# Highly Stereoselective Heterogeneous Diene Polymerization by Co-MFU-4*l*: A Single-Site Catalyst Prepared by Cation Exchange

**Romain J.-C. Dubey,[§] Robert J. Comito,[§] Zhenwei Wu,[°] Guanghui Zhang,[°] Adam J. Rieth,[§] Christopher H. Hendon,[§] Jeffrey T. Miller,[°] Mircea Dincă[§]\***

[§] Department of Chemistry, Massachusetts Institute of Technology, 77 Massachusetts Avenue, Cambridge, Massachusetts 02139, United States.

[°] Davidson School of Chemical Engineering, Purdue University, 480 Stadium Mall Dr., West Lafayette, Indiana 47907, United States.

## Supporting Information

**Contents**

# 1. General Information.

Modified methylaluminoxane-12 (MMAO-12, 7 % w/w in toluene, Sigma), 1,3-Butadiene (20 wt% in toluene, Sigma) and 1,3-butadiene (≥99%, with *p-tert*-butylcatechol as inhibitor, Sigma) were used as received. Other commercial reagents were purified prior to use following the guidelines of Perrin and Armarego.[1] Dry, deaerated toluene (HPLC Grade, 99.8%) was obtained by passing the solution through two silica columns in a Glass Contour Solvent System and degassing with a flow of argon gas for 30 min followed by three freeze-pump-thaw cycles. Sonication was performed using a VWR bath sonicator. Yields refer to purified compounds, unless otherwise indicated.

X-ray absorption spectroscopy measurements at the Co K edge (7.9090 keV) were performed on the 10-BM bending magnet beamline of the Materials Research Collaborative Access Team (MRCAT) at the Advanced Photon Source (APS), Argonne National Laboratory.

Powder X-ray diffraction (PXRD) patterns were recorded on a Bruker Advance II diffractometer equipped with $\theta/2\theta$ Bragg-Brentano geometry and Ni-filtered Cu-K$_\alpha$ radiation (K$\alpha$1 = 1.5406 Å). Unless otherwise noted, PXRD analysis was performed immediately after samples were exposed to air. Benchtop infrared (IR) spectra were recorded on a Bruker Tensor 37 instrument with a germanium attenuated total reflectance (ATR) sample holder. Nitrogen adsorption isotherms were performed using a Micromeritics ASAP 2020 Surface Area and Porosity Analyzer and UHP grade nitrogen (99.999% purity).

Elemental analysis was performed by Robertson Microlit Laboratories, using combustion analysis for carbon, nitrogen, and hydrogen and inductively coupled optical emission spectroscopy (ICP-OES) for transition metals. Additional transition metal analysis was provided by inductively coupled plasma mass spectrometry (ICP-MS) on an Agilent 7900 at the MIT Center for Environmental Health Sciences (MIT CEHS). Calibration standards were prepared for ICP-MS analysis using analytical standard solutions purchased from Ricca Chemicals and 1% $HNO_3$ solution (prepared from EMD Millipore

Omnitrace® HNO$_3$ and ultrafiltered water). $^1$H and $^{13}$C NMR spectra were recorded on a Jeol 502 JNM‑ECZ500R/S1 (500 MHz) ($^1$H, 500.2; $^{13}$C{$^1$H}, 125.8). $^1$H NMR spectra are internally referenced relative to residual protio solvent signals at δ 7.26 ppm (CDCl$_3$) or at δ 7.16 ppm (benzene-d$_6$) and are reported as follows: chemical shift (δ ppm), multiplicity (s = singlet, d = doublet, ap = apparent), integration, coupling constant (Hz). $^{13}$C NMR spectra are referenced relative to CDCl$_3$ at δ 77.16 ppm or benzene-d$_6$ at 128.06 ppm and are reported in terms of chemical shift (δ ppm) and multiplicity where appropriate. Gel permeation chromatography (GPC) data were recorded on an Agilent 1260 Infinity Series with THF as elution solvent. The molecular weights are reported against polystyrene standards. The elution traces were integrated with the Agilent GPC-Addon Rev. B.01.01.

## 2. Metal-Organic Framework Synthesis.

**MFU-4***l.* Prepared according to the published procedure.[2]

**Ti(IV)-MFU-4***l.* was synthesized after the procedure of Comito et al.[3] ICP-OES indicated a Ti : Zn molar ratio of 0.037 : 1 = 0.18 : 4.82. Formula: $Ti_{0.18}Zn_{4.82}Cl_{4.36}(BTDD)_3$ $(Ti_{0.18}Zn_{4.82}Cl_{4.36}C_{36}N_{18}H_{12}O_6)$. Ti = 0.98 wt%.

**Ti(III)-MFU-4***l.* was synthesized after the procedure of Comito et al.[3] ICP-OES indicated a Ti : Zn molar ratio of 0.464 : 1 = 1.59 : 3.41. Formula: $Ti_{1.6}Zn_{3.4}Cl_{5.6}(BTDD)_3$ • 8.34 $H_2O$ $(Ti_{1.6}Zn_{3.4}Cl_{5.6}C_{36}N_{18}H_{12}O_6$ • 8.34 $H_2O)$. Ti = 5.34 wt%.

**Cr(II)-MFU-4***l.* was synthesized after the procedure of Comito et al.[3] ICP-OES indicated a Cr : Zn molar ratio of 0.07633 : 1. Formula: $Cr_{0.35}Zn_{4.65}Cl_4(BTDD)_3$ $(Cr_{0.35}Zn_{4.65}Cl_4C_{36}N_{18}H_{12}O_6)$. Cr = 1.45 wt%.

**Cr(III)-MFU-4***l.* was synthesized after the procedure of Comito et al.[3] ICP-OES indicated a Cr : Zn molar ratio of 0.05 : 1. Formula: $Cr_{0.25}Zn_{4.75}Cl_{4.25}(BTDD)_3$ • 1.76 $H_2O$ • 0.98 $CH_3OH$ $(Cr_{0.25}Zn_{4.75}Cl_{4.25}C_{36}N_{18}H_{12}O_6$ • 1.76 $H_2O$ • 0.98 $CH_3OH)$. Cr = 0.98 wt%.

**Fe(II)-MFU-4***l.* was synthesized after the procedure of Denysenko et al.[4] ICP-OES indicated a Fe : Zn molar ratio of 0.63 : 1. Formula: $Fe_{1.94}Zn_{3.06}Cl_4(BTDD)_3$ $(Fe_{1.94}Zn_{3.06}Cl_4C_{36}N_{18}H_{12}O_6)$. Fe = 8.72 wt%.

**Ni(II)-MFU-4***l.* was synthesized after the procedure of Metzger et al.[5] ICP-OES indicated a Ni : Zn ratio of 0.13 : 1. Formula: $Ni_{0.58}Zn_{4.42}Cl_{1.82}(NO_3)_{2.18}$ $(BTDD)_3$ $(Ni_{0.58}Zn_{4.42}Cl_{1.82}C_{36}H_{12}N_{20.18}O_{12.54})$. Ni = 2.69 wt%.

**Co(II)-MFU-4***l.* (exchange Co : Zn ratio = 0.2) was synthesized after the procedure of Denysenko et al.[6] The exchange temperature was 155 °C. ICP-OES indicated a Co : Zn ratio of 0.19 : 1: Elemental analysis calculated (%) for $Co_{0.90}Zn_{4.10}(BTDD)_3$ • 1.5 DMF $(Co_{0.90}Zn_{4.10}C_{40.5}H_{22.5}N_{19.5}O_{7.5}Cl_4)$; C 35.63, H 1.66, N 20.01; found: C 35.61, H 1.25, N 20.49. Co = 3.88 wt%.

**Co(II)-MFU-4***l.* (exchange Co : Zn ratio = 0.2) was synthesized after the procedure of Denysenko et al.[6] The exchange was performed at 155 °C. ICP-OES indicated a Co : Zn ratio of 0.19 : 1: Elemental analysis calculated (%) for $Co_{0.90}Zn_{4.10}(BTDD)_3$ • 1.5 DMF

($Co_{0.90}Zn_{4.10}C_{40.5}H_{22.5}N_{19.5}O_{7.5}Cl_4$); C 35.63, H 1.66, N 20.01; found: C 35.61, H 1.25, N 20.49. Co = 3.88 wt%.

**Co(II)-MFU-4*l*.** (exchange Co : Zn ratio = 0.3) was synthesized after the procedure of Denysenko et al.[6] The exchange was performed at 155 °C. ICP-OES indicated a Co : Zn ratio of 0.39 : 1: Elemental analysis calculated (%) for $Co_{1.53}Zn_{3.47}(BTDD)_3 \bullet$ DMF ($Co_{1.53}Zn_{3.47}C_{39}H_{15}N_{19}O_7Cl_4$); C 35.36, H 1.44, N 20.09; found: C 35.68, H 0.84, N 20.20. Co = 6.81 wt%.

**Co(II)-MFU-4*l*.** (exchange Co : Zn ratio = 0.45) was synthesized after the procedure of Denysenko et al.[6] The exchange was performed at 155 °C. ICP-OES indicated a Co : Zn ratio of 0.66 : 1: Elemental analysis calculated (%) for $Co_{2.14}Zn_{2.86}(BTDD)_3 \bullet$ DMF ($Co_{2.14}Zn_{2.86}C_{39}H_{15}N_{19}O_7Cl_4$); C 35.47, H 1.45, N 20.15; found: C 35.65, H 0.80, N 20.34. Co = 9.55 wt%.

**Co(II)-MFU-4*l*.** (exchange Co : Zn ratio = 0.85) was synthesized after the procedure of Denysenko et al.[6] The exchange was performed at 155 °C. ICP-OES indicated a Co : Zn ratio of 1.54 : 1: Elemental analysis calculated (%) for $Co_{3.16}Zn_{1.84}(BTDD)_3 \bullet$ 0.7 DMF ($Co_{3.16}Zn_{1.84}C_{38.1}H_{16.9}N_{18.7}O_{6.7}Cl_4$); C 35.41, H 1.32, N 20.27; found: C 35.46, H 0.70, N 20.36. Co = 14.41 wt%.

**Co(II)-MFU-4*l*.** (full exchange) was synthesized after the procedure of Denysenko et al.[6] The exchange was performed at 155 °C. ICP-OES indicated a Co : Zn ratio of 4.00 : 1: Elemental analysis calculated (%) for $Co_4Zn(BTDD)_3$ ($Co_4ZnC_{36}H_{12}N_{18}O_6Cl_4$); C 34.99, H 0.98, N 20.41; found: C 32.78, H 1.42, N 18.64. Co = 19.07 wt%.

# 3. Analytical Data for Metal-Organic Frameworks.

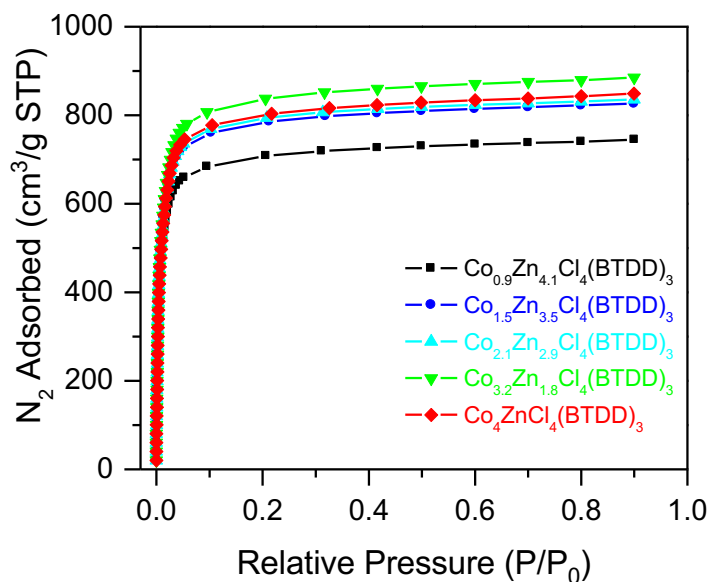## 3.1. Nitrogen Adsorption Isotherms for different Co-loadings.



**Figure S3.1.** Nitrogen adsorption analysis Co-MFU-4*l* with different loadings.

**Table S3.1.** Nitrogen adsorption analysis Co-MFU-4*l* with different loadings.

| Co-MFU-4*l* loading | Mass weighted in | Surface area per mass | MW | Surface area per mmol |
|---|---|---|---|---|
| $Co_4ZnCl_4(BTDD)_3$ | 90.2 mg | 3532 ± 13 m²/g | 1235.5 | 4364 ± 16 m²/mmol |
| $Co_{3.2}Zn_{1.8}Cl_4(BTDD)_3 \cdot$ 0.7 DMF | 65.7 mg | 3543 ± 20 m²/g | 1292.1 | 4577 ± 25 m²/mmol |
| $Co_{2.1}Zn_{2.9}Cl_4(BTDD)_3 \cdot$ DMF | 46.2 mg | 3349 ± 22 m²/g | 1320.6 | 4420 ± 30 m²/mmol |
| $Co_{1.5}Zn_{3.5}Cl_4(BTDD)_3 \cdot$ DMF | 66.3 mg | 3364 ± 11 m²/g | 1324.5 | 4450 ± 15 m²/mmol |
| $Co_{0.9}Zn_{4.1}Cl_4(BTDD)_3 \cdot$ 1.5 DMF | 60.3 mg | 3040 ± 8 m²/g | 1365.1 | 4149 ± 11 m²/mmol |

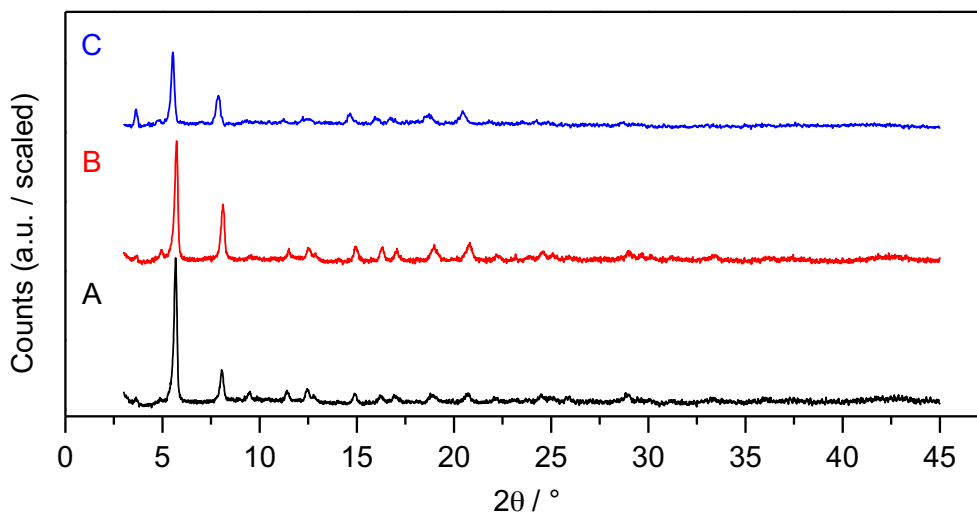## 3.2. Powder X-Ray Diffraction Patterns.



**Figure S3.2.** Comparison of powder diffraction patterns of Co-MFU-4*l*. (A) Activated at 280°C under ultra-high vacuum. (B) Treated 7 h with MMAO in toluene. (C) After a 1 h polymerization reaction at 60 °C. The baselines were corrected.

# 4. Experimental Data for Butadiene Polymerization.

## 4.1 "Semi-batch" Polymerization.

**General Procedure.** In a nitrogen glovebox, MMAO-12 (a solution 7 w% Al in toluene) was added to a suspension of precatalyst in dry, degassed toluene (4.5 mL) in a Parr reactor equipped with a magnetic stirbar. The reactor was sealed, and then connected to a 1,3-butadiene gas bottle, stirring vigorously for 6 h. The reactor was then carefully depressurized, opened, and quenched with a 1 : 5 hydrochloric acid/methanol solution (25 mL). The resulting mixture was transferred to a flask and then sonicated for 30 s. The product was isolated by filtration of the resulting precipitate. The solid was dried under high-vacuum for 20 h. The yield was determined gravimetrically.

Analytical samples were then prepared for NMR by dissolving 20-30 mg polymer in 1.2 mL $CDCl_3$. The suspension was centrifuged and an NMR sample of the supernatant was measured. To obtain very high signal-to-noise ratios, the paramagnetic catalyst was removed from the solution according to the "hot-filtration" procedure. The ratio between 1,2-vinyl polybutadiene, 1,4-cis-polybutadiene and 1,4-trans polybutadiene was determined by the relative integrals in a quantitative $^{13}C$ NMR experiment with 5 s relaxation delay ($\delta$ = 34.42 (-$CH_2$-, 1,2-vinyl), 32.89 (-$CH_2$-, 1,4-trans), 27.54 (-$CH_2$-, 1,4-cis), 25.12 (-$CH_2$-, 1,2-vinyl).[7] The 1,2-vinyl content was then controlled by $^1$H-NMR spectroscopy evaluating the ratio between 1,4-insertion and 1,2-vinyl content ($\delta$ = 5.38 (-$CH$=, 1,4-cis/trans), 4.98 (-CH=$CH_2$, 1,2-vinyl)).[8]

Number-average molecular weights ($M_N$) and polydispersity indices (PDI) were determined by GPC. A solution of the polymer (1 mg/mL) in THF was prepared. In case of poor solubility, the polymer was stirred in THF at 40 °C during 72 h. The solution was filtrated through a 0.2 μm PTFE syringe filter. Injection volume 50 μL, temperature = 25 °C, eluent flow 1 mL/min, column pressure 94 bar.

**Ti(IV)-MFU-4*l* Polymerization (Table 1, entry 2).** According to the general procedure with Ti(IV)-MFU-4*l* (0.98 % Ti, 5.0 mg, 1.0 μmol Ti, 1.00 equiv.) and MMAO-12 (0.5

mL, 1.16 mmol, 1160 equiv.). Yield: 326 mg, 6.0 mmol. Stereoselectivity: 22.9 % 1,4-cis, 73.8 % 1,4-trans, 3.3 % 1,2-vinyl.

**Ti(III)-MFU-4*l* Polymerization (Table 1, entry 3).** According to the general procedure with Ti(III)-MFU-4*l* (5.34 % Ti, 5.2 mg, 5.8 μmol Ti, 1.00 equiv.) and MMAO-12 (0.5 mL, 1.16 mmol, 181 equiv.). Yield: 19 mg, 0.36 mmol. Stereoselectivity: not determined.

**Cr(II)-MFU-4*l* Polymerization (Table 1, entry 4).** According to the general procedure with Cr(II)-MFU-4*l* (5.1 mg, 3.8 μmol Cr, 1.00 equiv.) and MMAO-12 (0.5 mL, 1.16 mmol, 305 equiv.). Yield: 20 mg, 0.37 mmol. Stereoselectivity: not determined.

**Cr(III)-MFU-4*l* Polymerization (Table 1, entry 5).** According to the general procedure with Cr(III)-MFU-4*l* (5.1 mg, 1.0 μmol Cr, 1.00 equiv.) and MMAO-12 (0.5 mL, 1.16 mmol, 305 equiv.). Yield: 20 mg, 0.37 mmol. Stereoselectivity: 91.0 % 1,4-cis, 6.9 % 1,4-trans, 2.1 % 1,2-vinyl.

**Fe(II)-MFU-4*l* Polymerization (Table 1, entry 6).** According to the general procedure with Fe(II)-MFU-4*l* (5.0 mg, 7.8 μmol Fe, 1.00 equiv.), and MMAO-12 (0.5 mL, 1.16 mmol, 148 equiv.). Yield: 360 mg, 6.7 mmol. Stereoselectivity: 68 % 1,4-cis, 22 % 1,4-trans, 10 % 1,2-vinyl.

**Co(II)-MFU-4*l* Polymerization (Table 1, entry 7).** According to the general procedure with Co(II)-MFU-4*l* (5.2 mg, 16.9 μmol Co, 1.00 equiv.), and MMAO-12 (0.5 mL, 1.16 mmol, 68 equiv.). Yield: 1468 mg, 27 mmol. Stereoselectivity: 99.3 % 1,4-cis, 0.4 % 1,4-trans, 0.3 % 1,2-vinyl. GPC data: $M_n$ = 200'000, $M_w$ = 252'000, PDI = 1.26.

**Ni(II)-MFU-4*l* Polymerization (Table 1, entry 8).** According to the general procedure with Ni(II)-MFU-4*l* (4.5 mg, 2.1 μmol Ni, 1.00 equiv.) and MMAO-12 (0.5 mL, 1.16 mmol, 552 equiv.). Yield: 1049 mg, 19 mmol. Stereoselectivity: 96.2 % 1,4-cis, 1.9 % 1,4-trans, 1.9 % 1,2-vinyl. GPC data: $M_n$ = 71'000, $M_w$ = 150'000, PDI = 2.12.

## 4.2 Batch Polymerization.

**Generation of a Monomer Solution.** 1,3-Butadiene was condensed via a cooling finger at -78 °C (dry ice/acetone) into dry toluene stored over activated 3 Å molecular sieves at -78 °C (dry ice/acetone). The concentration in the cold solution was measured gravimetrically. Concentration: 33.24 wt%. Density at -78 °C estimated: 0.81 g/mL via the Mixtures Property Prediction program of the Dortmund Data Bank (DDSB).

**General Procedure.** In a glovebox, the activator was added to a suspension of precatalyst in dry, degassed toluene in a flame-dried Schlenk flask equipped with a J Young valve and a magnetic stirbar. The precatalyst/activator mixture was aged, stirring for 10 min at 21 °C. A dry, degassed solution of 1,3-butadiene in toluene at − 78 °C was injected rapidly, the Schlenk flask was sealed tightly immediately, stirring vigorously during the desired time. Upon completion, the flask was carefully opened, quenched with a 1 : 5 hydrochloric acid/methanol solution (15 mL) and sonicated for 30 s. The precipitate was washed with methanol (30 mL) and the solid was dried under vacuum for 20 h. NMR and GPC analysis samples were prepared and performed according to the procedure described in the semi-batch section.

**Activator Screen (Table 2).**

**MMAO-12.** According to the general procedure with $Co_4ZnCl_4(BTDD)_3$ (3.1 mg, 10 $\mu$mol Co, 1 equiv.), MMAO-12 (0.46 mL, 1 mmol, 100 equiv.), toluene (1 mL) and 1,3-butadiene solution (3.63 mL, 1 g, 18.5 mmol, 1850 equiv., resulting monomer conc. 3.5 M). Reaction time = 2 h at 21 °C. Yield: 290 mg, 5.36 mmol. Stereoselectivity: 99.3 % 1,4-cis, 0.4 % 1,4-trans, 0.3 % 1,2-vinyl.

**Et₂AlCl.** According to the general procedure with $Co_4ZnCl_4(BTDD)_3$ (3.1 mg, 10 $\mu$mol Co, 1 equiv.), Et₂AlCl (0.54 mL, 1 mmol, 100 equiv.), toluene (1 mL) and 1,3-butadiene solution (3.63 mL, 1 g, 18.5 mmol, 1850 equiv., resulting monomer conc. 3.5 M). Reaction time = 2 h at 21 °C. Yield: 212 mg, 3.92 mmol. Stereoselectivity: 88.8 % 1,4-cis, 6.4 % 1,4-trans, 4.8 % 1,2 vinyl.

**Me$_3$Al.** According to the general procedure with Co$_4$ZnCl$_4$(BTDD)$_3$ (3.1 mg, 10 $\mu$mol Co, 1 equiv.), Me$_3$Al (0.5 mL, 1 mmol, 100 equiv.), toluene (1 mL) and 1,3-butadiene solution (3.63 mL, 1 g, 18.5 mmol, 1850 equiv., resulting monomer conc. 3.5 M). Reaction time = 6 h at 21 °C. Yield: 9 mg, 0.17 mmol. Stereoselectivity: not determined.

**$^i$Bu$_3$Al.** According to the general procedure with Co$_4$ZnCl$_4$(BTDD)$_3$ (3.1 mg, 10 $\mu$mol Co, 1 equiv.), $^i$Bu$_3$Al (0.93 mL, 1 mmol, 100 equiv.), toluene (1 mL) and 1,3-butadiene solution (3.63 mL, 1 g, 18.5 mmol, 1850 equiv., resulting monomer conc. 3.5 M). Reaction time = 6 h at 21 °C. Yield: 21 mg, 0.39 mmol. Stereoselectivity: not determined.

**Et$_3$Al.** According to the general procedure with Co$_4$ZnCl$_4$(BTDD)$_3$ (3.1 mg, 10 $\mu$mol Co, 1 equiv.), Et$_3$Al (0.15 mL, 1 mmol, 100 equiv.), toluene (1.35 mL) and 1,3-butadiene solution (3.63 mL, 1 g, 18.5 mmol, 1850 equiv., resulting monomer conc. 3.5 M). Reaction time = 6 h at 21 °C. Yield: 18 mg, 0.33 mmol. Stereoselectivity: not determined.

**Activator Concentration Dependence (Figure 4).** According to the general procedure with Co$_4$ZnCl$_4$(BTDD)$_3$ (3.1 mg, 10 $\mu$mol Co, 1 equiv.), MMAO-12 (0.22 – 0.86 mL, 0.5 - 2 mmol, 50 - 200 equiv.), toluene (3.72 – 4.35 mL) and 1,3-butadiene solution (3.63 mL, 1 g, 18.5 mmol, 1850 equiv., resulting monomer conc. 2.25 M). Reaction time = 2 h at 21 °C (Table S4.1.).

**Table S4.1.** Effect of the MMAO loading on the polymerization.

| Catalyst[a] | $T$ (°C) | Time (h) | Al/Co | Yield (mg) | 1,4-cis % | $M_n$ (x 10$^{-5}$) | $M_x/M_n$ |
|---|---|---|---|---|---|---|---|
| Co$_4$ZnCl$_4$(BTDD)$_3$ | 21 | 2 | 50 | 86.0 | 99.3 | 6.7 | 1.63 |
| Co$_4$ZnCl$_4$(BTDD)$_3$ | 21 | 2 | 100 | 113.1 | 99.3 | 6.7 | 1.68 |
| Co$_4$ZnCl$_4$(BTDD)$_3$ | 21 | 2 | 125 | 120.2 | 99.3 | 7.2 | 1.64 |
| Co$_4$ZnCl$_4$(BTDD)$_3$ | 21 | 2 | 150 | 124.4 | 99.2 | 6.7 | 1.55 |
| Co$_4$ZnCl$_4$(BTDD)$_3$ | 21 | 2 | 200 | 130.9 | 99.1 | 7.1 | 1.71 |

[a]Co-MFU-4*l*: 3.1 mg; cobalt = 10 μmol; [BD$_o$] = 2.25 M

**Investigating Cobalt Loading.** According to the general procedure with Co$_x$Zn$_{5-x}$Cl$_4$(BTDD)$_3$ (3.1-15.2 mg, 10.0 $\mu$mol Co, 1 equiv.), MMAO-12 (0.53 mL, 125 mmol,

125 equiv.), toluene (5.08 mL) and 1,3-butadiene solution (3.63 mL, 1 g, 18.5 mmol, 1850 equiv., resulting monomer conc. 2.0 M). Reaction time = 2 h at 21 °C. (Table S4.2.)

**Table S4.2.** Effect of the cobalt loading in Co-MFU-4*l* on the polymerization rate.

| Catalyst[a] | Amount of MFU-4*l* (mg) | Cobalt Amount (μmol) | Time (h) | [BD$_o$] | Al/Co | Yield (mg) | TOF[b] |
|---|---|---|---|---|---|---|---|
| Co$_{0.9}$Zn$_{4.1}$Cl$_4$(BTDD)$_3$ | 15.2 | 10 | 2 | 2.0 M | 125 | 93.7 | 86.9 |
| Co$_{1.5}$Zn$_{3.5}$Cl$_4$(BTDD)$_3$ | 8.9 | 10 | 2 | 2.0 M | 125 | 85.4 | 79.1 |
| Co$_{2.1}$Zn$_{2.9}$Cl$_4$(BTDD)$_3$ | 6.2 | 10 | 2 | 2.0 M | 125 | 86.6 | 80.2 |
| Co$_{3.2}$Zn$_{1.8}$Cl$_4$(BTDD)$_3$ | 4.1 | 10 | 2 | 2.0 M | 125 | 81.4 | 75.4 |
| Co$_4$ZnCl$_4$(BTDD)$_3$ | 3.1 | 10 | 2 | 2.0 M | 125 | 94.5 | 87.6 |

[a]Temperature = 21 °C; [b]Defined as mmol polymer / mmol cobalt h.

**Time Study (Figure 3A).** According to the general procedure with Co$_{2.1}$Zn$_{2.9}$Cl$_4$(BTDD)$_3$ (3.1 mg, 5.0 $\mu$mol Co, 1 equiv.), MMAO-12 (0.27 mL, 0.625 mmol, 125 equiv.), toluene (4.3 mL) and 1,3-butadiene solution (3.63 mL, 1 g, 18.5 mmol, 3700 equiv., resulting monomer conc. 2.25 M). After addition of monomer, the sealed Schlenk flask was placed into a pre-heated oil bath at 40 °C. Reaction time = 30 – 180 min. (Table S4.3.)

**Table S4.3.** Effect of the reaction time on the molecular weight.

| Catalyst[a] | Cobalt Amount | Time (min) | Yield (mg) | TON[b] | 1,4-cis %[c] | M$_w$ (x 10$^5$) | M$_n$ (x 10$^5$) | M$_w$/M$_n$ |
|---|---|---|---|---|---|---|---|---|
| Co$_{2.1}$Zn$_{2.9}$Cl$_4$(BTDD)$_3$ | 5 μmol | 30 | 33.8 | 124 | 98.3 | 9.27 | 5.5 | 1.68 |
| Co$_{2.1}$Zn$_{2.9}$Cl$_4$(BTDD)$_3$ | 5 μmol | 60 | 56.6 | 210 | 98.4 | 11.5 | 6.8 | 1.69 |
| Co$_{2.1}$Zn$_{2.9}$Cl$_4$(BTDD)$_3$ | 5 μmol | 90 | 72.1 | 267 | 98.3 | 11.6 | 6.9 | 1.68 |
| Co$_{2.1}$Zn$_{2.9}$Cl$_4$(BTDD)$_3$ | 5 μmol | 120 | 86.9 | 322 | 98.3 | 11.0 | 6.7 | 1.66 |
| Co$_{2.1}$Zn$_{2.9}$Cl$_4$(BTDD)$_3$ | 5 μmol | 150 | 87.7 | 325 | 98.3 | 11.4 | 6.8 | 1.67 |
| Co$_{2.1}$Zn$_{2.9}$Cl$_4$(BTDD)$_3$ | 5 μmol | 180 | 89.9 | 333 | 98.5 | 11.8 | 7.0 | 1.68 |

[a]MOF mass = 3.1 mg, Co = 9.55 wt%; Al/Co ratio = 125; temperature = 40 °C [b]Defined in mmol polymer / mmol cobalt. [c]Determined by quantitative $^{13}$C NMR.

**Investigating Temperature Dependence (Figure 3B).** According to the general procedure with Co$_4$ZnCl$_4$(BTDD)$_3$ (3.1 mg, 10 $\mu$mol Co, 1 equiv.), MMAO-12 (0.46 mL, 1.00 mmol, 100 equiv.), toluene (4.13 mL) and 1,3-butadiene solution (3.63 mL, 1 g, 18.5 mmol, 1850 equiv., resulting monomer conc. 2.25 M). After addition of monomer, the

sealed Schlenk flask was placed into a pre-heated oil bath at the desired temperature. Reaction time = 1 – 2 h. (Table S4.4.).

**Table S4.4.** Effect of the temperature on the selectivity.

| $T$ (°C) | Time (h) | Cobalt[a] Amount ($\mu$mol) | Yield (mg) | TOF[b] | 1,4-cis %[c] | 1,4-trans %[c] | 1,2-vinyl %[c] | $M_w$ (x $10^5$) | $M_n$ (x $10^5$) | $M_w/M_n$ |
|---|---|---|---|---|---|---|---|---|---|---|
| 0 | 2 | 10 | 31 | 29.6 | 99.4 | 0.4 | 0.2 | 12.8 | 8.5 | 1.51 |
| 21 | 2 | 10 | 113 | 104 | 99.3 | 0.5 | 0.2 | 11.3 | 6.7 | 1.68 |
| 35 | 2 | 10 | 132 | 124 | 98.9 | 0.8 | 0.3 | 13.6 | 8.4 | 1.62 |
| 50 | 1 | 10 | 162 | 300 | 97.5 | 2.2 | 0.3 | 11.6 | 7.1 | 1.64 |
| 65 | 1 | 10 | 204 | 378 | 96.2 | 3.2 | 0.6 | 7.6 | 4.6 | 1.64 |

[a]$Co_4ZnCl_4(BTDD)_3$ = 3.1 mg; $[BD_o]$ = 1 g, 18.5 mmol, conc. = 2.25 M; Al/Co = 100. [b]Defined as mmol polymer / mmol cobalt h. [c]Determined by quantitative $^{13}C$ NMR.

**Effect of Initial Monomer Concentration.** According to the general screening procedure with $Co_4ZnCl_4(BTDD)_3$ (3.1 mg, 10 $\mu$mol Co, 1 equiv.), MMAO-12 (0.65 mL, 1.5 mmol, 150 equiv.), toluene (1.00 – 14.22 mL) and 1,3-butadiene solution (3.63 mL, 1 g, 18.5 mmol, 1850 equiv., resulting monomer conc. 1.0 – 3.5 M). Reaction time = 2 h at 21 °C. (Table S4.5.)

**Table S4.5.** Effect of the initial monomer concentration on the polymerization.

| Catalyst[a] | $[BD_o]$ | Toluene (mL) | Yield (mg) | TOF[b] | 1,4-cis %[c] | $M_n$ (x $10^{-5}$) | $M_x/M_n$ |
|---|---|---|---|---|---|---|---|
| $Co_4ZnCl_4(BTDD)_3$ | 1.0 M | 14.22 | 36.0 | 33.3 | 98.0 | 4.1 | 1.64 |
| $Co_4ZnCl_4(BTDD)_3$ | 1.5 M | 8.05 | 66.1 | 61.3 | 98.9 | 5.0 | 1.71 |
| $Co_4ZnCl_4(BTDD)_3$ | 2.0 M | 4.96 | 100.4 | 93.0 | 99.2 | 6.3 | 1.67 |
| $Co_4ZnCl_4(BTDD)_3$ | 2.25 M | 3.93 | 124.4 | 115 | 99.3 | 6.7 | 1.55 |
| $Co_4ZnCl_4(BTDD)_3$ | 2.5 M | 3.11 | 176.7 | 164 | 99.3 | 9.3 | 1.61 |
| $Co_4ZnCl_4(BTDD)_3$ | 3.0 M | 1.88 | 247.7 | 229 | 99.3 | -[d] | -[d] |
| $Co_4ZnCl_4(BTDD)_3$ | 3.5 M | 1.00 | 289.9 | 269 | 99.3 | -[d] | -[d] |

[a]Co-MFU-4*l*: 3.1 mg; cobalt = 10 $\mu$mol; temperature = 21 °C; reaction time = 2 h, BD = 1 g, 18.5 mmol, 1850 equiv. [b]Defined as mmol polymer / mmol cobalt h. [c]Determined by quantitative $^{13}C$ NMR. [d]Product insoluble in tetrahydrofuran.

**Ni-MFU-4*l* in batch.** According to the general procedure with Ni(II)-MFU-4*l* (10.7 mg, 5.0 $\mu$mol Ni, 1 equiv.), MMAO-12 (0.25 mL, 0.58 mmol, 116 equiv.), toluene (1.4 mL) and 1,3-butadiene solution (3.63 mL, 1 g, 18.5 mmol, 3700 equiv., resulting monomer conc. 3.5 M). Reaction time = 1 h at 21 °C. Yield = 383 mg. TOF = 76.6 g / mmol h.

Stereoselectivity: 96.2 % 1,4-cis, 1.9 % 1,4-trans, 1.9 % 1,2-vinyl. GPC data: $M_n$ = 42'000, $M_w$ = 75'000, PDI = 1.79.

**Tp$^{Mes}$NiCl in batch.** According to the general procedure with Tp$^{Mes}$NiCl (6.6 mg, 10.0 $\mu$mol Ni, 1 equiv.), MMAO-12 (0.5 mL, 1.16 mmol, 116 equiv.), toluene, 1.1 mL and 1,3-butadiene solution (3.63 mL, 1 g, 18.5 mmol, 1850 equiv., resulting monomer conc. 3.5 M). Reaction time = 1 h at 21 °C. Yield = 221.6 mg, TOF = 22.2 g / mmol h. Stereoselectivity: 94.0 % 1,4-cis, 4.1 % 1,4-trans, 1.9 % 1,2-vinyl. GPC data: $M_n$ = 43'000, $M_w$ = 72'000, PDI = 1.68.

**Tp$^{Mes}$CoCl and MMAO-12 in batch.** According to the general procedure with Tp$^{Mes}$CoCl (2.2 mg, 3.33 $\mu$mol Co, 1 equiv.), MMAO-12 (0.18 mL, 0.39 mmol, 116 equiv.), toluene, 4.4 mL and 1,3-butadiene solution (3.63 mL, 1 g, 18.5 mmol, 5555 equiv., resulting monomer conc. 2.25 M). Reaction time = 2 h at 21 °C. Yield = 580.2 mg, TOF = 87 g / mmol h. Stereoselectivity: 98.2 % 1,4-cis, 1.3 % 1,4-trans, 0.5 % 1,2-vinyl. GPC data: $M_n$ = 316'000, $M_w$ = 550'000, PDI = 1.74.

**Tp$^{Mes}$Co($\eta^3$-allyl) only in batch.** According to the general procedure with Tp$^{Mes}$Co-allyl (2.2 mg, 3.33 $\mu$mol Co, 1 equiv.), toluene, 4.6 mL and 1,3-butadiene solution (3.63 mL, 1 g, 18.5 mmol, 5555 equiv., resulting monomer conc. 2.25 M). Reaction time = 8 h at 21 °C. Yield = 0 mg.

**Tp$^{Mes}$Co($\eta^3$-allyl) and MMAO-12 in batch.** According to the general procedure with Tp$^{Mes}$Co-allyl (3.3 mg, 5 $\mu$mol Co, 1 equiv.), MMAO-12 (0.23 mL, 0.5 mmol, 100 equiv.), toluene (4.34 mL) and 1,3-butadiene solution (3.63 mL, 1 g, 18.5 mmol, 3700 equiv., resulting monomer conc. 2.25 M). Reaction time = 2 h at 21 °C. Yield = 363 mg, 6.7 mmol.

Stereoselectivity: 98.5 % 1,4-cis, 0.9 % 1,4-trans, 0.6 % 1,2-vinyl. GPC data: $M_n$ = 47'000, $M_w$ = 100'000, PDI = 2.12.
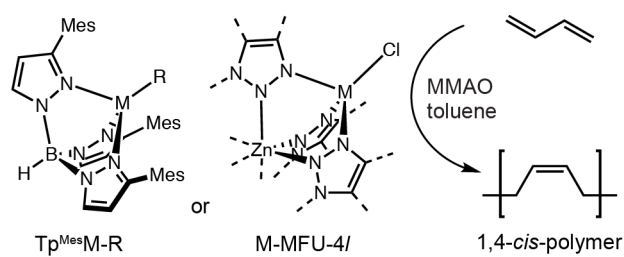
| Entry | Precatalyst | TOF[a] | % 1,4-*cis*[b] | PDI[c] |
|---|---|---|---|---|
| 1[d] | Ni-MFU-4*l* | 1400 | 96% | 1.8 |
| 2[d] | Tp[Mes]NiCl | 410 | 94% | 1.7 |
| 3[e] | Co-MFU-4*l* | 100 | 99.3% | 1.6 |
| 4[e] | Tp[Mes]CoCl | 1,700 | 98% | 1.7 |
| 5[e] | Tp[Mes]Co($\eta^3$-allyl) | 670 | 99% | 2.1 |

[a]Determined by isolated yield. [b]1,4-cis content determined by ^{13}C-NMR. [c]Determined by GPC. [d]Batch conditions with 3.5 M diene for 1 hour. [e]Batch conditions with 2.25 M diene for 2 hours.

**Table S4.6**. Comparing the reactivity and selectivity of cation-exchanged MOFs and their small molecule counterparts.

# 5 Experimental Data for Catalyst Stability Determination.

**5.1 Catalyst Recovery for PXRD Measurement.**

**Treatment of Co-MFU-4*l* with MMAO.** MMAO-12 (0.5 ml, 1.16 mmol as a 7 w% solution Al in toluene) was added to a suspension of $Co_4ZnCl_4(BTDD)_3$ (8 mg, 25.9 $\mu$mol Co, 1 equiv.) in dry toluene (2 ml) in a vial under inert conditions at 21 °C. The mixture was stirred at 21 °C for 7 h. The suspension was transferred under inert conditions to a centrifuge tube and centrifuged for 10 min. The supernatant was removed and a powder x-ray diffraction pattern of the solid phase was measured.

**Recovery of Co-MFU-4*l* after Polymerization (21 °C).** According to the general procedure, MMAO-12 (0.5 mL, 1.16 mmol, 116 equiv.) was added to a suspension of $Co_4ZnCl_4(BTDD)_3$ (3.1 mg, 10 $\mu$mol Co, 1 equiv.) in dry toluene (4.08 mL) in a flame dried 50 mL Schlenk flask with a J Young valve. The catalyst/cocatalyst mixture was stirred for 10 min at 21 °C. A dry, degassed 1,3-butadiene solution in toluene at -78°C (3.63 mL, 1 g, 18.5 mmol, 1850 equiv., resulting monomer conc. 2.25 M) was injected rapidly and the Schlenk flask was sealed tightly immediately. The reaction was stirred for 2 h at 21 °C. The mixture was cooled down to -78°C, diluted with dry dichloromethane (15 mL) and dry toluene (5 mL) under inert conditions and the diluted mixture was centrifuged. The solid phase was collected, dried under vacuum and a powder x-ray diffraction pattern was measured.
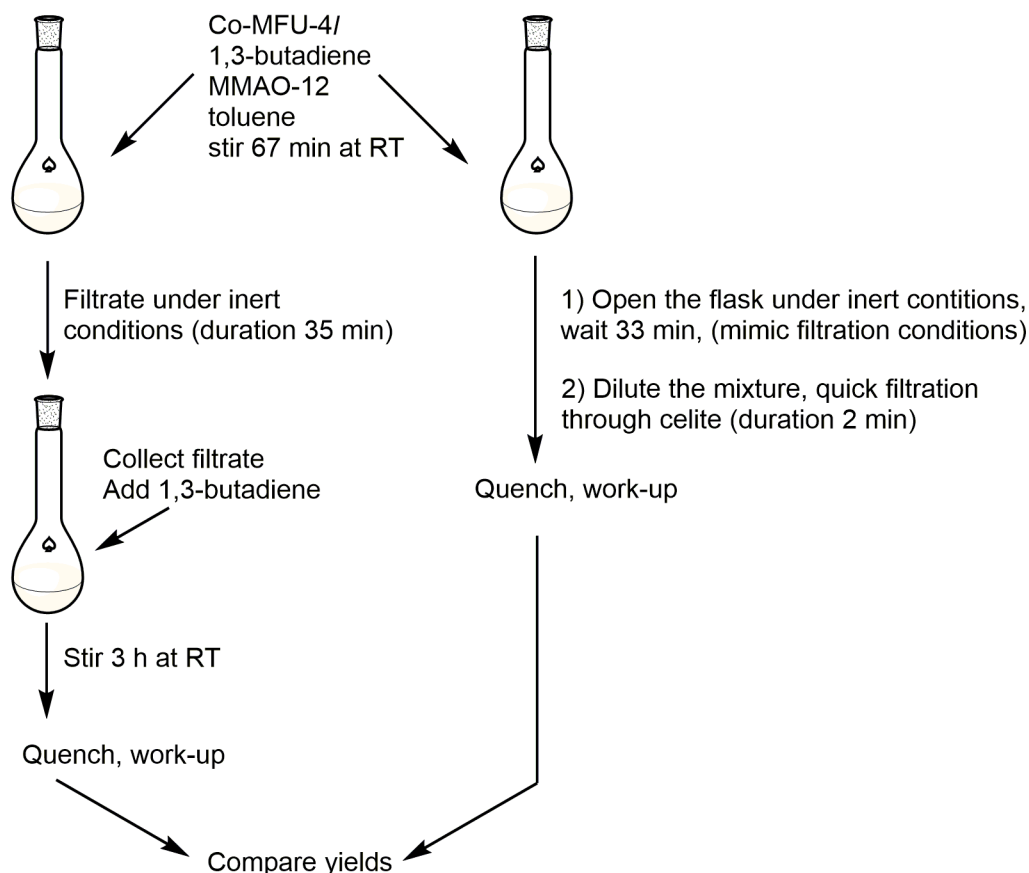
**Recovery of Co-MFU-4*l* after Polymerization (50 °C).** According to the general procedure, MMAO-12 (0.5 mL, 1.16 mmol, 116 equiv., as a 7 wt% Al solution in toluene) was added to a suspension of $Co_4ZnCl_4(BTDD)_3$ (3.1 mg, 10 $\mu$mol Co, 1 equiv.) in dry toluene (4.08 mL) in a flame dried 50 mL Schlenk flask with a J Young valve. The catalyst/cocatalyst mixture was stirred for 10 min at 21 °C. A dry/degassed 1,3-butadiene solution in toluene at -78°C (3.63 mL, 1 g, 18.5 mmol, 1850 equiv., resulting monomer conc. 2.25 M) was injected rapidly and the Schlenk flask was sealed tightly immediately.

The reaction was stirred for 1 h at 50 °C in a pre-heated oil bath. The mixture was cooled down to -78°C, diluted with dry dichloromethane (15 mL) and dry toluene (5 mL) under inert conditions and the diluted mixture was centrifuged. The solid phase was collected, dried under vacuum and a powder x-ray diffraction pattern was measured.

## 5.2 Hot-filtration Experiment.



Co-MFU-4/
1,3-butadiene
MMAO-12
toluene
stir 67 min at RT

Filtrate under inert
conditions (duration 35 min)

Collect filtrate
Add 1,3-butadiene

Stir 3 h at RT

Quench, work-up

1) Open the flask under inert contitions,
wait 33 min, (mimic filtration conditions)

2) Dilute the mixture, quick filtration
through celite (duration 2 min)

Quench, work-up

Compare yields

**Figure S5.1.** Schematic description of the performed "hot-filtration" experiment.

**Hot-Filtration Reaction.** MMAO-12 (0.5 mL, 1.16 mmol, 106 equiv.) was added to a suspension of $Co_4ZnCl_4(BTDD)_3$ (3.4 mg, 10.9 $\mu$mol Co, 1 equiv.) in dry toluene (4.08 mL) in a flame dried 50 mL Schlenk flask with a J Young valve. The catalyst/cocatalyst mixture was stirred for 10 min at 21 °C. A dry/degassed 1,3-butadiene solution in toluene at -78 °C (3.63 mL, 1 g, 18.5 mmol, 1697 equiv., resulting monomer conc. 2.25 M) was injected rapidly, the Schlenk flask was sealed tightly immediately and the reaction was stirred at 21 °C for 67 min. The green reaction mixture was filtrated under inert conditions through a short pad of celite. A dry/degassed 1,3-butadiene solution in toluene at -78 °C (3.63 mL, 1 g, 18.5 mmol, 1697 equiv.) was injected to the colorless filtrate in a flame dried 50 mL Schlenk flask with a J Young valve. The reaction mixture was stirred

for 3 h at 21 °C and quenched with. a 1 : 5 hydrochloric acid/methanol solution (15 mL). The resulting precipitate was washed with methanol (15 mL) and dried under high vacuum for 20 h. Yield: 120.5 mg.

**Control for the Hot-Filtration Reaction.** MMAO-12 (0.5 mL, 1.16 mmol, 106 equiv.) was added to a suspension of $Co_4ZnCl_4(BTDD)_3$ (3.4 mg, 10.9 $\mu$mol Co, 1 equiv.) in dry toluene (4.08 mL) in a flame dried 50 mL Schlenk flask with a J Young valve. The catalyst/cocatalyst mixture was stirred for 10 min at 21 °C. A dry/degassed 1,3-butadiene solution in toluene at -78°C (3.63 mL, 1 g, 18.5 mmol, 1697 equiv., resulting monomer conc. 2.25 M) was injected rapidly, the Schlenk flask was sealed tightly immediately and the reaction was stirred at 21 °C for 67 min. The Schlenk flask was opened under inert conditions and let age for 33 min. The reaction mixture was diluted with toluene (15 mL) and filtrated through a short pad of celite. The filtrate was quenched with. a 1 : 5 hydrochloric acid/methanol solution (15 mL). The resulting precipitate was washed with methanol (15 mL) and dried under vacuum. Yield: 115.4 mg.

**5.3 Co-MFU-4*l* Leaching Experiments.**

**After filtration of Polymer Reaction Mixture.** MMAO-12 (0.5 mL, 1.16 mmol, 106 equiv., as a 7 wt% Al solution in toluene) was added to a suspension of $Co_4ZnCl_4(BTDD)_3$ (3.4 mg, 10.9 $\mu$mol Co, 1 equiv.) in dry toluene (4.08 mL) in a flame dried 50 mL Schlenk flask with a J Young valve. The catalyst/cocatalyst mixture was stirred for 10 min at 21 °C. A dry/degassed 1,3-butadiene solution in toluene at -78 °C (3.63 mL, 1 g, 18.5 mmol, 1697 equiv., resulting monomer conc. 2.25 M) was injected rapidly, the Schlenk flask was sealed tightly immediately and the reaction was stirred at 21 °C for 90 min. The reaction mixture was diluted with toluene (15 mL) and filtered through a short pad of celite. The solvent was removed from the colorless filtrate *in vacuo*. The resulting solid was sonicated for 1 h in ICP-grade conc. nitric acid (5 mL). 1 mL of this solution was diluted 20 times and the resulting cobalt concentration was

determined via ICP-MS. Resulting cobalt concentration = 160 ppb. This corresponds to a max. 0.94 % cobalt leaching. Fe internal standard: calc. 100 ppb, found 160 ppb.

**$Co_4ZnCl_4(BTDD)_3$ after Treatment with MMAO.** In a glovebox, MMAO-12 (0.5 ml, 1.16 mmol, 106 equiv. as a 7 w% solution Al in toluene) was added to a solution of $Co_4ZnCl_4(BTDD)_3$ (3.4 mg, 10.9 $\mu$mol Co) in dry toluene (5 mL) in a 20 mL vial. The sealed vial was stirred for 1 h at 21 °C. The suspension was filtrated through a 0.2 $\mu$m Teflon filter. The filtrate was added to a flame dried 50 mL Schlenk flask with a J Young valve. A dry/degassed 1,3-butadiene solution in toluene at -78 °C (3.63 mL, 1 g, 18.5 mmol, 1697 equiv., resulting monomer conc. 2.0 M) was injected rapidly, the Schlenk flask was sealed tightly immediately and the reaction was stirred at 21 °C for 4 h. The reaction mixture was quenched with. a 1 : 5 hydrochloric acid/methanol solution (25 mL) and no precipitate was observed. The solvent was removed from the colorless filtrate *in vacuo*. The resulting solid (12 mg, trace polymer, mostly aluminum oxide) was sonicated for 1 h in ICP-grade conc. nitric acid (5 mL). 1 mL of this solution was diluted 20 times and the resulting cobalt concentration was determined via ICP-MS. Resulting cobalt concentration = 23 ppb. This corresponds to a max. 0.35 % cobalt leaching. Fe internal standard: calc. 100 ppb, found 174 ppb.

## 5.4 Heterogeneity of $CoCl_2$ / MMAO-12

In a nitrogen glovebox, a vial (A) was charged with $CoCl_2$ (1.4 mg, 10.8 $\mu$mol), MMAO-12 (0.5 ml, 1.16 mmol, 106 equiv. as a 7 w% solution Al in toluene), and toluene (4.5 mL). As control, a second vial (B) was charged with $CoCl_2$ and toluene only. The two vials were stirred for one hour. Vial A was observed to form a homogeneous olive-green solution in a matter of minutes, while the mixture in vial B remained a bluish suspension. Both mixtures were filtered through 0.45 $\mu$m Supor filters. The filtered solution from vial A remained olive in color. This filtrate was quenched with methanol and then concentrated in vacuo. The resulting light blue solid was found to contain 23.22% Al and 0.46% Co (molar ratio of 110 : 1), consistent with complete dissolution of $CoCl_2$. By contrast, filtration of the sample in vial B afforded a clear, colorless toluene solution.

Thus, $CoCl_2$ is a homogeneous catalyst in the presence of alkaluminum reagents, whereas our material is a robust solid with no detectable "leaching" of active Co species.

## 6. Analytical Data for Polyolefin Products.

### 6.1 Fourier transformed infrared spectra and nuclear magnetic resonance spectra.

### Typical IR Spectrum of cis-1,4-polybutadiene Produced with Co-MFU-4*l* at 21 °C.

IR (Ge-ATR): $\tilde{v}$= 995 (1,2-vinyl, w), 965 (1,4-trans, w), 910 (1,2-vinyl, w), 735 cm$^{-1}$ (1,4-cis, s).[9] Possible interferences with residual Co-MFU-4*l* IR (Ge-ATR): $\tilde{v}$=3078 (w), 1576 (w), 1460 (s), 1351(s), 1239 (w), 1220 (m), 1204 (m), 1173 (s), 919 (m), 869 (m), 818 (w), 533 cm$^{-1}$ (m).
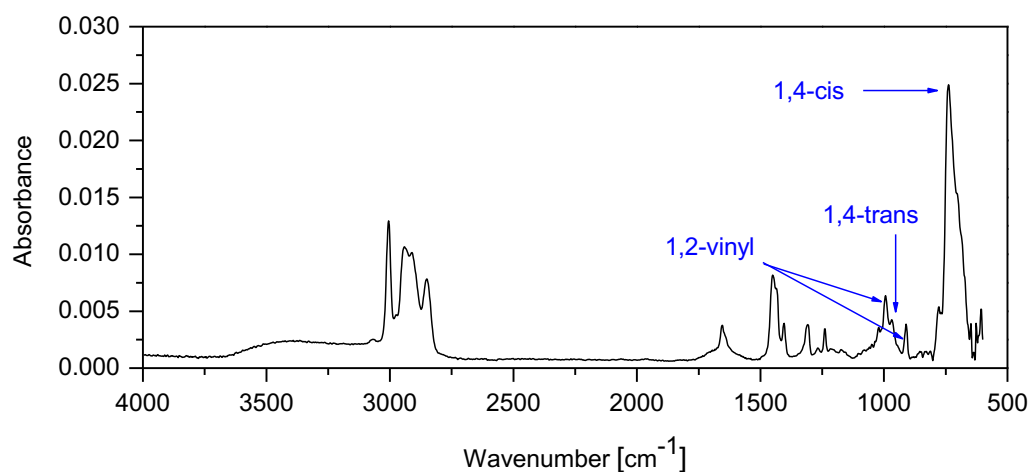


**Figure S6.1.** Ge-ATR IR-spectrum of cis-1,4-polybutadiene produced at 21 °C with Co-MFU-4*l*.

## Typical ¹H-NMR Spectrum of cis-1,4-polybutadiene Produced with Co-MFU-4*l* at 21 °C.

¹H NMR (500 MHz, CDCl₃) δ 5.58 (-C*H*=CH₂, 1,2-vinyl), 5.38 (-C*H*=, 1,4-cis/trans), 4.98 (-CH=C*H*₂, 1,2-vinyl), 2.09 (-C*H*₂-, 1,4-cis/trans), 1.96 (-C*H*₂-, 1,2-vinyl) 1.45 (-C*H*, 1,2-vinyl).
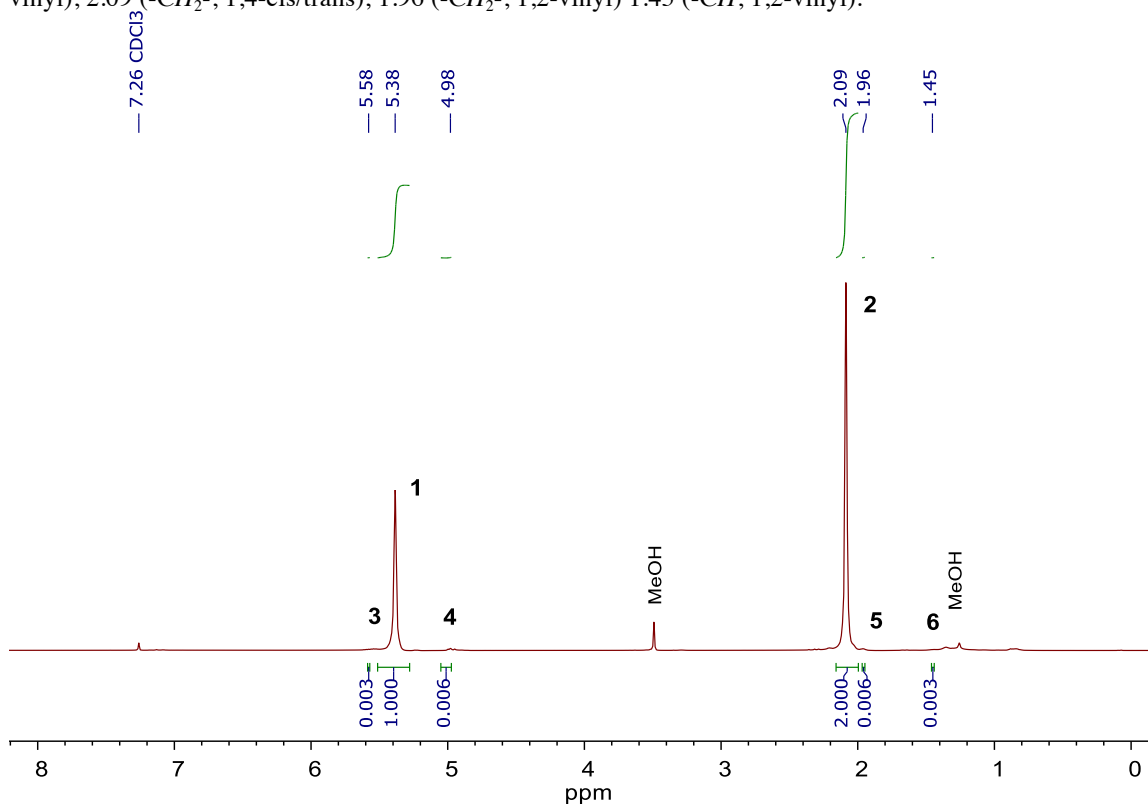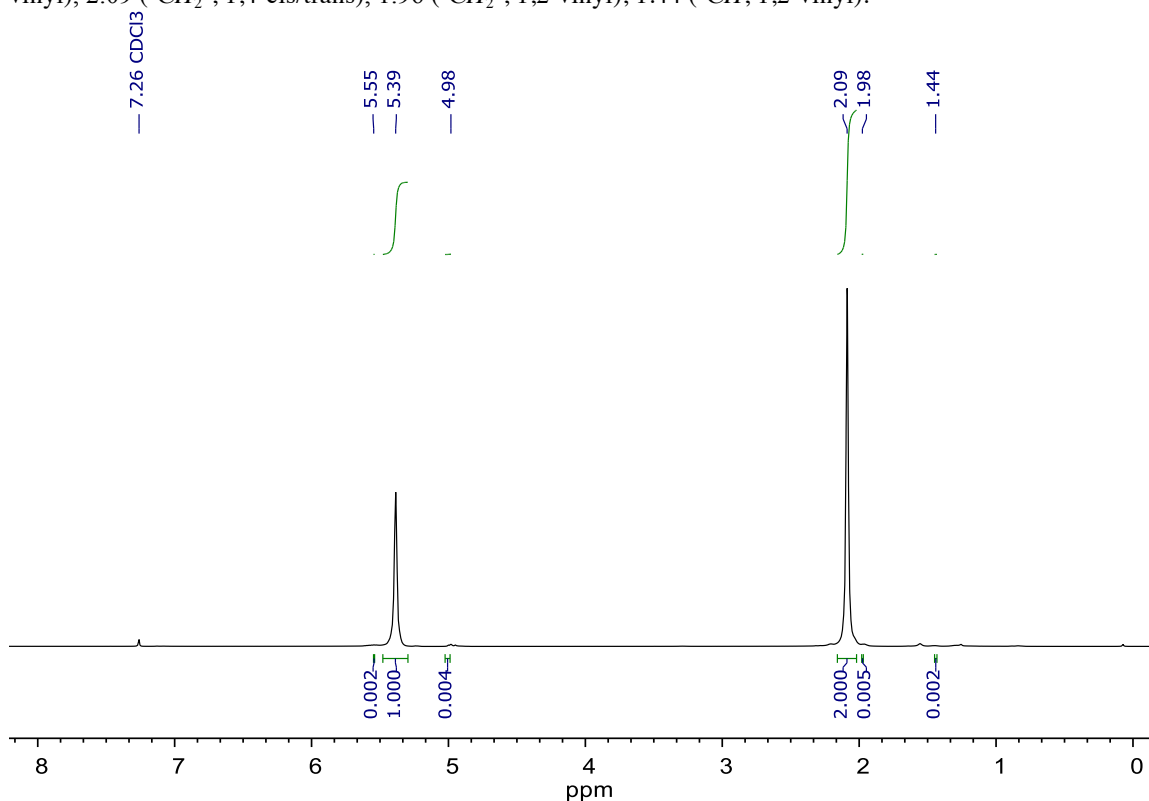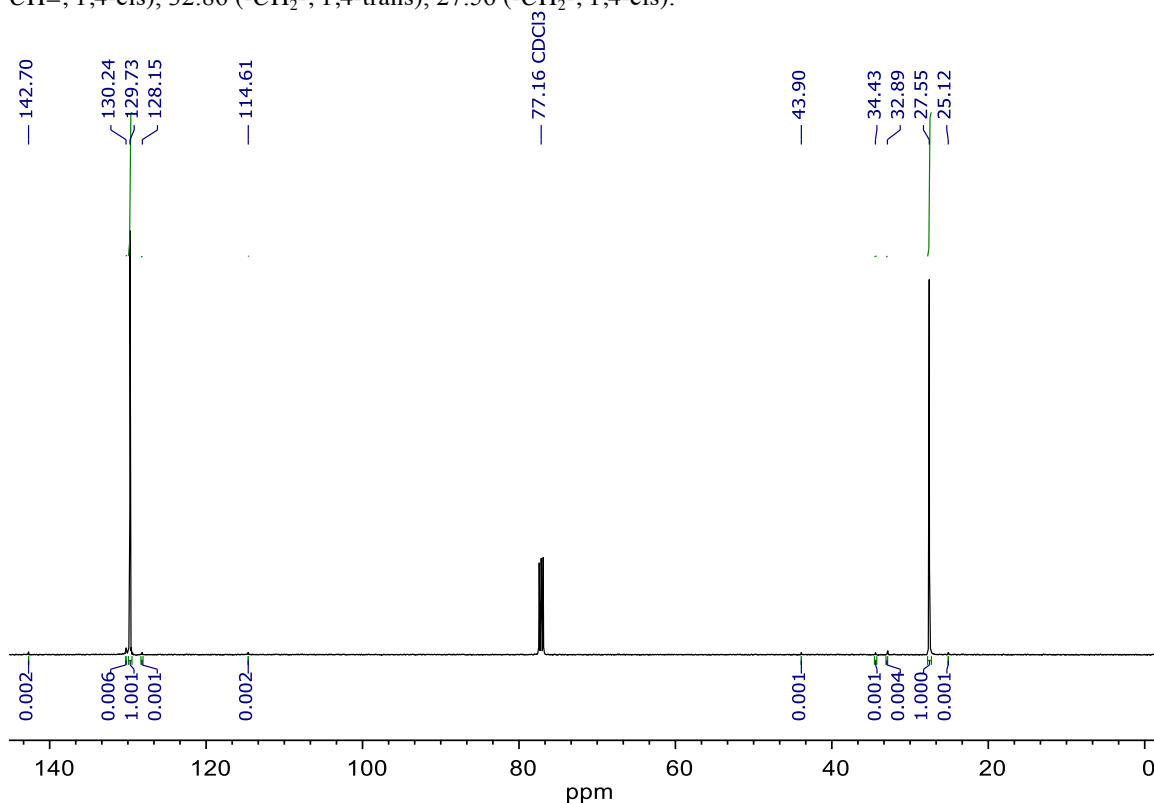


**Figure S6.2.** ¹H-NMR-spectrum of cis-1,4-polybutadiene produced at 21 °C with Co-MFU-4*l*. This S/N ratio could be obtained after removal of the catalyst. Here [BD₀] = 3.5 M, Al/Co = 116, 21 °C, 2 h.
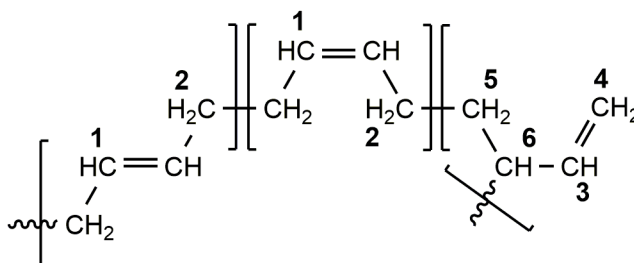


**Figure S6.3.** Schematic representation of all possible stereoisomers of polybutadiene and assignment of the observed protons.

## Typical $^{13}$C-NMR Spectrum of cis-1,4-polybutadiene Produced with Co-MFU-4*l* at 21 °C.

Quantitative $^{13}$C NMR (126 MHz, CDCl$_3$, relaxation delay = 5 s) δ 142.70 (-*CH*=CH$_2$, 1,2-vinyl), 130.24 (-*CH*=, 1,4-trans), 129.73 (-*CH*=, 1,4-cis), 128.16 (-*CH*-, 1,2-vinyl), 114.60 (-CH=*CH*$_2$, 1,2-vinyl), 43.89(-*CH*-, 1,2-vinyl), 34.42 (-*CH*$_2$-, 1,2-vinyl), 32.89 (-*CH*$_2$-, 1,4-trans), 27.54 (-*CH*$_2$-, 1,4-cis), 25.12 (-*CH*$_2$-, 1,2-vinyl).
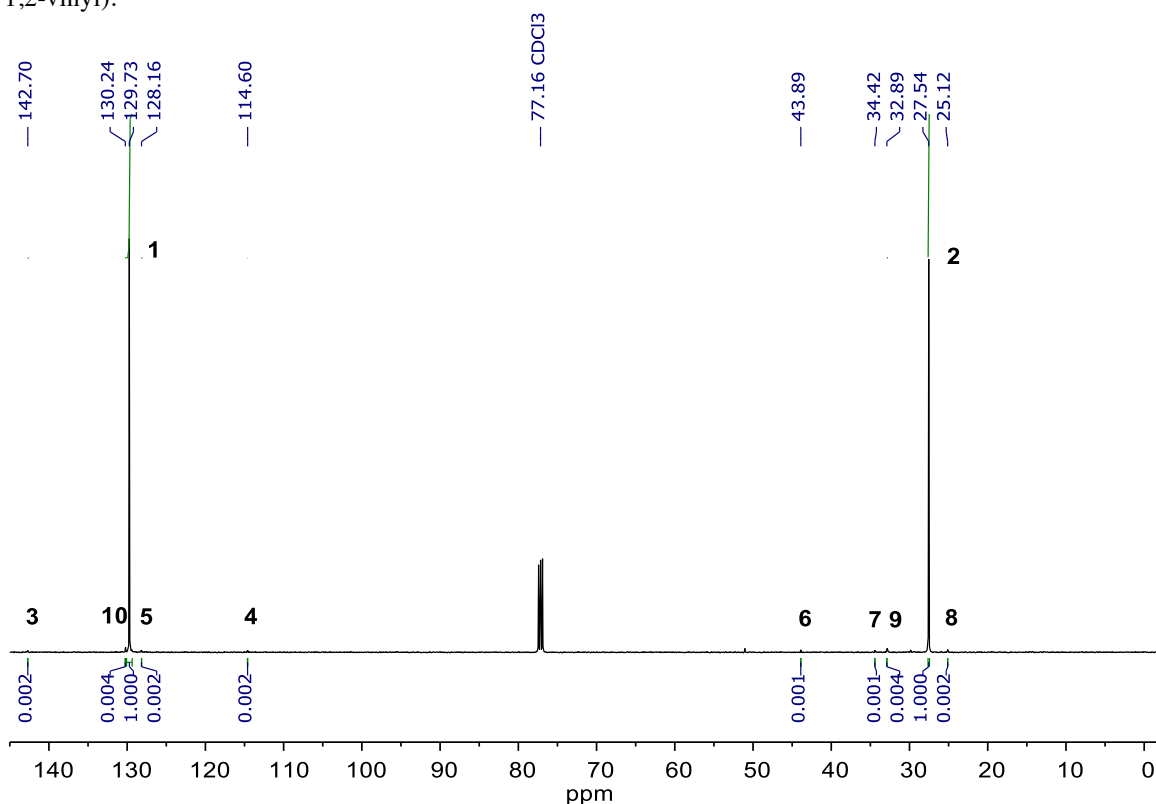


**Figure S6.4.** $^{13}$C-NMR-spectrum of cis-1,4-polybutadiene produced at 21 °C with Co-MFU-4*l*. This S/N ratio could be obtained after removal of the catalyst through the "hot filtration procedure". Quantitative $^{13}$C NMR, 5 s relaxation delay, 1024 scans. Here [BD$_0$] = 3.5 M, Al/Co = 116, 21 °C, 2 h.
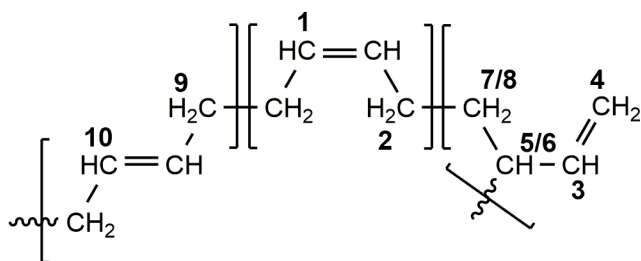


**Figure S6.5.** Schematic representation of all possible stereoisomers of polybutadiene and assignment of the observed carbon resonances.

## IR Spectrum of cis-1,4-polybutadiene Produced with Co-MFU-4*l* at 0 °C.

IR (Ge-ATR): $\tilde{v}$= 995 (1,2-vinyl, w), 965 (1,4-trans, w), 910 (1,2-vinyl, w), 735 cm$^{-1}$ (1,4-cis, s). Possible interferences with residual Co-MFU-4*l* IR (Ge-ATR): $\tilde{v}$=3078 (w), 1576 (w), 1460 (s), 1351(s), 1239 (w), 1220 (m), 1204 (m), 1173 (s), 919 (m), 869 (m), 818 (w), 533 cm$^{-1}$ (m).
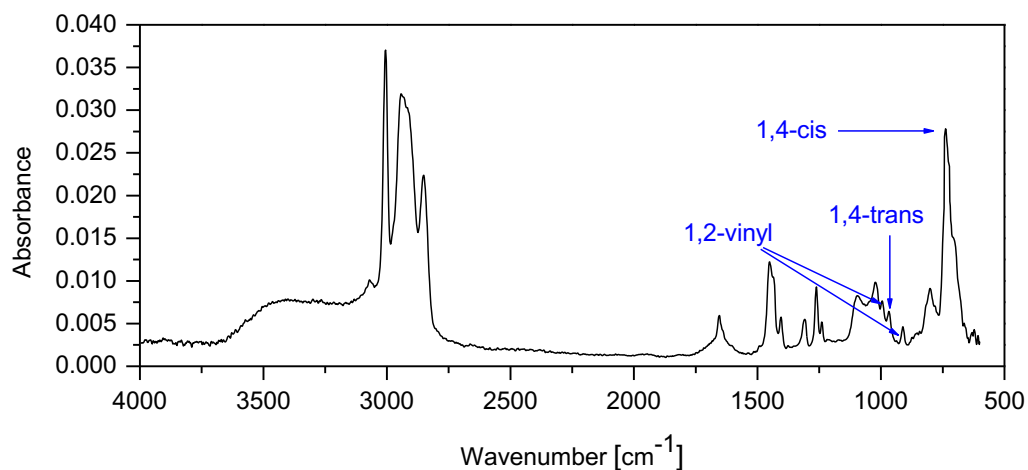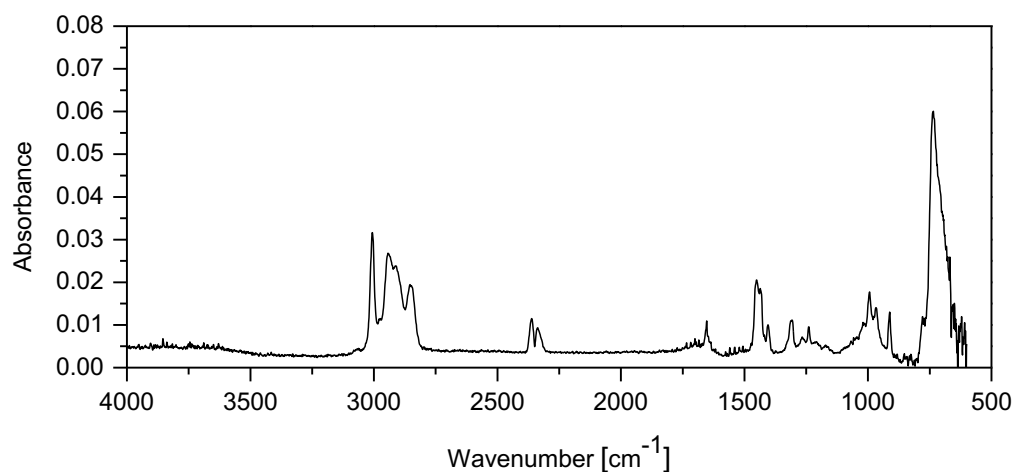


**Figure S6.6.** Ge-ATR IR-spectrum of cis-1,4-polybutadiene produced at 0 °C with Co-MFU-4*l*.

## ¹H-NMR Spectrum of cis-1,4-polybutadiene Produced with Co-MFU-4*l* at 0 °C.

¹H NMR (500 MHz, CDCl₃) δ 5.57 (-C$H$=CH₂, 1,2-vinyl), 5.38 (-C$H$=, 1,4-cis/trans), 4.98 (-CH=C$H$₂, 1,2-vinyl), 2.09 (-C$H$₂-, 1,4-cis/trans), 1.96 (-C$H$₂-, 1,2-vinyl), 1.44 (-C$H$, 1,2-vinyl).
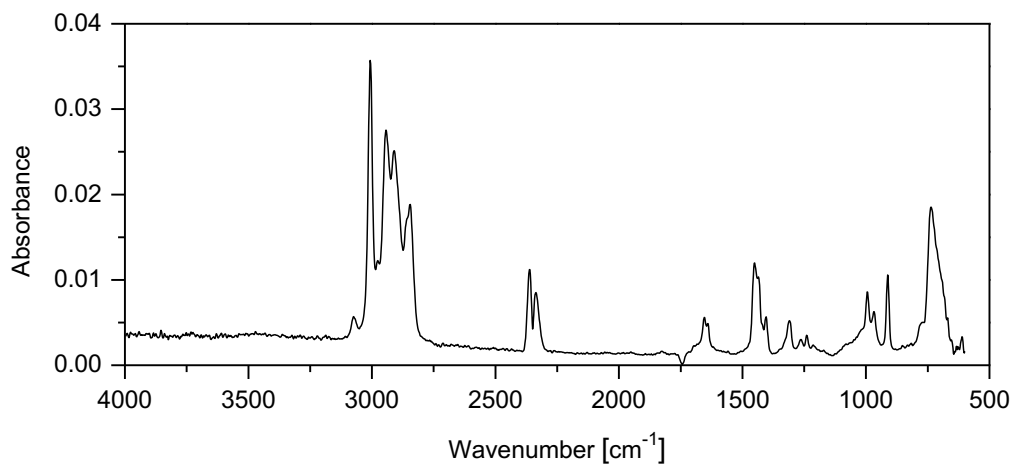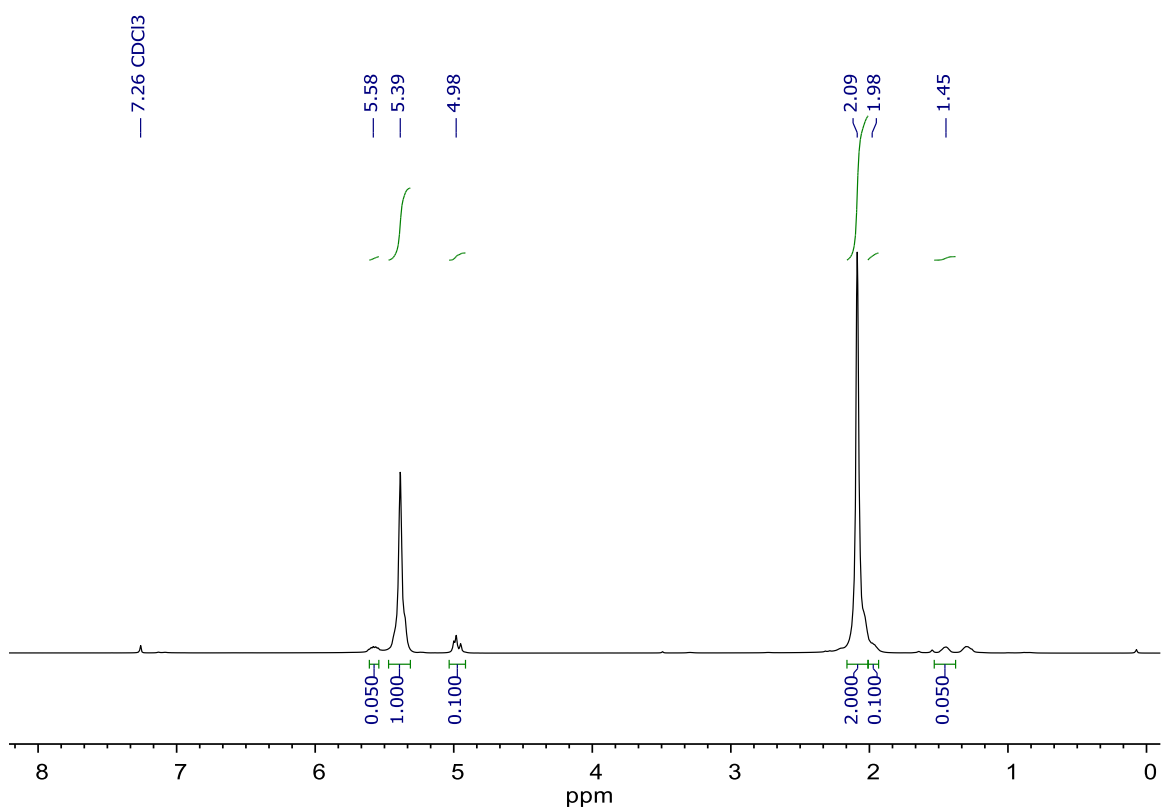


**Figure S6.7.** ¹H-NMR-spectrum of cis-1,4-polybutadiene produced at 0 °C with Co-MFU-4*l*. Spectrum obtained after the "hot-filtration" method. 64 scans.

# $^{13}$C-NMR Spectrum of cis-1,4-polybutadiene Produced with Co-MFU-4*l* at 0 °C.

Quantitative $^{13}$C NMR (126 MHz, CDCl$_3$, relaxation delay = 5 s) δ 130.25 (-*C*H=, 1,4-trans), 129.74 (-*C*H=, 1,4-cis), 32.86 (-*C*H$_2$-, 1,4-trans), 27.56 (-*C*H$_2$-, 1,4-cis).



**Figure S6.8.** $^{13}$C-NMR-spectrum of cis-1,4-polybutadiene produced at 0 °C with Co-MFU-4*l*. This S/N ratio was obtained after removal of the catalyst through the "hot-filtration" procedure. Quantitative $^{13}$C, 5 s relaxation delay, 2048 scans.

## IR Spectrum of cis-1,4-polybutadiene Produced with Ni-MFU-4*l* at 21°C.

IR (Ge-ATR): $\tilde{v}$= 995 (1,2-vinyl, w), 965 (1,4-trans, w), 910 (1,2-vinyl, w), 735 cm$^{-1}$ (1,4-cis, s). Possible interferences with residual Co-MFU-4*l* IR (Ge-ATR): $\tilde{v}$=3078 (w), 1576 (w), 1460 (s), 1351(s), 1239 (w), 1220 (m), 1204 (m), 1173 (s), 919 (m), 869 (m), 818 (w), 533 cm$^{-1}$ (m).



**Figure S6.9.** Ge-ATR IR-spectrum of cis-1,4-polybutadiene produced at 21 °C with Ni-MFU-4*l*.

## [1]H Spectrum of cis-1,4-polybutadiene Produced with Ni-MFU-4*l* at 21°C.

^{1}H NMR (500 MHz, CDCl$_3$) δ 5.58 (-C*H*=CH$_2$, 1,2-vinyl), 5.39 (-C*H*=, 1,4-cis/trans), 4.98 (-CH=C*H*$_2$, 1,2-vinyl), 2.09 (-C*H*$_2$-, 1,4-cis/trans), 1.96 (-C*H*$_2$-, 1,2-vinyl), 1.45 (-C*H*, 1,2-vinyl).
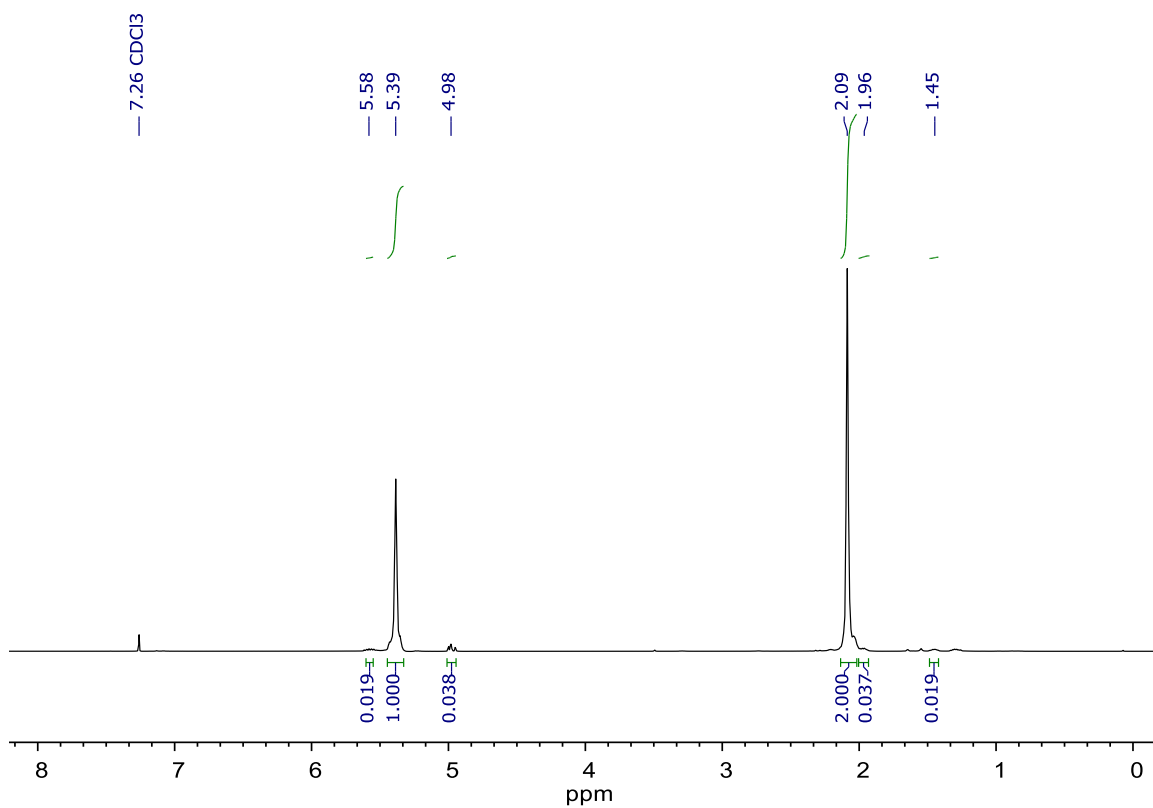


**Figure S6.10.** ^{1}H-NMR-spectrum of cis-1,4-polybutadiene produced at 21 °C with Ni-MFU-4*l*. 64 scans.

## $^{13}$C-NMR Spectrum of cis-1,4-polybutadiene Produced with Ni-MFU-4*l* at 21 °C.

Quantitative $^{13}$C NMR (126 MHz, CDCl$_3$, relaxation delay = 5 s) δ 142.70 (-*C*H=CH$_2$, 1,2-vinyl), 130.24 (-*C*H=, 1,4-trans), 129.73 (-*C*H=, 1,4-cis), 128.16 (-*C*H-, 1,2-vinyl), 114.60 (-CH=*C*H$_2$, 1,2-vinyl), 43.89(-*C*H-, 1,2-vinyl), 34.42 (-*C*H$_2$-, 1,2-vinyl), 32.89 (-*C*H$_2$-, 1,4-trans), 27.54 (-*C*H$_2$-, 1,4-cis), 25.12 (-*C*H$_2$-, 1,2-vinyl).
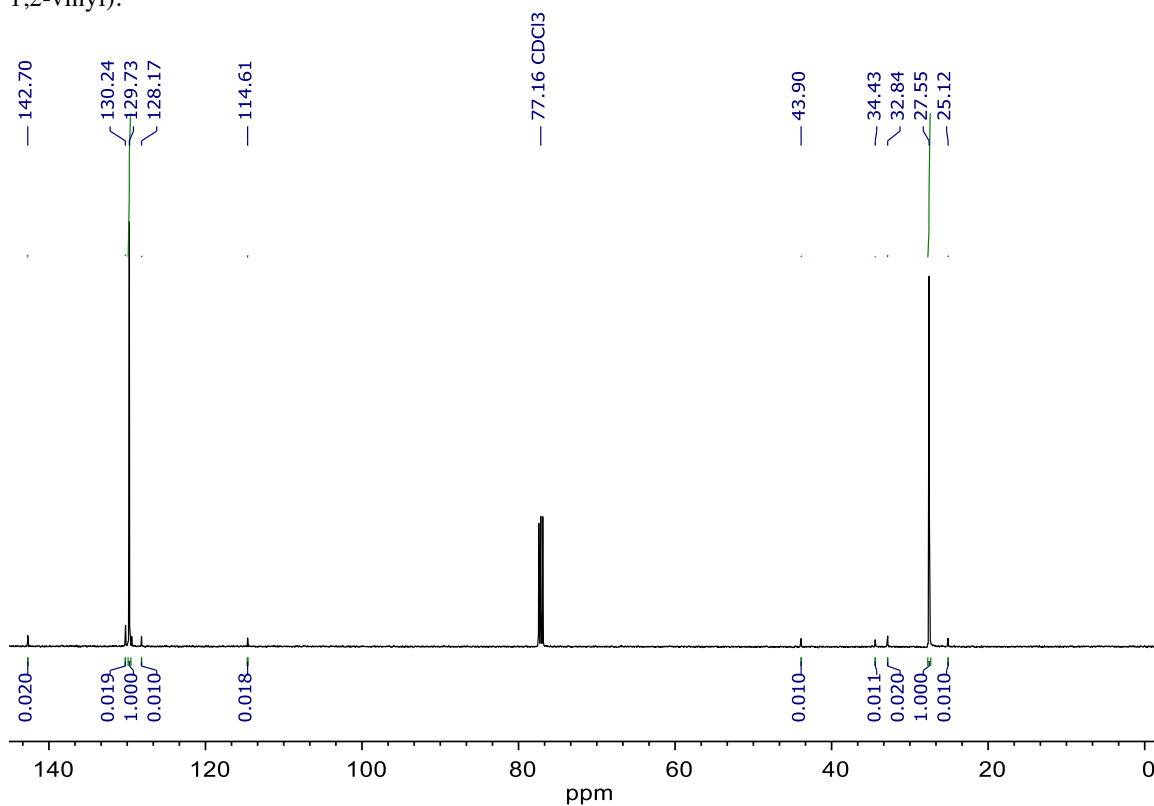


**Figure S6.11.** $^{13}$C-NMR-spectrum of cis-1,4-polybutadiene produced at 21 °C with Ni-MFU-4*l*. Quantitative $^{13}$C, 5 s relaxation delay, 1024 scans.

# IR Spectrum of cis-1,4-polybutadiene Produced with Co-MFU-4*l* and Et$_2$AlCl at 21°C.

IR (Ge-ATR): $\tilde{v}$= 995 (1,2-vinyl, w), 965 (1,4-trans, w), 910 (1,2-vinyl, w), 735 cm$^{-1}$ (1,4-cis, s).



**Figure S6.12.** Ge-ATR IR-spectrum of cis-1,4-polybutadiene produced at 21 °C with Co-MFU-4*l* and Et$_2$AlCl.

# $^1$H-NMR Spectrum of cis-1,4-polybutadiene Produced with Co-MFU-4*l* and Et$_2$AlCl at 21 °C.

$^1$H NMR (500 MHz, CDCl$_3$) δ 5.58 (-C$H$=CH$_2$, 1,2-vinyl), 5.39 (-C$H$=, 1,4-cis/trans), 4.98 (-CH=C$H_2$, 1,2-vinyl), 2.09 (-C$H_2$-, 1,4-cis/trans), 1.98 (-C$H_2$-, 1,2-vinyl), 1.45 (-C$H$, 1,2-vinyl).



**Figure S6.13.** $^1$H-NMR-spectrum of cis-1,4-polybutadiene produced at 21 °C with Co-MFU-4*l* and Et$_2$AlCl. 64 scans.

## ^{13}C-NMR Spectrum of cis-1,4-polybutadiene Produced with Co-MFU-4*l* and Et₂AlCl at 21 °C.

Quantitative ^{13}C NMR (126 MHz, CDCl₃, relaxation delay = 5 s) δ 142.71 (-CH=CH₂, 1,2-vinyl), 130.25 (-CH=, 1,4-trans), 129.74 (-CH=, 1,4-cis), 114.59 (-CH=CH₂, 1,2-vinyl), 43.90(-CH-, 1,2-vinyl), 34.44 (-CH₂-, 1,2-vinyl), 32.84 (-CH₂-, 1,4-trans), 27.55 (-CH₂-, 1,4-cis), 25.13 (-CH₂-, 1,2-vinyl).
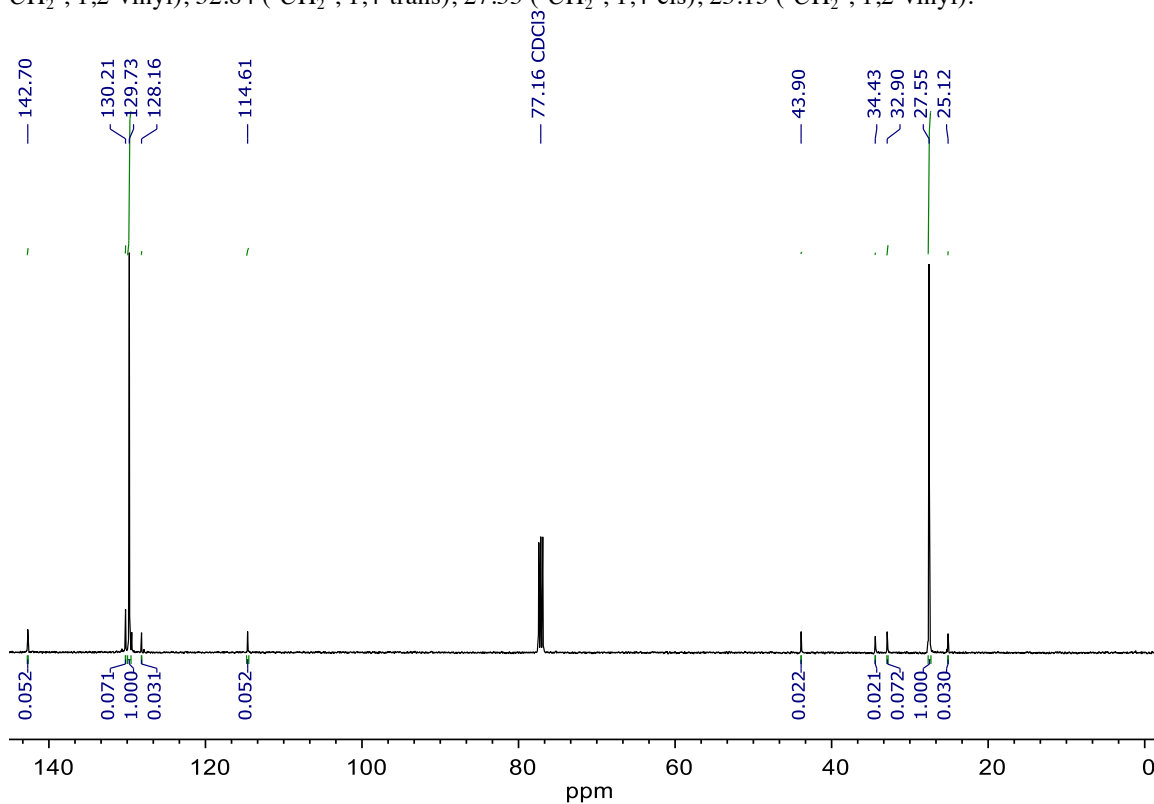


**Figure S6.14.** ^{13}C-NMR-spectrum of cis-1,4-polybutadiene produced at 21 °C with Co-MFU-4*l* and Et₂AlCl. Quantitative ^{13}C, 5 s relaxation delay, 1024 scans.

## IR Spectrum of polybutadiene produced with Ti(IV)-MFU-4*l*

IR (Ge-ATR): $\tilde{\nu}$= 995 (1,2-vinyl, w), 965 (1,4-trans, w), 910 (1,2-vinyl, w), 735 cm$^{-1}$ (1,4-cis, s).
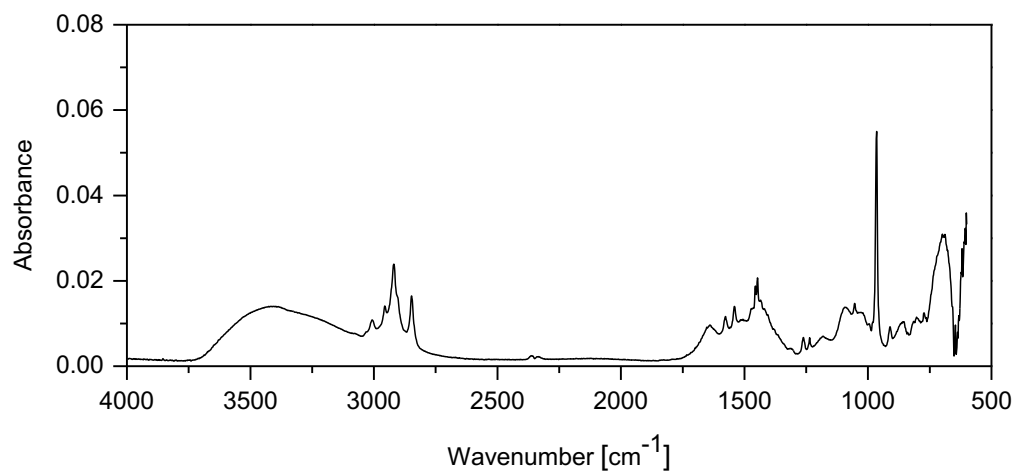


**Figure S6.15.** Ge-ATR IR-spectrum of polybutadiene produced at 21 °C with Ti(IV)-MFU-4*l*.

# ¹H NMR Spectrum of polybutadiene produced with Ti(IV)-MFU-4*l*

¹H NMR (500 MHz, CDCl₃) δ 5.56 (-C$H$=CH₂, 1,2-vinyl), 5.41 (-C$H$=, 1,4-cis/trans), 4.98 (-CH=C$H_2$, 1,2-vinyl), 2.08 (-C$H_2$-, 1,4-cis/trans), 1.97 (-C$H_2$-, 1,2-vinyl), 1.44 (-C$H$, 1,2-vinyl).
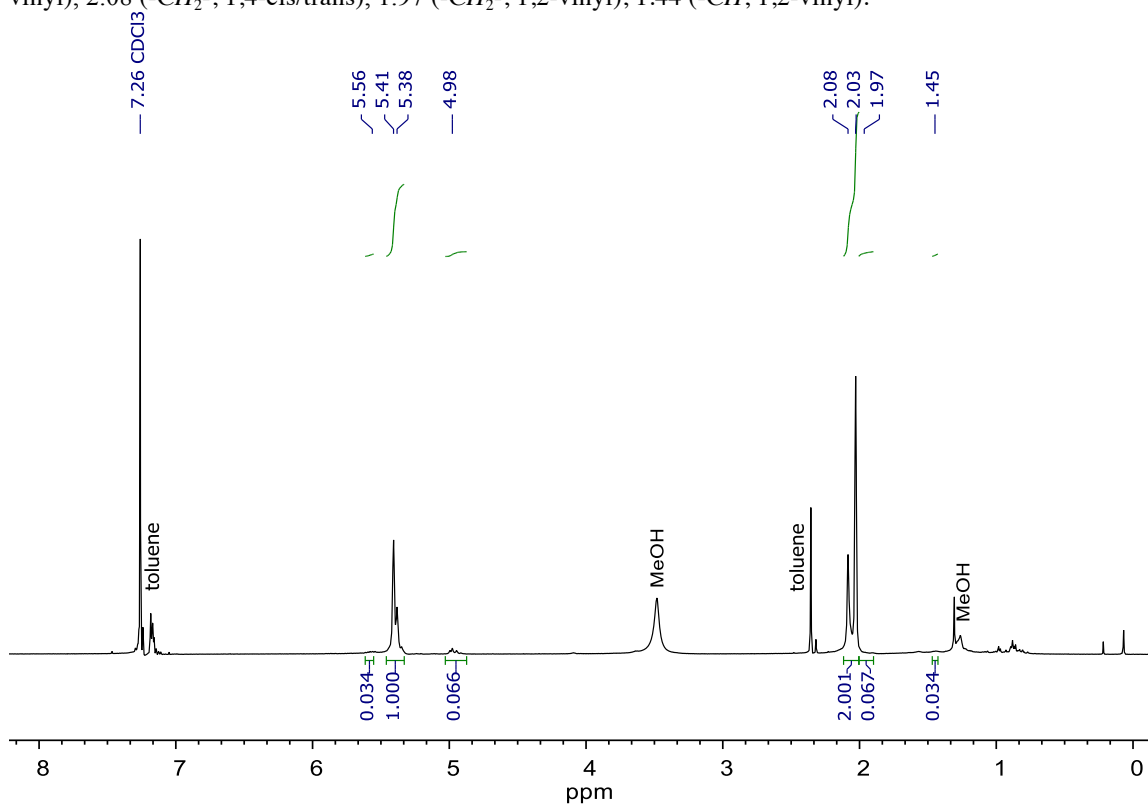


**Figure S6.16.** ¹H-NMR-spectrum of polybutadiene produced at 21 °C with Ti(IV)-MFU-4*l*. 64 scans.

## $^{13}$C NMR Spectrum of polybutadiene produced with Ti(IV)-MFU-4*l*

Quantitative $^{13}$C NMR (126 MHz, CDCl$_3$, relaxation delay = 5 s) δ 130.16 (-*C*H=, 1,4-trans), 129.74 (-*C*H=, 1,4-cis), 32.88 (-*C*H$_2$-, 1,4-trans), 27.56 (-*C*H$_2$-, 1,4-cis).
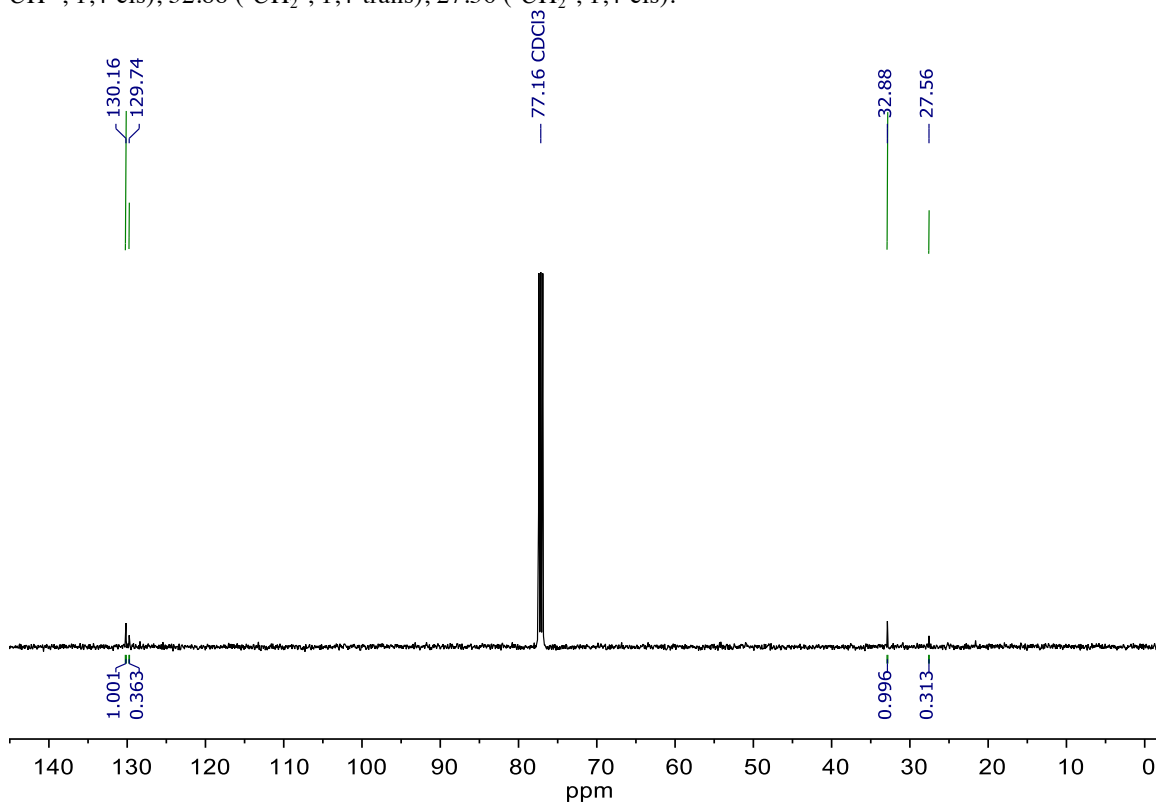


**Figure S6.17.** $^{13}$C-NMR-spectrum of polybutadiene produced at 21 °C with Ti(IV)-MFU-4*l*. Quantitative $^{13}$C, 5 s relaxation delay, 1024 scans.

## IR Spectrum of polybutadiene produced with Cr(III)-MFU-4*l*

IR (Ge-ATR): $\tilde{v}$= 995 (1,2-vinyl, w), 965 (1,4-trans, w), 910 (1,2-vinyl, w), 735 cm$^{-1}$ (1,4-cis, s).
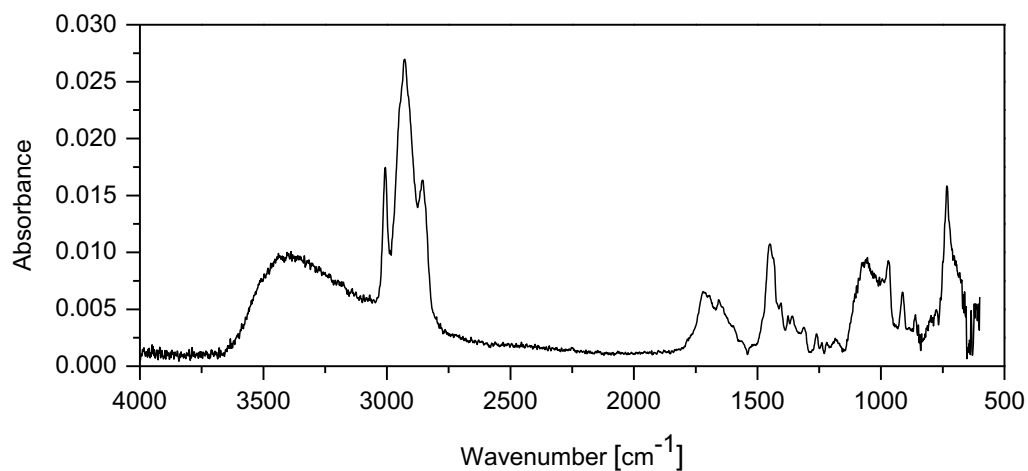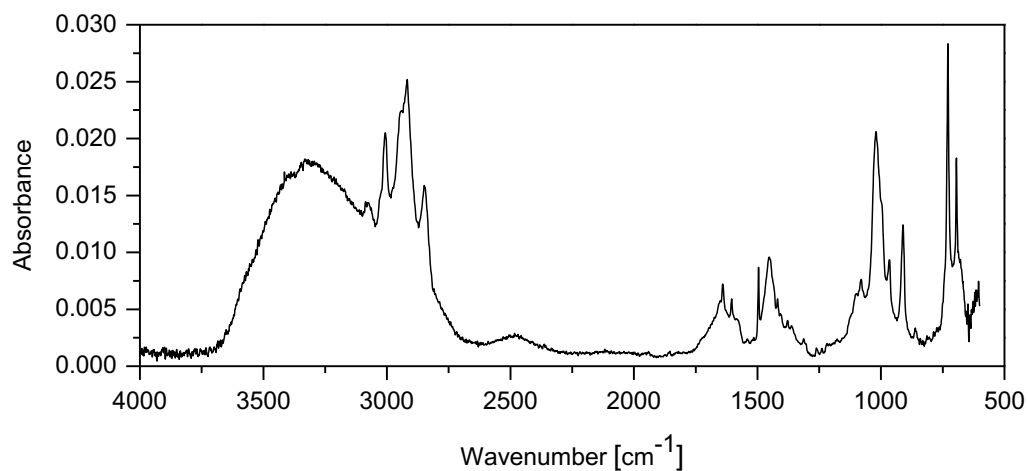


**Figure S6.18.** Ge-ATR IR-spectrum of cis-1,4 polybutadiene produced at 21 °C with Cr(III)-MFU-4*l*.

# <sup>1</sup>H NMR Spectrum of polybutadiene produced with Cr(III)-MFU-4*l*

[^1]H NMR (500 MHz, CDCl₃) δ 5.58 (-C*H*=CH₂, 1,2-vinyl), 5.39 (-C*H*=, 1,4-cis/trans), 4.98 (-CH=C*H₂*, 1,2-vinyl), 2.09 (-C*H₂*-, 1,4-cis/trans), 1.97 (-C*H₂*-, 1,2-vinyl), 1.46 (-C*H*, 1,2-vinyl).
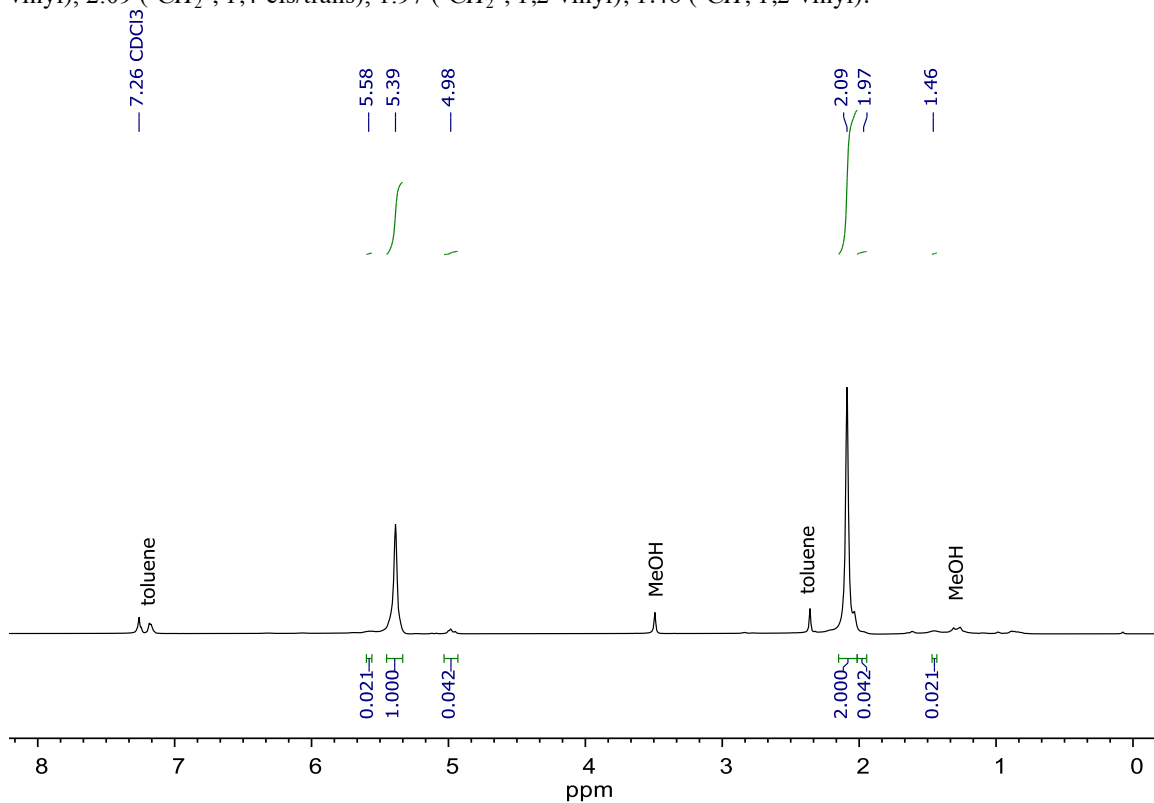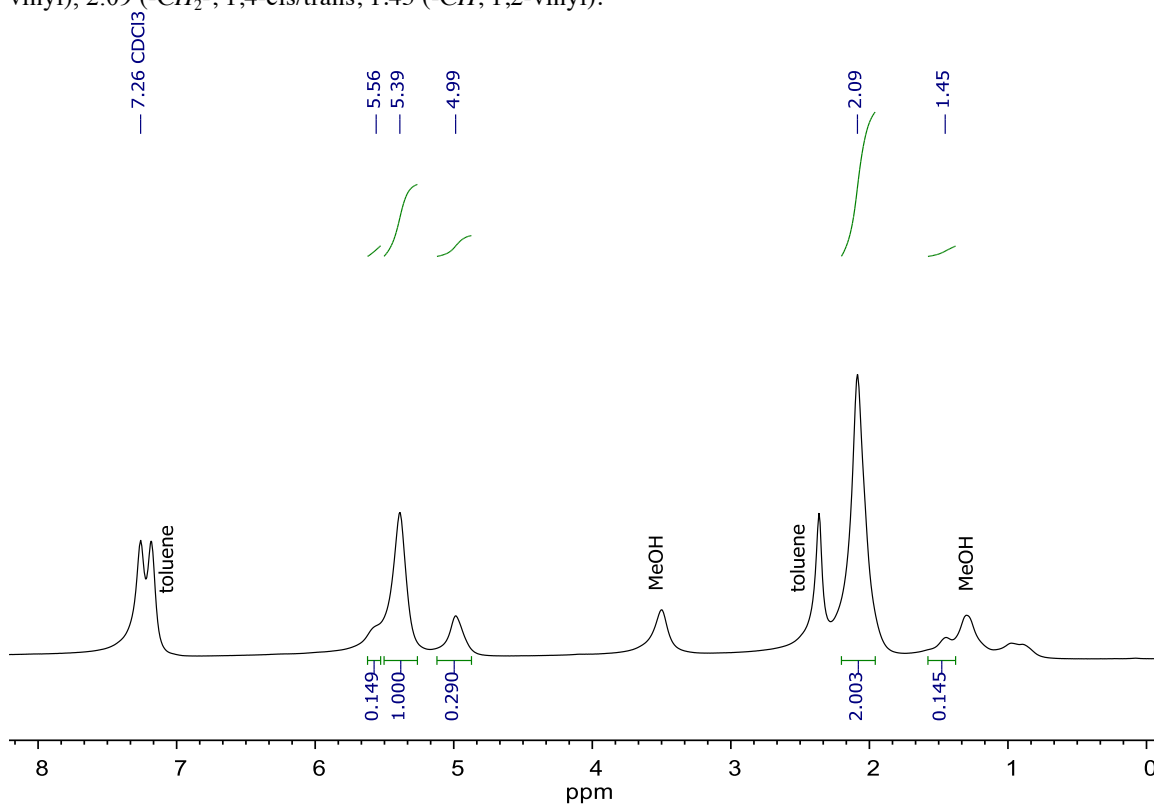


**Figure S6.19.** [^1]H-NMR-spectrum of cis-1,4 polybutadiene produced at 21 °C with Cr(III)-MFU-4*l*.

## ¹³C NMR Spectrum of polybutadiene produced with Cr(III)-MFU-4*l*

Quantitative ¹³C NMR (126 MHz, CDCl₃, relaxation delay = 5 s) δ 142.71 (-$CH$=CH₂, 1,2-vinyl), 130.25 (-$CH$=, 1,4-trans), 129.74 (-$CH$=, 1,4-cis), 114.59 (-CH=$CH_2$, 1,2-vinyl), 43.90(-$CH$-, 1,2-vinyl), 34.44 (-$CH_2$-, 1,2-vinyl), 32.84 (-$CH_2$-, 1,4-trans), 27.55 (-$CH_2$-, 1,4-cis), 25.13 (-$CH_2$-, 1,2-vinyl).
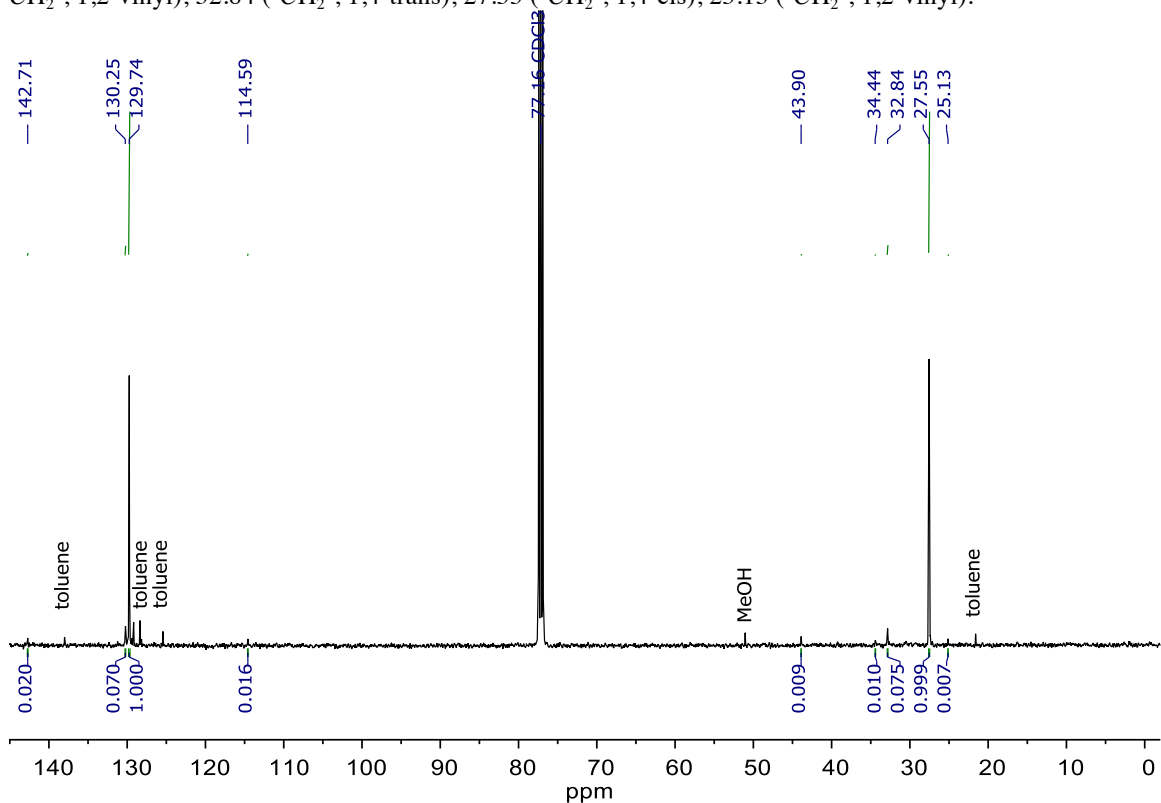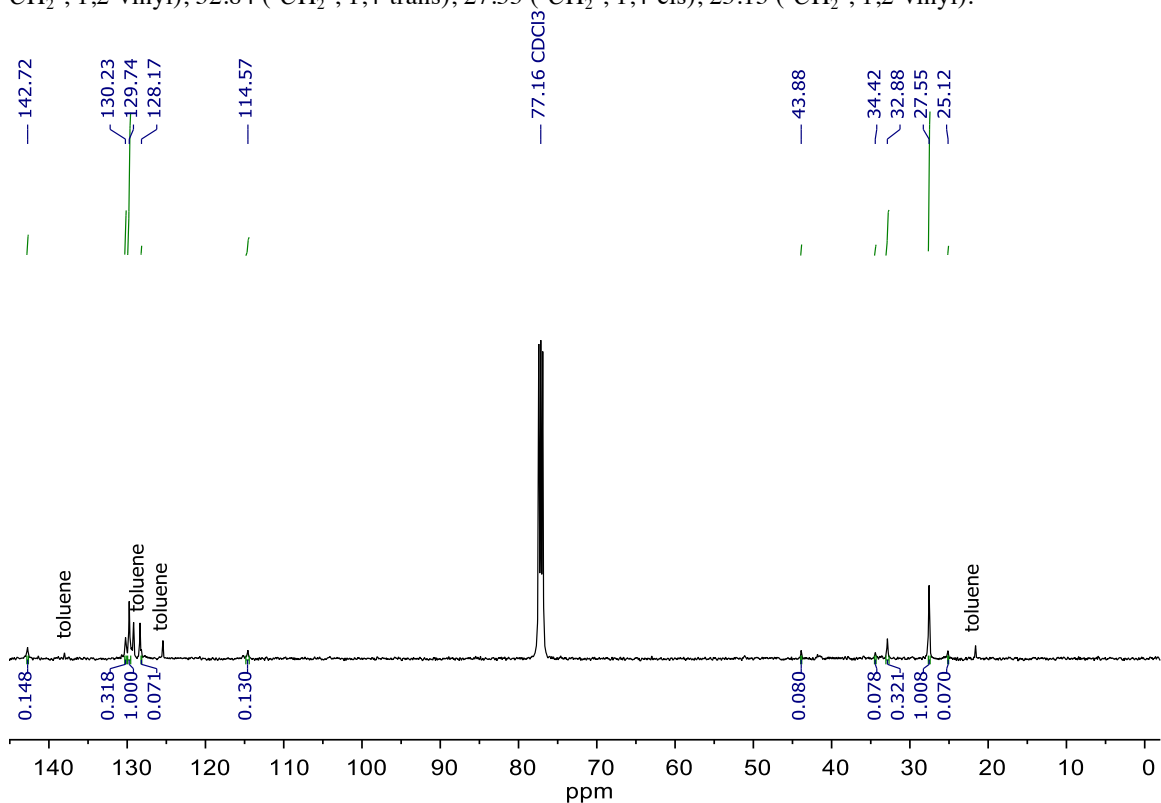


**Figure S6.20.** ¹³C-NMR-spectrum of cis-1,4 polybutadiene produced at 21 °C with Cr(III)-MFU-4*l*.

## IR Spectrum of polybutadiene produced with Fe(II)-MFU-4*l*

IR (Ge-ATR): $\tilde{v}$= 995 (1,2-vinyl, w), 965 (1,4-trans, w), 910 (1,2-vinyl, w), 735 cm$^{-1}$ (1,4-cis, s).

**Figure S6.21.** Ge-ATR IR-spectrum of polybutadiene produced at 21 °C with Fe(II)-MFU-4*l*.

# ¹H NMR Spectrum of polybutadiene produced with Fe(II)-MFU-4*l*

¹H NMR (500 MHz, CDCl₃) δ 5.56 (-C*H*=CH₂, 1,2-vinyl), 5.39 (-C*H*=, 1,4-cis/trans), 4.99 (-CH=C*H₂*, 1,2-vinyl), 2.09 (-C*H₂*-, 1,4-cis/trans, 1.45 (-C*H*, 1,2-vinyl).



**Figure S6.22.** ¹H-NMR-spectrum of cis-1,4 polybutadiene produced at 21 °C with Fe(II)-MFU-4*l*. 64 scans.

## $^{13}$C NMR Spectrum of polybutadiene produced with Fe(II)-MFU-4*l*

Quantitative $^{13}$C NMR (126 MHz, CDCl$_3$, relaxation delay = 5 s) δ 142.71 (-$CH$=CH$_2$, 1,2-vinyl), 130.25 (-$CH$=, 1,4-trans), 129.74 (-$CH$=, 1,4-cis), 114.59 (-CH=$CH_2$, 1,2-vinyl), 43.90(-$CH$-, 1,2-vinyl), 34.44 (-$CH_2$-, 1,2-vinyl), 32.84 (-$CH_2$-, 1,4-trans), 27.55 (-$CH_2$-, 1,4-cis), 25.13 (-$CH_2$-, 1,2-vinyl).



**Figure S6.23.** $^{13}$C-NMR-spectrum of cis-1,4 polybutadiene produced at 21 °C with Fe(II)-MFU-4*l*. Quantitative $^{13}$C, 5 s relaxation delay.

## IR Spectrum of cis-1,4-polybutadiene Produced with Tp^Mes^NiCl at 21°C.

IR (Ge-ATR): $\tilde{\nu}$= 995 (1,2-vinyl, w), 965 (1,4-trans, w), 910 (1,2-vinyl, w), 735 cm$^{-1}$ (1,4-cis, s).
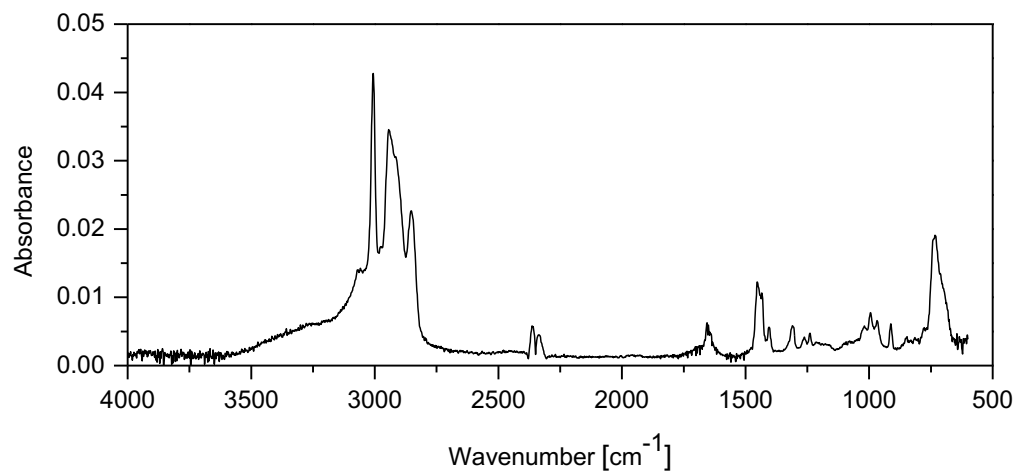


**Figure S6.24.** Ge-ATR IR-spectrum of cis-1,4-polybutadiene produced at 21 °C with Tp^Mes^NiCl.

# ¹H-NMR Spectrum of cis-1,4-polybutadiene Produced with Tp$^{Mes}$NiCl at 21°C.

¹H NMR (500 MHz, CDCl₃) δ 5.57 (-C*H*=CH₂, 1,2-vinyl), 5.39 (-C*H*=, 1,4-cis/trans), 4.98 (-CH=C*H₂*, 1,2-vinyl), 2.09 (-C*H₂*-, 1,4-cis/trans), 1.97 (-C*H₂*-, 1,2-vinyl), 1.44 (-C*H*, 1,2-vinyl).
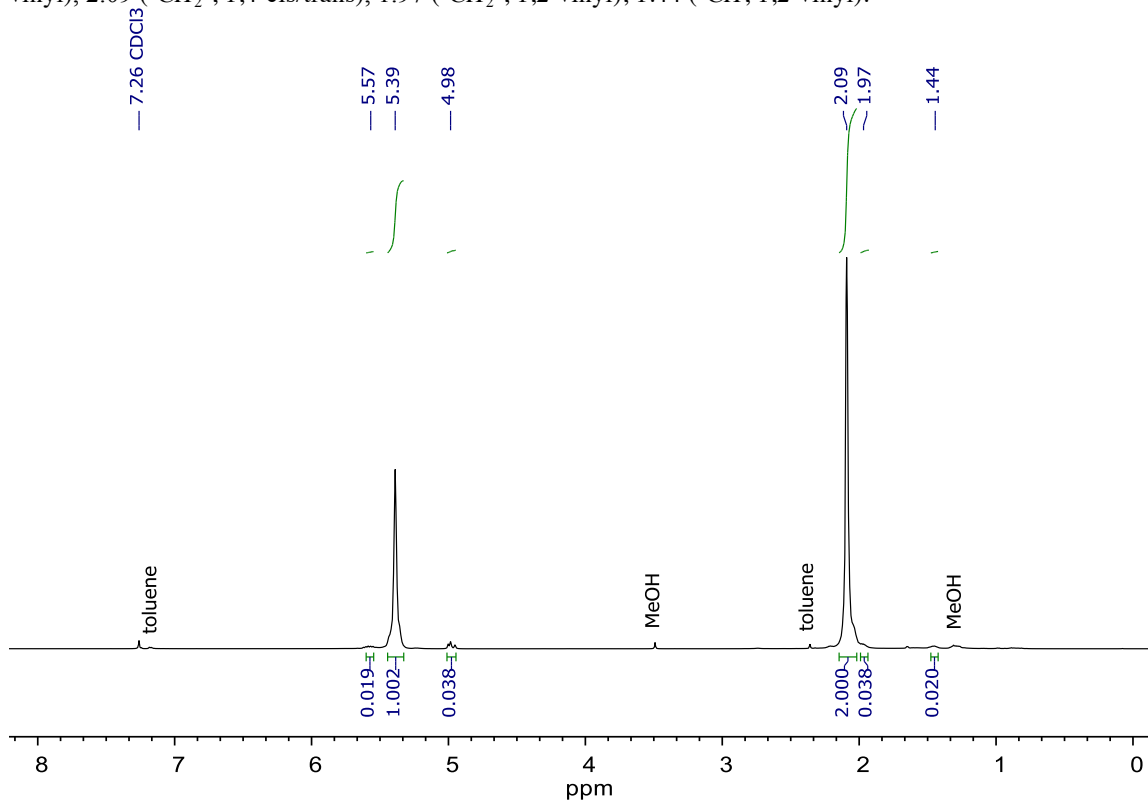


**Figure S6.25.** ¹H-NMR-spectrum of cis-1,4-polybutadiene produced at 21 °C with Tp$^{Mes}$NiCl. 64 scans.

## ^{13}C-NMR Spectrum of cis-1,4-polybutadiene Produced with Tp[Mes]NiCl at 21°C.

Quantitative ^{13}C NMR (126 MHz, CDCl$_3$, relaxation delay = 5 s) δ 142.71 (-*C*H=CH$_2$, 1,2-vinyl), 130.22 (-*C*H=, 1,4-trans), 129.73 (-*C*H=, 1,4-cis), 128.16 (-*C*H-, 1,2-vinyl), 114.58 (-CH=*C*H$_2$, 1,2-vinyl), 43.89(-*C*H-, 1,2-vinyl), 34.43 (-*C*H$_2$-, 1,2-vinyl), 32.86 (-*C*H$_2$-, 1,4-trans), 27.55 (-*C*H$_2$-, 1,4-cis), 25.12 (-*C*H$_2$-, 1,2-vinyl).
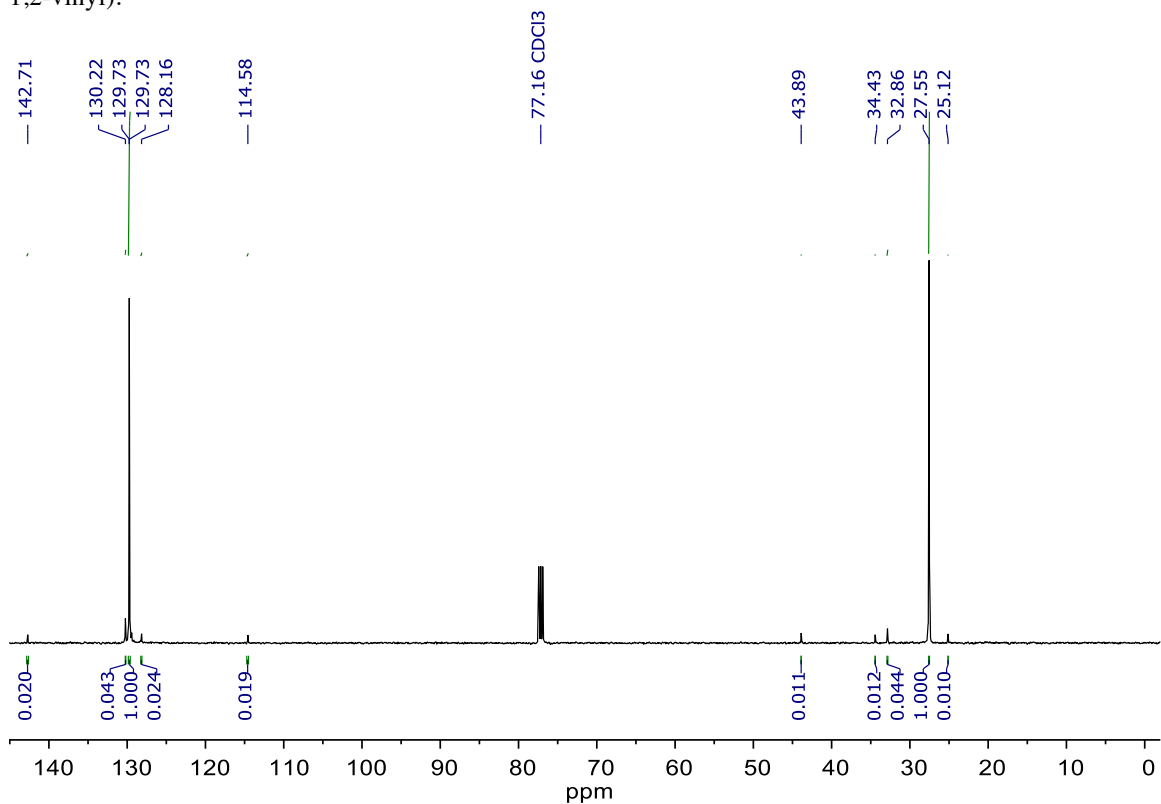


**Figure S6.26.** ^{13}C-NMR-spectrum of cis-1,4-polybutadiene produced at 21 °C with Tp[Mes]NiCl. Quantitative ^{13}C, 5 s relaxation delay.

## IR Spectrum of cis-1,4-polybutadiene Produced with Tp<sup>Mes</sup>CoCl at 21°C.

IR (Ge-ATR): $\tilde{v}$= 995 (1,2-vinyl, w), 965 (1,4-trans, w), 910 (1,2-vinyl, w), 735 cm⁻¹ (1,4-cis, s).



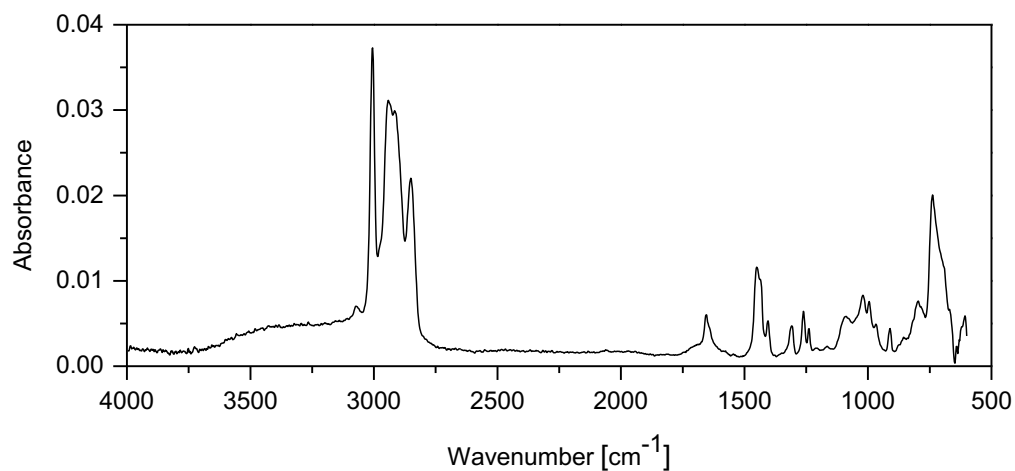**Figure S6.27.** Ge-ATR IR-spectrum of cis-1,4-polybutadiene produced at 21 °C with Tp<sup>Mes</sup>CoCl.

# ¹H-NMR Spectrum of cis-1,4-polybutadiene Produced with Tp$^{Mes}$CoCl at 21°C.

¹H NMR (500 MHz, CDCl₃) δ 5.56 (-C$H$=CH₂, 1,2-vinyl), 5.39 (-C$H$=, 1,4-cis/trans), 4.97 (-CH=C$H_2$, 1,2-vinyl), 2.09 (-C$H_2$-, 1,4-cis/trans), 1.97 (-C$H_2$-, 1,2-vinyl), 1.45 (-C$H$, 1,2-vinyl).
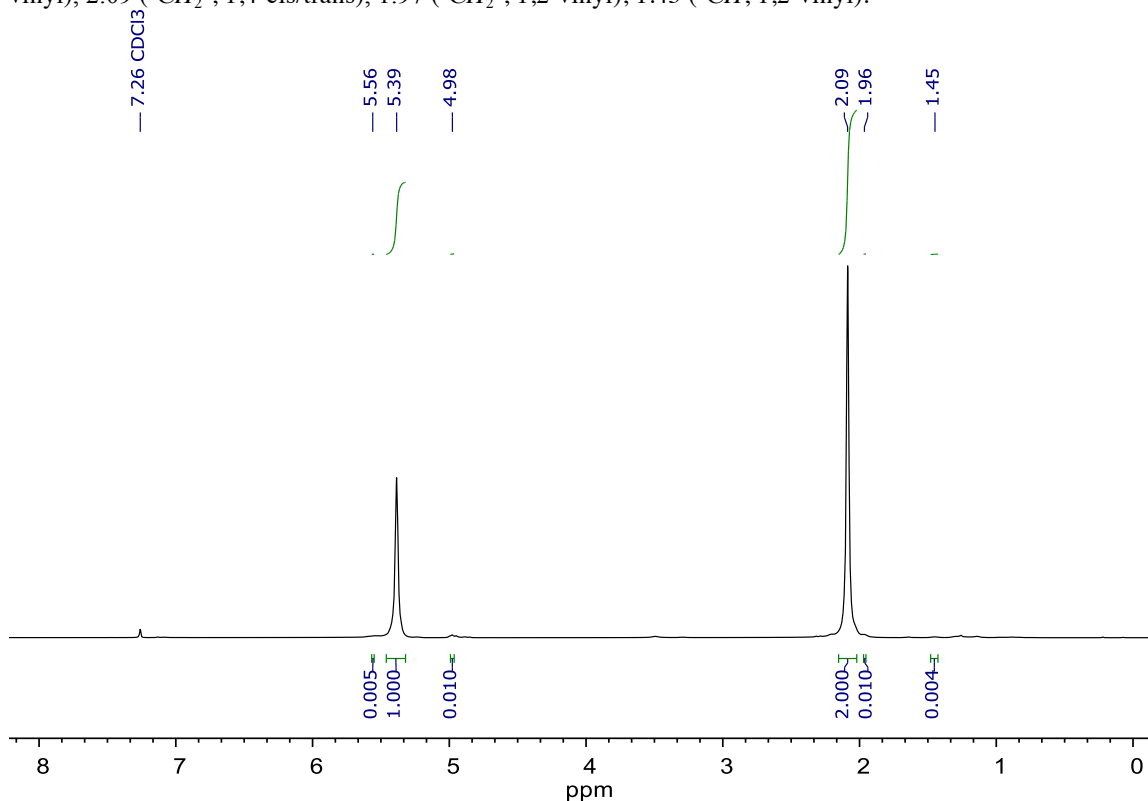


**Figure S6.28.** ¹H-NMR-spectrum of cis-1,4-polybutadiene produced at 21 °C with Tp$^{Mes}$CoCl. 64 scans.

## <sup>13</sup>C-NMR Spectrum of cis-1,4-polybutadiene Produced with Tp<sup>Mes</sup>CoCl at 21°C.

Quantitative $^{13}$C NMR (126 MHz, CDCl$_3$, relaxation delay = 5 s) δ 142.70 (-*C*H=CH$_2$, 1,2-vinyl), 130.20 (-*C*H=, 1,4-trans), 129.72 (-*C*H=, 1,4-cis), 128.14 (-*C*H-, 1,2-vinyl), 114.60 (-CH=*C*H$_2$, 1,2-vinyl), 43.91(-*C*H-, 1,2-vinyl), 34.42 (-*C*H$_2$-, 1,2-vinyl), 32.84 (-*C*H$_2$-, 1,4-trans), 27.55 (-*C*H$_2$-, 1,4-cis), 25.12 (-*C*H$_2$-, 1,2-vinyl).



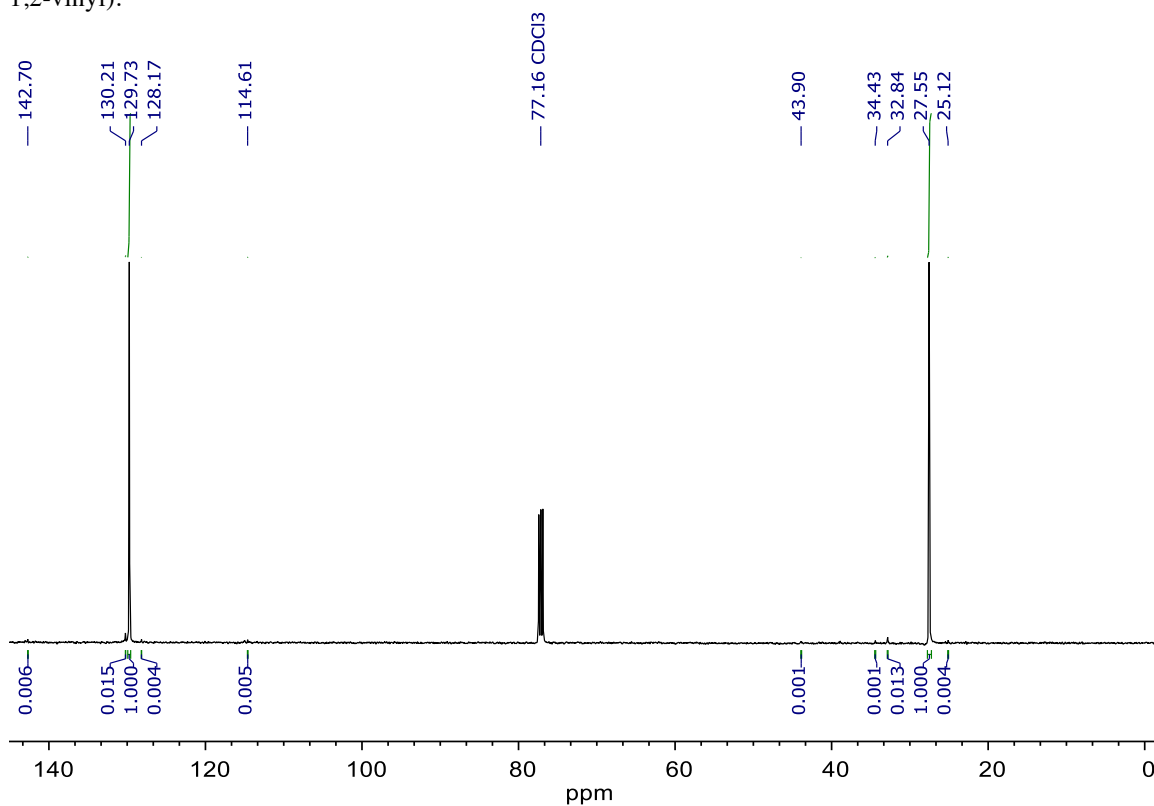**Figure S6.29.** $^{13}$C-NMR-spectrum of cis-1,4-polybutadiene produced at 21 °C with Tp$^{Mes}$CoCl. Quantitative $^{13}$C, 5 s relaxation delay.

## IR Spectrum of cis-1,4-polybutadiene Produced with Tp$^{Mes}$Co-allyl at 21°C.

IR (Ge-ATR): $\tilde{v}$= 995 (1,2-vinyl, w), 965 (1,4-trans, w), 910 (1,2-vinyl, w), 735 cm$^{-1}$ (1,4-cis, s).



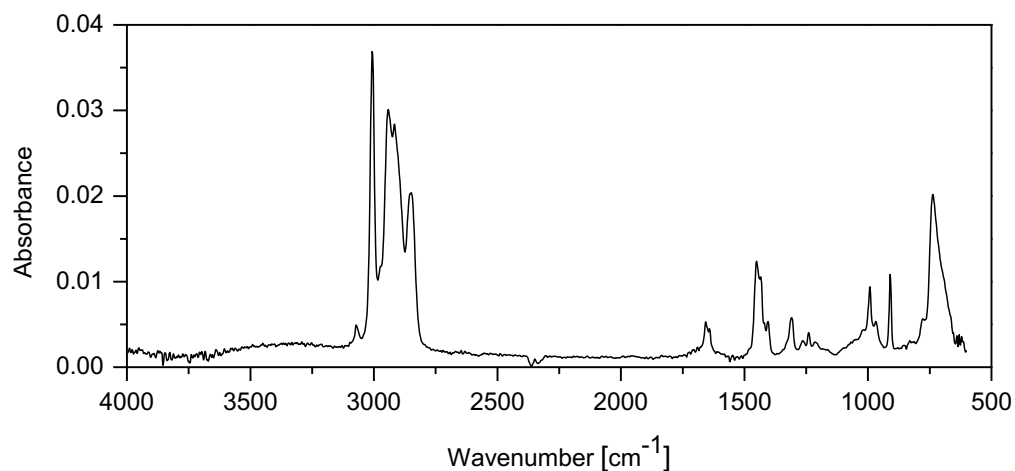**Figure S6.30.** Ge-ATR IR-spectrum of cis-1,4-polybutadiene produced at 21 °C with Tp$^{Mes}$Co-allyl.

# $^1$H-NMR Spectrum of cis-1,4-polybutadiene Produced with Tp$^{Mes}$Co-allyl at 21°C.

$^1$H NMR (500 MHz, CDCl$_3$) δ 5.56 (-C*H*=CH$_2$, 1,2-vinyl), 5.39 (-C*H*=, 1,4-cis/trans), 4.97 (-CH=C*H*$_2$, 1,2-vinyl), 2.09 (-C*H*$_2$-, 1,4-cis/trans), 1.97 (-C*H*$_2$-, 1,2-vinyl), 1.45 (-C*H*, 1,2-vinyl).
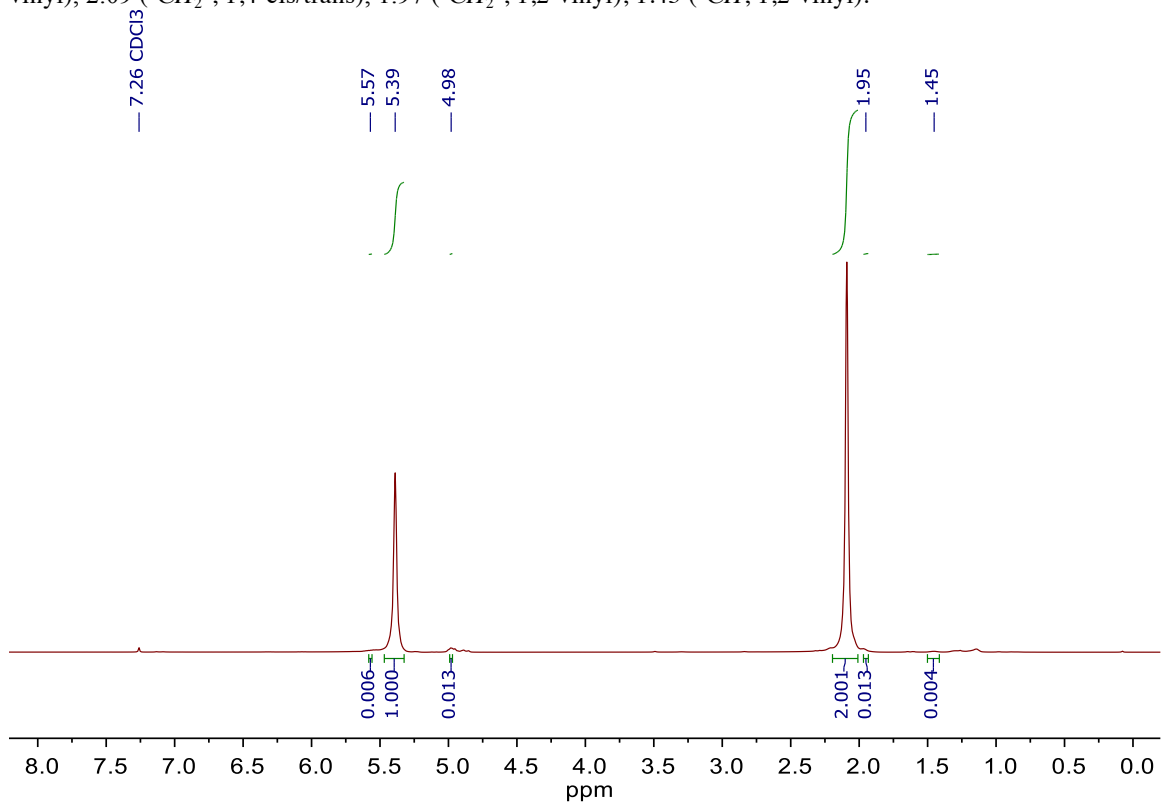


**Figure S6.31.** $^1$H-NMR-spectrum of cis-1,4-polybutadiene produced at 21 °C with Tp$^{Mes}$Co-allyl. 64 scans.

## $^{13}$C-NMR Spectrum of cis-1,4-polybutadiene Produced with Tp$^{Mes}$Co-allyl at 21°C.

Quantitative $^{13}$C NMR (126 MHz, CDCl$_3$, relaxation delay = 5 s) δ 142.70 (-*C*H=CH$_2$, 1,2-vinyl), 130.20 (-*C*H=, 1,4-trans), 129.72 (-*C*H=, 1,4-cis), 128.14 (-*C*H-, 1,2-vinyl), 114.60 (-CH=*C*H$_2$, 1,2-vinyl), 43.91(-*C*H-, 1,2-vinyl), 34.42 (-*C*H$_2$-, 1,2-vinyl), 32.84 (-*C*H$_2$-, 1,4-trans), 27.55 (-*C*H$_2$-, 1,4-cis), 25.12 (-*C*H$_2$-, 1,2-vinyl).



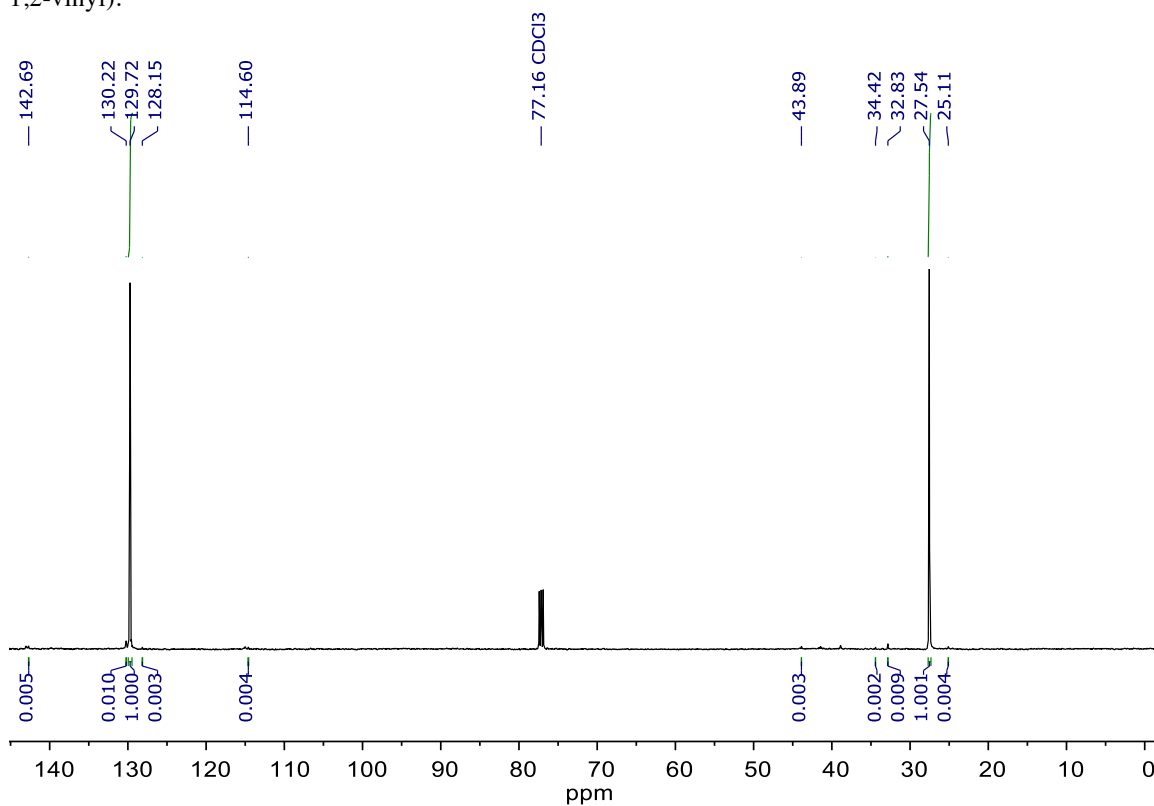**Figure S6.32.** $^{13}$C-NMR-spectrum of cis-1,4-polybutadiene produced at 21 °C with Tp$^{Mes}$Co-allyl. Quantitative $^{13}$C, 5 s relaxation delay.
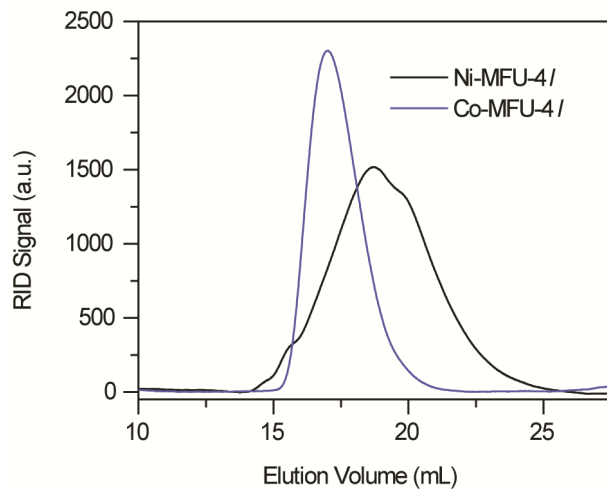
## 6.2 GPC elution curves.

### Ni-MFU-4*l* and Co-MFU-4*l* in semi-batch.



**Figure S6.33.** GPC elution curves of polybutadiene produced in semi-batch mode with Ni-MFU-4*l* and Co-MFU-4*l*.
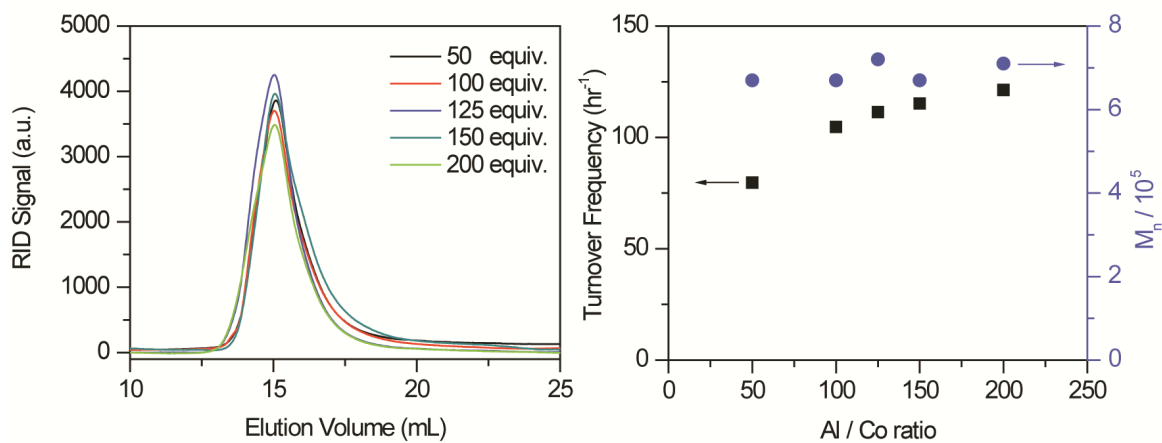
## Effect of the MMAO loading on the molecular weight.



**Figure S6.34.** (Left) cis-1,4-polybutadiene GPC elution curves produced with different equivalents of MMAO. (Right) Resulting molecular weight and turnover frequency.
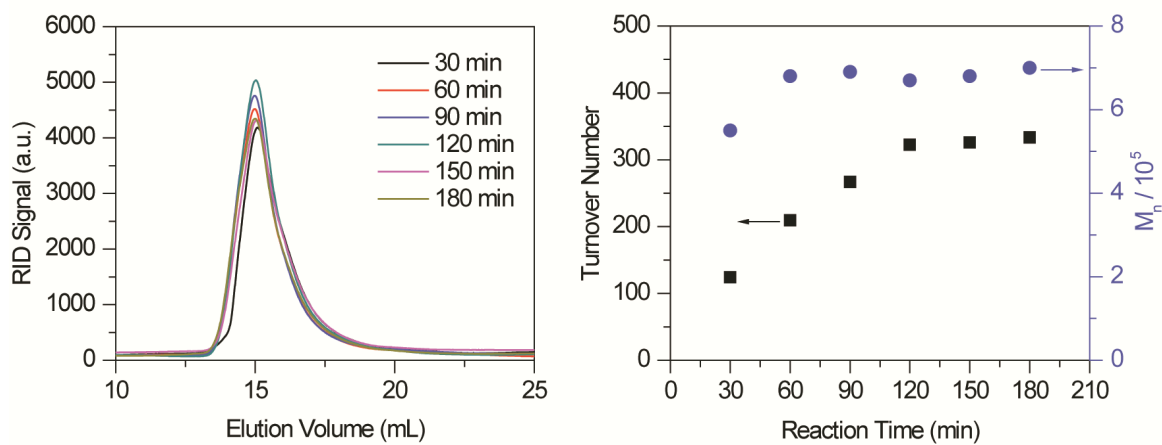
## Effect of the reaction time on the molecular weight.



**Figure S6.35.** (Left) cis-1,4-polybutadiene GPC elution curves at different polymerization times. (Right) Resulting molecular weight and turnover frequency.
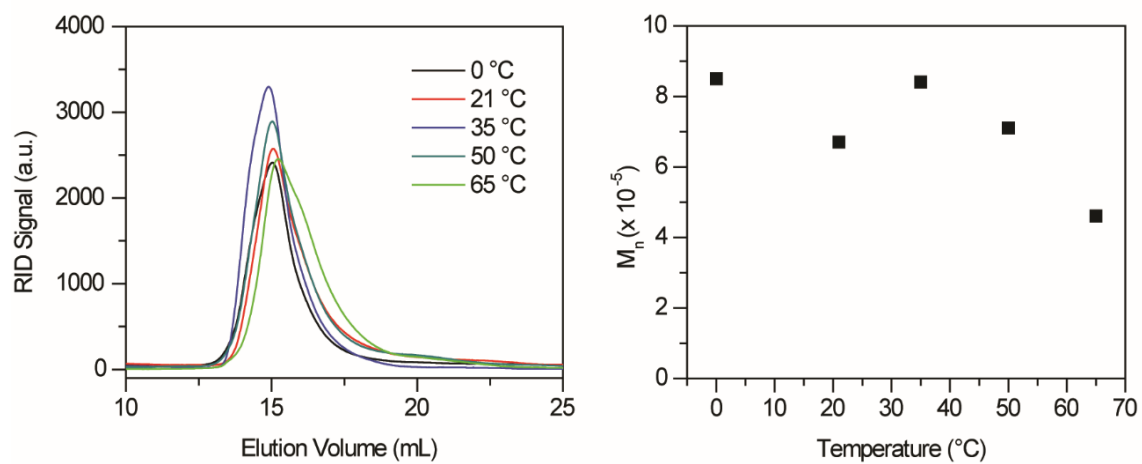
**Effect of temperature on the molecular weight.**



**Figure S6.36** (Left) cis-1,4-polybutadiene GPC elution curves produced at different temperatures. (Right) Resulting molecular weight.

## Effect of the monomer concentration on the molecular weight.
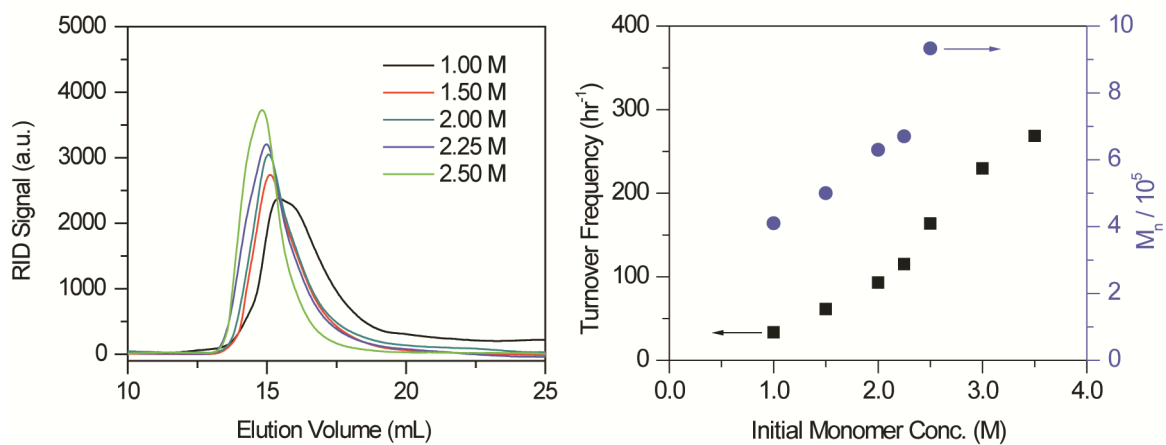


**Figure S6.37.** (Left) cis-1,4-polybutadiene GPC elution curves produced with different initial monomer concentrations. (Right) Resulting molecular weight and turnover frequency. There are no elution curves for 3.0 and 3.5 M, because the product was not soluble in THF.

## Ni-MFU-4*l* in batch vs. Tp$^{Mes}$NiCl.
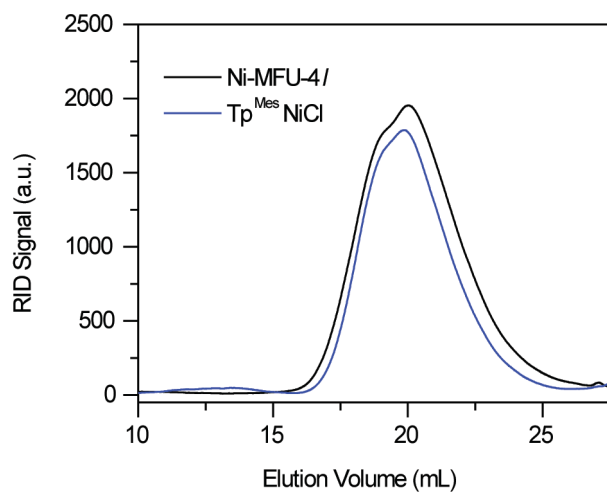


**Figure S6.38.** GPC elution curves of cis-1,4-polybutadiene obtained with the MOF Ni-MFU-4*l* and the molecular complex Tp$^{Mes}$NiCl.

## Co-MFU-4*l* in batch vs. Tp$^{Mes}$CoCl.
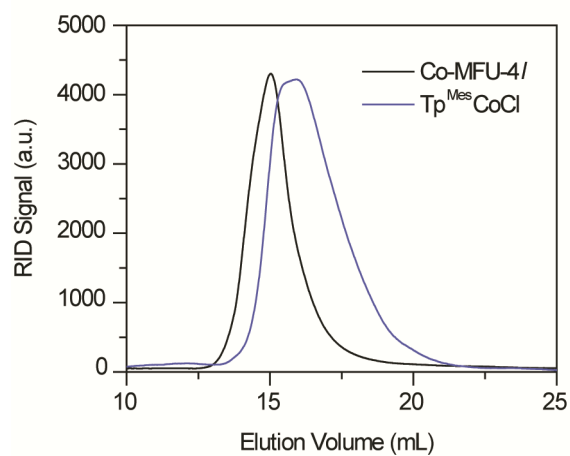


**Figure S6.39.** GPC elution curves of cis-1,4-polybutadiene obtained with the MOF Co-MFU-4*l* and the molecular complex Tp$^{Mes}$CoCl.
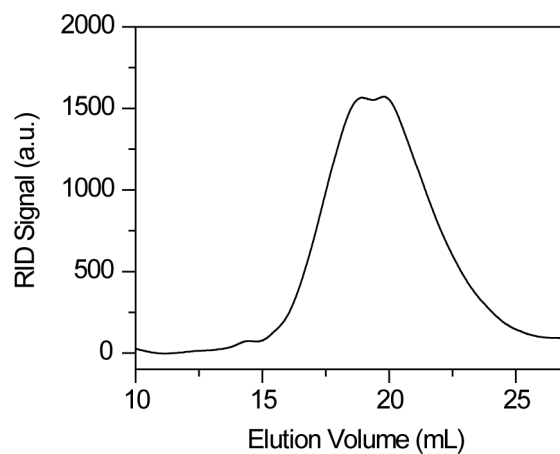
## Tp^MesCo-allyl with MMAO-12.



**Figure S6.40.** GPC elution curve of cis-1,4-polybutadiene obtained with the MOF Co-MFU-4*l* and the molecular complex Tp^MesCo-allyl.

# 7. Electron Microscopy Data.

**General.** To mount samples for analysis, the powdery solids were smeared onto carbon tape and then cleaned with a fine stream of nitrogen to remove loosely affixed particles. Mounted samples were then sputter coated with Pt/Pd at a thickness of 5 nm. High resolution scanning electron microscopy (SEM) analysis was performed using a Zeiss Ultra 55 model field emission scanning electron (FESEM) microscope in Everhart-Thornley (SE2) detector mode.

**Co-MFU-4*l* after Polymerization Sample Preparation.** A polymerization was run after the general screening procedure. After a reaction time of 1 h, the reaction mixture was diluted under inert conditions with dry toluene (5 mL) and centrifuged. The solid phase was washed with dry toluene (10 mL), separated through centrifugation, washed with dichloromethane (10 mL) and separated through centrifugation. The powdery solid was dried *in vacuo*. The sample mounting then followed the general procedure.

## 7.1. SEM of Co-MFU-4*l* Before Polymerization.



**Figure S7.1.** Scanning Electron Microscopy representations of activated Co-MFU-4*l* before polymerization.
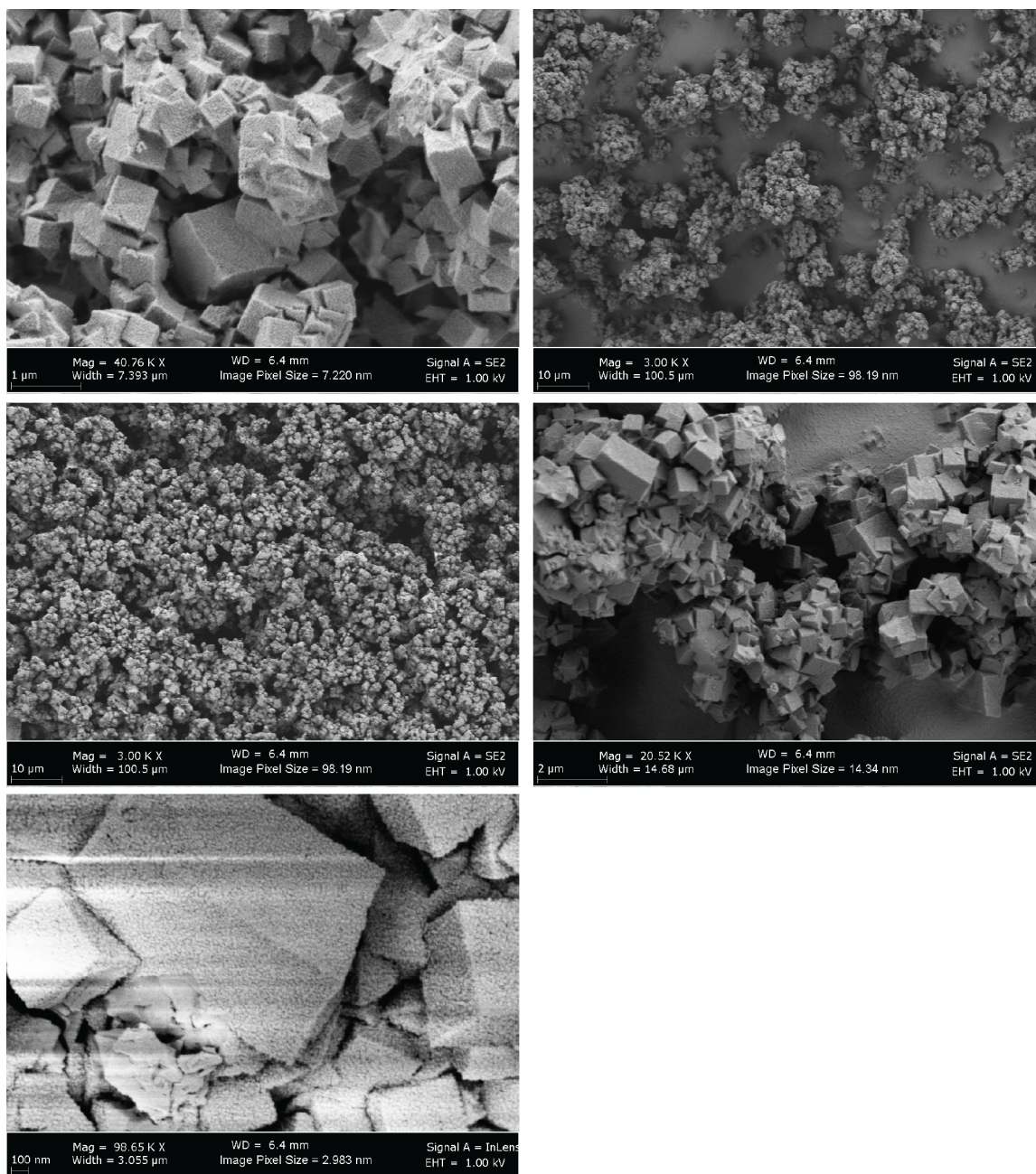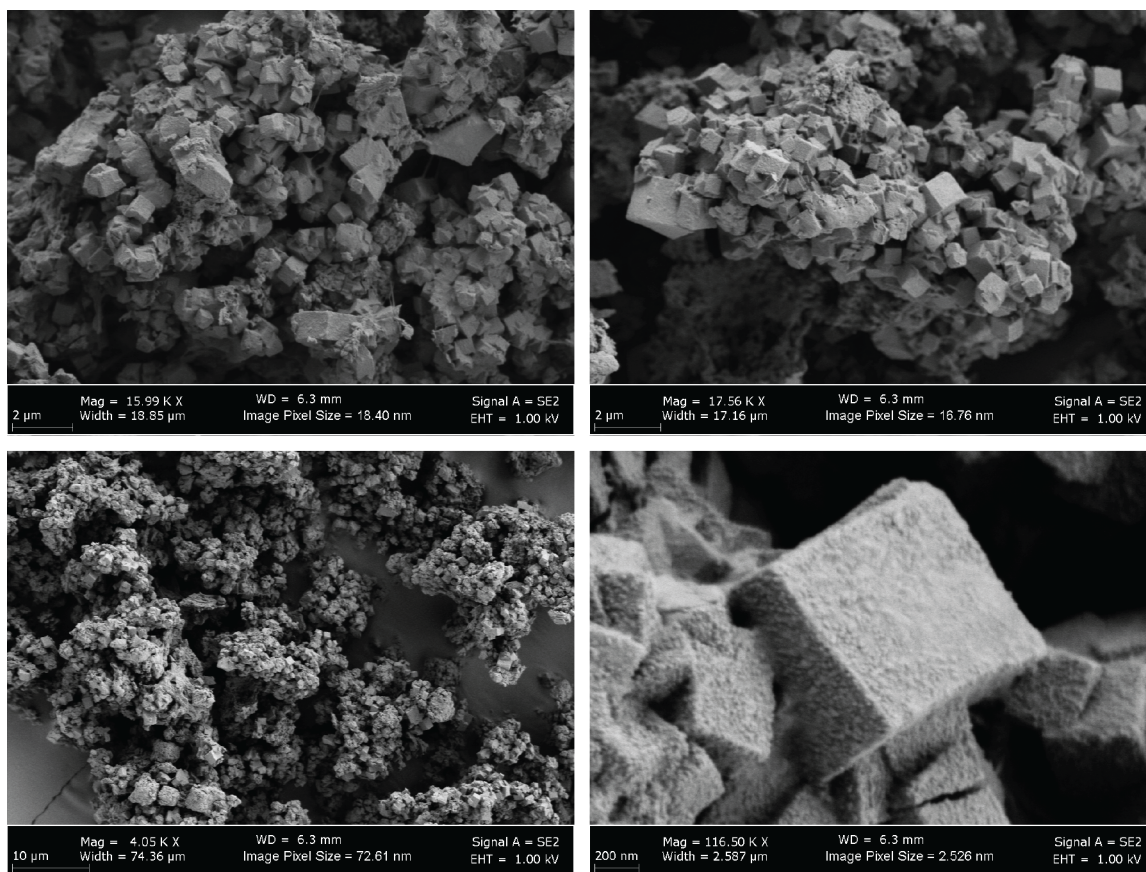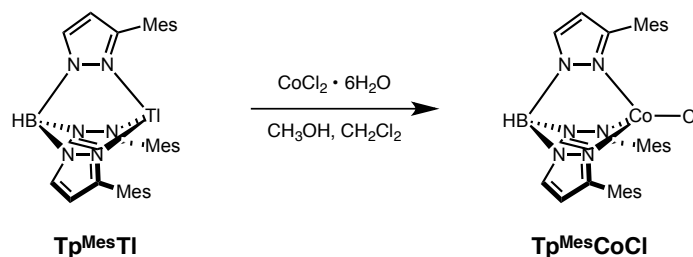
## 7.2. SEM of Co-MFU-4*l* After Polymerization.



**Figure S7.1.** Scanning Electron Microscopy representations of activated Co-MFU-4*l* after polymerization. The MOF was washed with toluene and dichloromethane to get rid of most of the surrounding polymer.

## 8. Preparation of Cobalt Complexes.



**Tp^MesTl** → **Tp^MesCoCl**

CoCl₂ • 6H₂O
CH₃OH, CH₂Cl₂

**Tp^Mes^CoCl (9)**. A solution of CoCl₂ • 6H₂O (68 mg, 0.285 mmol, 1.1 equivalents) and methanol (3.0 mL) was added dropwise to a suspension of Tp^Mes^Tl[10] (200 mg, 0.259 mmol, 1.0 equivalents), immediately forming a blue suspension. After three hours, the reaction was filtered through a plug of celite, rinsing with CH₂Cl₂ until the blue solution finished eluting. The filtrate was then partitioned between CH₂Cl₂ and brine (25 mL each). The brine solution was backrinsed with CH₂Cl₂ (25 mL), and the combined pink organic solution was dried over sodium sulfate, filtered, and concentrated in vacuo to afford the title compound as a flaky blue solid (164.6 mg, 0.249 mmol, 96% yield). IR 2968, 2926, 2860, 2478 (υ[B–H]), 1616, 1525, 1483, 1477, 1358, 1263, 1180, 1048, 851, 798, 783, 744, 705 cm⁻¹. Elemental Analysis (C₃₆H₄₀BClCoN₆): carbon (theoretical: 65.32%, experimental: 65.24%, difference: 0.08%), hydrogen (theoretical: 6.09%, experimental: 6.00%, difference 0.09%), nitrogen (theoretical: 12.70%, experimental: 12.59%, difference: 0.11%). ¹H-NMR (tetrahydrofuran-d8, 500 MHz): δ 72.39 (3 H), 39.08 (3 H), 10.86 (18 H), 6.44 (6 H), 1.41 (9 H), –29.18 (1 H). Single crystals suitable for X-ray diffraction analysis were obtained from a dichloromethane solution by vapor diffusion with hexane.



**Tp^MesCoCl** → **Tp^MesCo(allyl)**

⌒⌒MgBr
Et₂O, THF
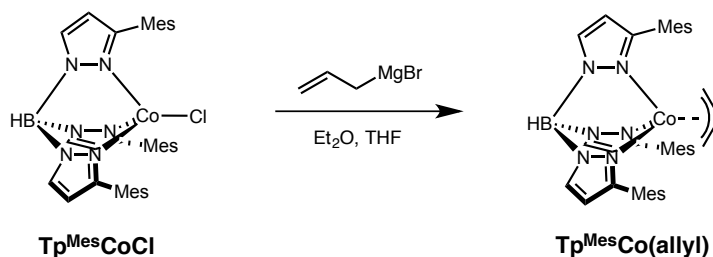
**Tp^Mes^Co(allyl) (10)**. In a nitrogen glovebox, allyl magnesium bromide (0.2 mL, 1 M solution in diethyl ether, 0.2 mmol, 4.3 equivalents) was added to a vial containing a

homogeneous blue solution of Tp$^{Mes}$CoCl (30 mg, 0.046 mmol, 1 equivalent) and tetrahydrofuran (4.0 mL). The solution immediately turned a dull orange color. After the reaction had stirred for one hour, the solvent was removed in vacuo. The resulting orange solid was dissolved in toluene (4.0 mL), stored in a −35 °C freezer for 18 hours, and then filtered cold to remove a white solid. The clear orange solution was then concentrated in vacuo. Diffraction quality crystals could be obtained by dissolving the material in diethyl ether followed by vapor diffusion with hexane. *Decomposition of this product upon exposure to air was evident by a light blue color.*

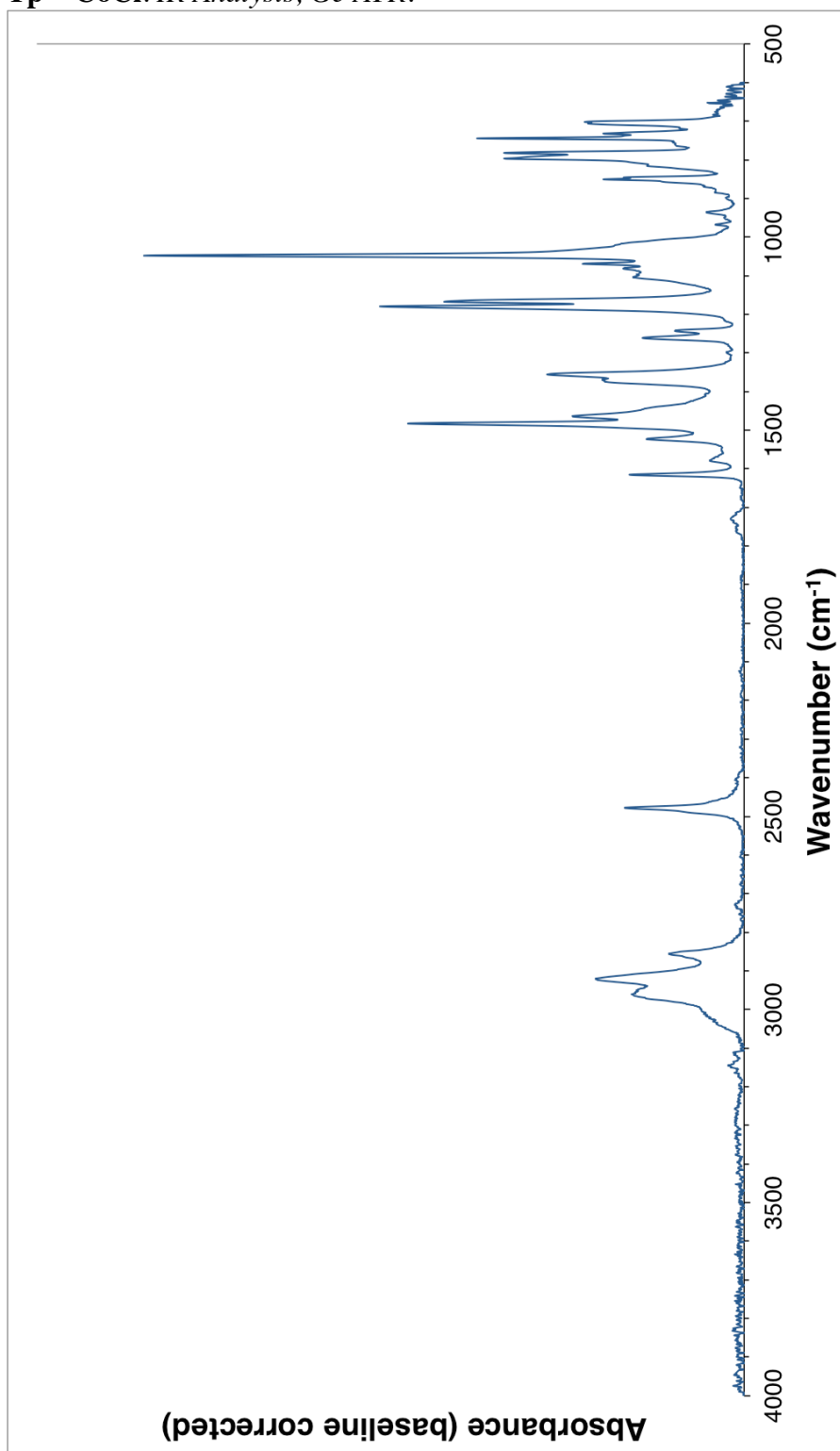**Tp^{Mes}CoCl**. *IR Analysis, Ge ATR*.



**Figure S8.1.** Ge ATR IR spectrum of Tp^{Mes}CoCl

**Tp<sup>Mes</sup>CoCl**, ¹H-NMR, tetrahydrofuran-d8, 500 MHz



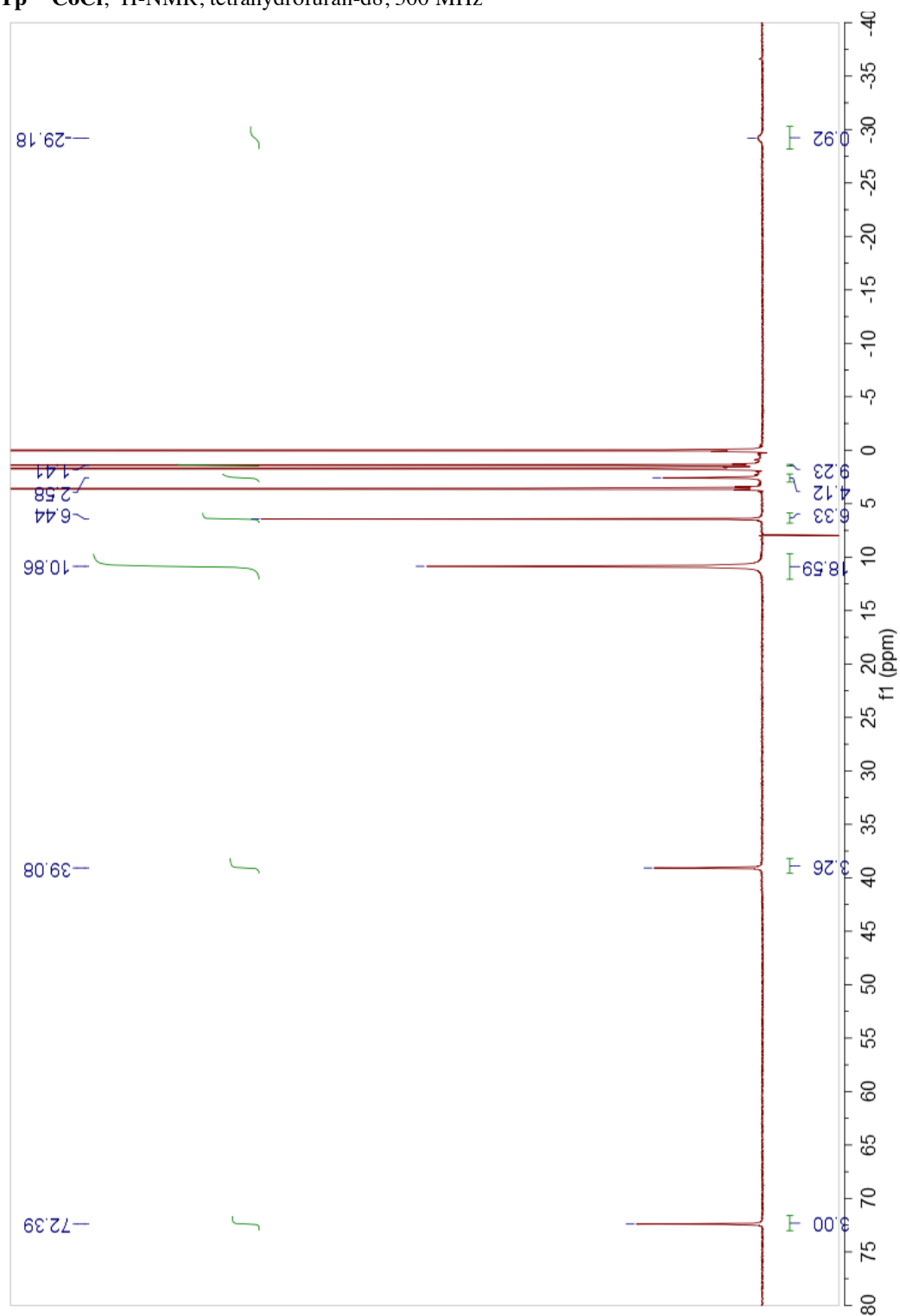**Figure S8.2**. 1H-NMR analysis of Tp<sup>Mes</sup>CoCl.

# 9. DFT Model of Co-MFU-4*l*.

**DFT-1. Model of Co-MFU-4*l*.** First-principles total energy and electronic structure calculations were performed within the Kohn-Sham DFT construct. A delocalised plane-wave basis set with PAW scalar-relativistic frozen-core potentials were employed as implemented in the Vienna ab initio simulation package (VASP). A 500 eV plane-wave kinetic energy cutoff and a 2 × 2 × 2 k-grid were combined to provide total energy convergence to within 0.01 eV/atom. Beginning with the experimentally determined crystallographic primitive cell of MFU-4*l*, all unit cell vectors and internal ionic positions were relaxed to their equilibrium values using the PBEsol functional. This functional provides a good description of the solid-state structures of MOFs, with all equilibrium lattice vectors being within 1% of experimental values. Cobalt substitutions were then installed by manually modifying the structural file to 4 $Co^{2+}$ per cluster with appropriate charge compensating metal-bound $Cl^-$ included. The structure was then further optimized using the same convergence criteria as the native framework. The resulting geometry-optimized structure is hereafter referred to as DFT-**1**.

**Transition state model.** A representative 1,3-butadiene insertion into a $C_7$-allyl was modeled using a representative truncated cluster, where the BTDD ligands were terminated at the bridging oxide with charge-compensating protons. Using a nudged elastic band approach as implemented in FHI-aims (PBEsol, 'tight' basis set, 0.005 eV/atom convergence, transition state confirmed by vibrational mode analysis), a transition state ($E_a$ = 17 kcal/mol) was obtained for the sigma bond formation of between the Co-bound allyl chain and the incoming 1,3-diene. We note that the formal $\eta^3$-allyl is transiently $\eta^1$, bound through the C3 carbon. Spin density is a useful gauge for the bond formation process, with the spin contributions of the allyl complex decreasing as the sigma bond is formed. Simultaneous formation of spin stabilization on the newly formed allyl anion is observed in Figure S9.1. We also probed the potential energy surface of the

Co-allyl species and found that the $\eta^3$- $\eta^1$ structures are all within 4 kcal/mol of each other.
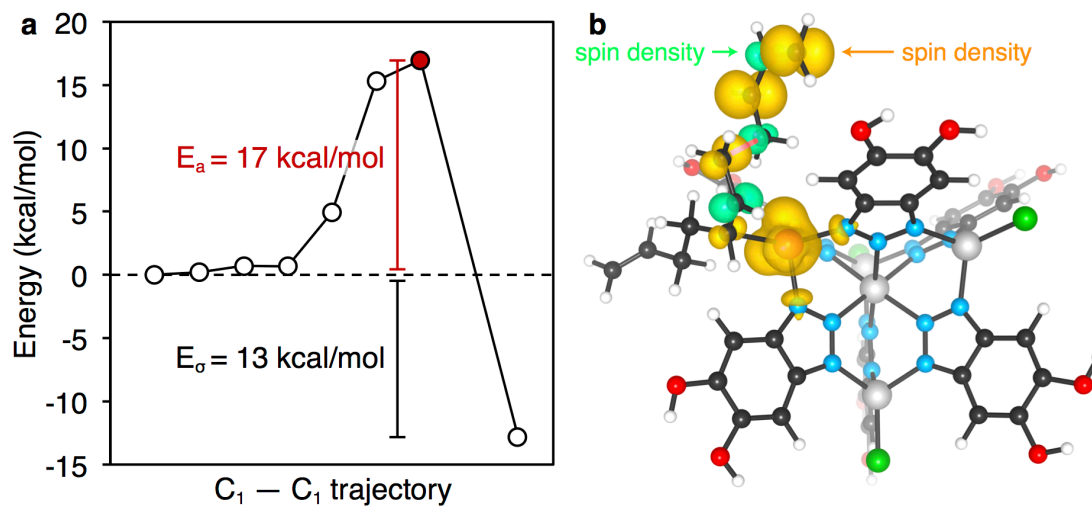


**Figure S9.1.** (**a**) A nudged elastic band calculation of a representative transition state in chain propagation yields an activation energy ($E_a$) of 17 kcal/mol. (**b**) the transition state shows the formation of a sigma bond (red), and spin density on the newly formed allyl.

**Table S9.1** Structural Comparison of Nickel Coordination in DFT-**1** and Tp$^{Mes}$CoCl (**10**).

| Structure | N–Co bond length* | Cl–Co bond length | N–Co–N bond angle* | N–Co–Cl bond angle* |
|---|---|---|---|---|
| DFT-**1** | 1.915 Å | 2.134 Å | 99.16 ° | 118.47 ° |
| Tp$^{Mes}$CoCl (**9**) | 2.023 Å | 2.175 Å | 92.41 ° | 123.44 ° |

*Average values within each structure (i.e., of three N–Co bonds)

## 10. X-Ray Absorption Spectroscopy Analysis of Co-MFU-4*l*.

X-ray absorption spectroscopy measurements at the Co K edge (7.7089 keV) were performed on the 10-BM bending magnet beamline of the Materials Research Collaborative Access Team (MRCAT) at the Advanced Photon Source (APS), Argonne National Laboratory. Data was acquired in transmission and step-scan mode using ionization chambers optimized for the maximum current with linear response ($\sim10^{10}$ photons detected/sec) with 10 % absorption in the incident ion chamber and 70 % absorption in the transmission X-ray detector. A Co foil spectrum was acquired simultaneously with each sample measurement for energy calibration. Catalyst samples were pressed in a $N_2$ glovebox into a cylindrical sample holder consisting of six wells, forming a self-supporting wafer which was then placed in a quartz tube (2.5 cm. OD, 10.0 cm. length) sealed with Kapton windows by two Ultra-Torr fittings. Artemis software was used to fit the XAS data.[11]

Below are the X-ray absorption near-edge spectroscopy (XANES) plots (Figure S10.1) and zoom in pre-edge feature (Figure S10.2) of Co-MFU-4*l*[12] and corresponding references. $CoCl_2$ and $Tp_2Co$[13] were also analyzed for comparison. From the shape of the XANES curve, Co-MFU-4*l* clearly has a different coordination environment than both $CoCl_2$ and $Tp_2Co$. Although the edge position and shape corresponding to Co-MFU-4*l* more closely resembles that of $Tp_2Co$ (with a lower white line intensity), the shape of Co-MFU-4*l*'s XANES spectra after the white line more closely resembles that of $CoCl_2$.
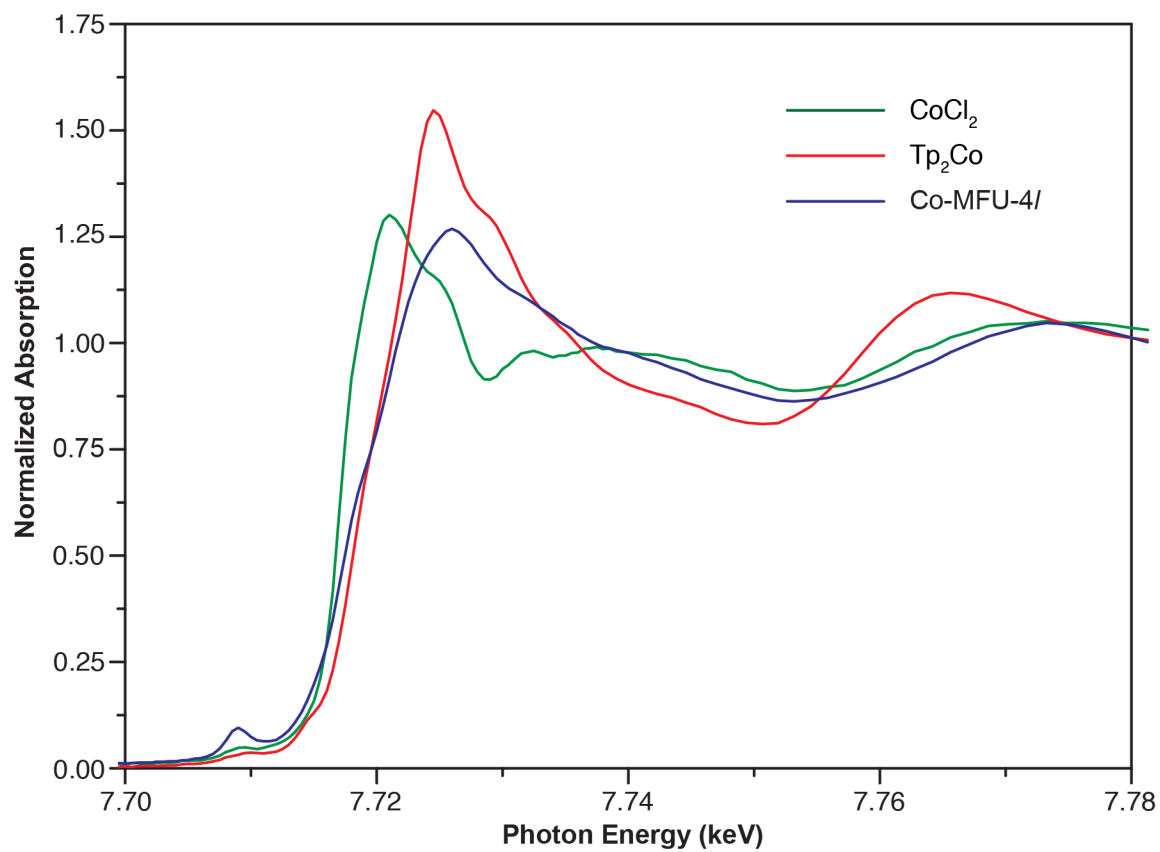
**Figure S10.1.** XANES plot for Co-MFU-4*l* and corresponding references.
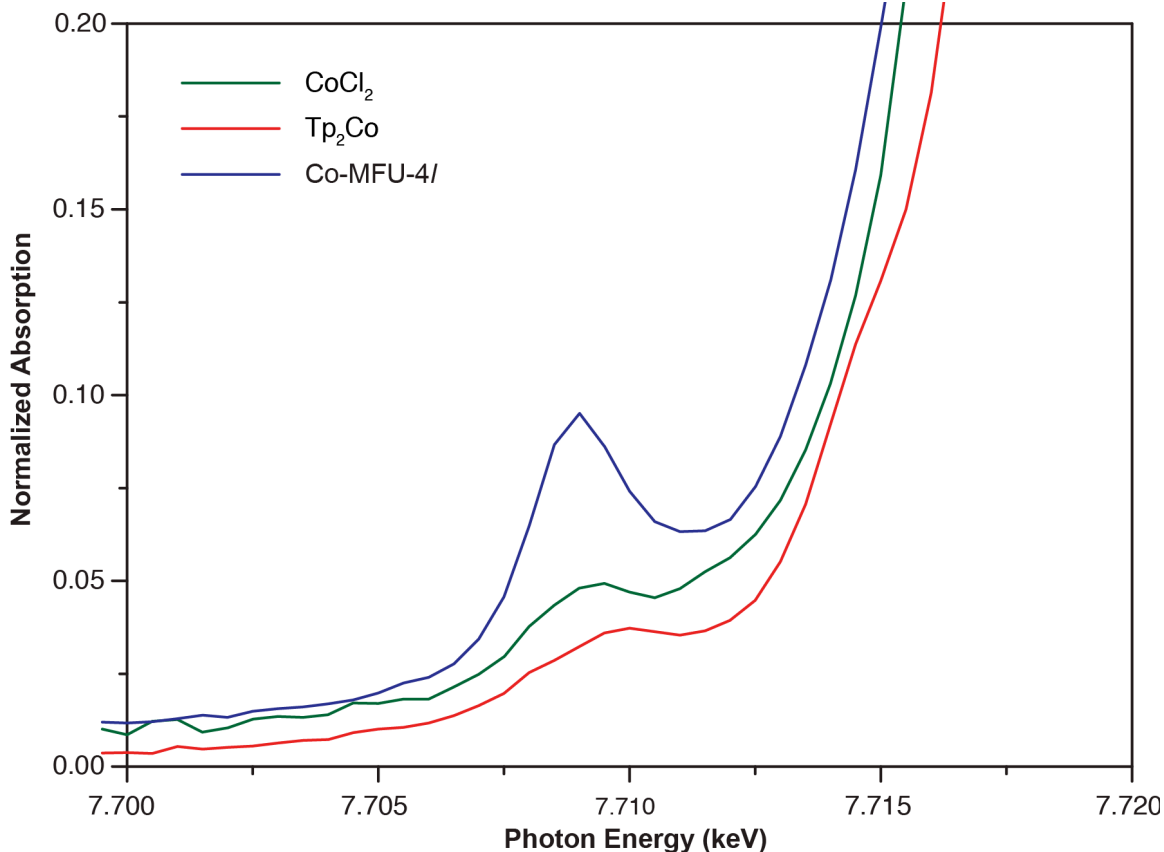
**Figure S10.2**. XANES Pre-edge plot for Co-MFU-4*l* and corresponding references.

The values of the edge energy (inflection point of the leading edge) and pre-edge energy can be determined from the spectra and are summarized below (Table S10.1). Co-MFU-4*l* has an edge and pre-edge energy similar to that of $CoCl_2$ and $Tp_2Co$, consistent with an oxidation state of Co(II) in the former. The pre-edge energy of $Tp_2Co$ is slightly higher than that of Co-MFU-4*l*, which can be explained by the difference in coordination geometry. In the octahedral structure of $Tp_2Co$, the $e_g$ orbitals are higher in energy than $t_{2g}$ orbitals. The pre-edge is due to the transition of 1s-$e_g$ since all the $t_{2g}$ orbitals are filled. In a tetrahedral structure, the $t_{2g}$ orbitals would be higher in energy than the $e_g$, so the pre-edge would be due to the transition of 1s-$t_{2g}$. Thus the higher XANES pre-edge energy in $Tp_2Co$ compared to Co-MFU-4*l* would be consistent with the larger crystal field splitting for Oh compared to Td symmetry. Although Co(II) resides in an octahedral

geometry for both Tp$_2$Co and CoCl$_2$, Tp$^-$ is a stronger field ligand than Cl$^-$, consistent with the higher pre-edge energy observed for Tp$_2$Co. Furthermore, the pre-edge features are higher in intensity for Co-MFU-4*l* than the two standards (Figure S10.2), indicating less symmetric coordination. Taken together, the pre-edge data are consistent with the proposed pseudo-tetrahedral environment of DFT-**1**.

**Table S10.1**. XANES edge energy and pre-edge energy.

| Sample | Edge Energy (keV) | Pre-Edge Energy (keV) |
|---|---|---|
| Co foil | 7.7090 | / |
| CoCl$_2$ | 7.7170 | 7.7092 |
| Tp$_2$Co | 7.7180 | 7.7097 |
| Co-MFU-4*l* | 7.7172 | 7.7090 |
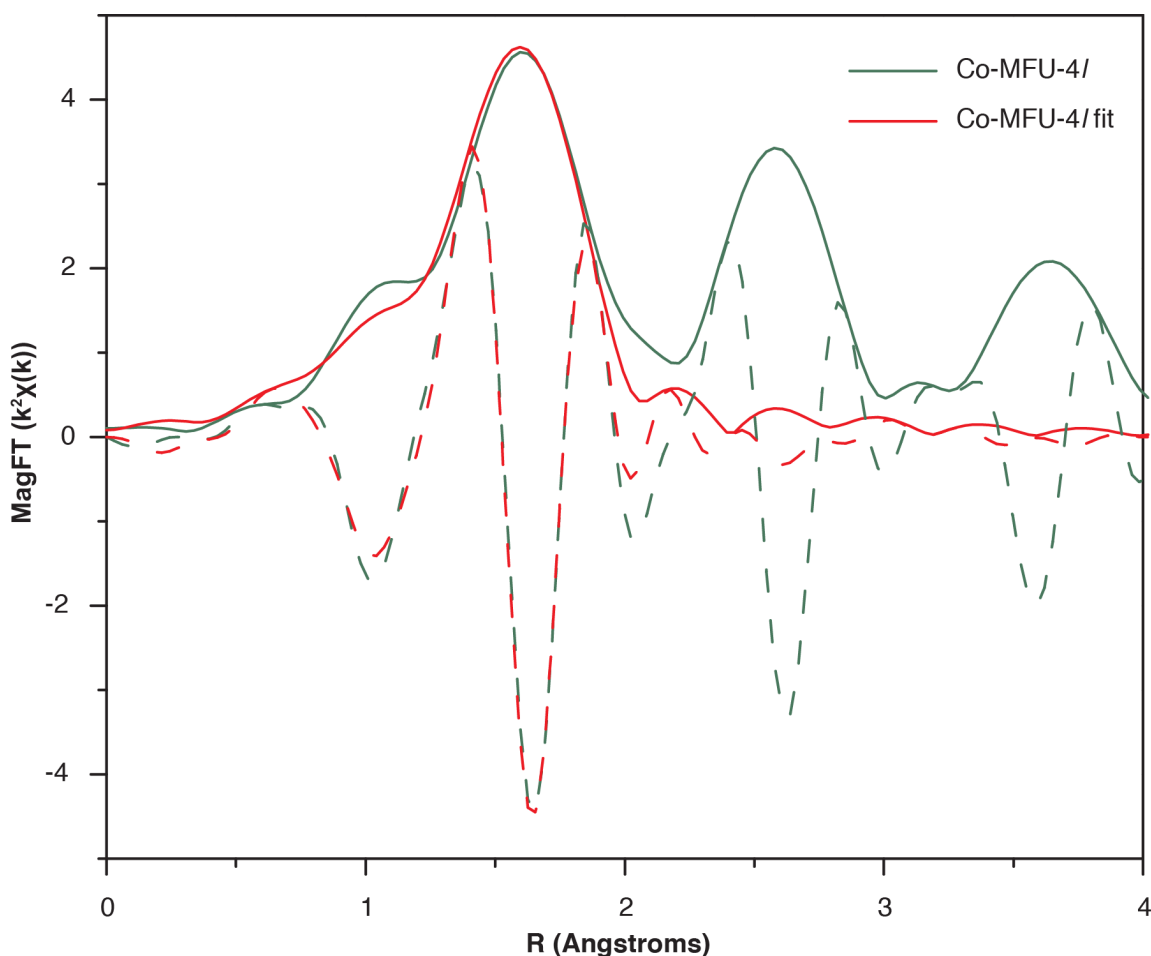
**Figure S10.3**. EXAFS plot for Co-MFU-4*l* and corresponding first shell fit. Solid lines indicate real and hashed lines indicate imaginary components.

**Quantitative Coordination Structure by EXAFS.** Figure S3 displays the EXAFS plot of Co-MFU-4*l* and the optimal first shell fits evaluated using Artemis software.[11] The initial bond lengths and coordination number were derived from DFT-**1**, and the model was adjusted until reasonable amplitude reduction factor ($S_0^2$), energy shift ($\Delta E_0$) and bond length difference ($\Delta R$) values are obtained. When comparing multiple samples, the $S_0^2$ value is typically determined from fitting a reference compound (in this case $Tp_2Co$). Guided by this value, the optimal bond lengths for the fit (3 Co–N at 2.02 Å and 1 Co–Cl at 2.15 Å) are slightly longer than those of DFT-**1** (3 Co–N at 1.915 Å and 1 Co–Cl at

2.134 Å). Nevertheless, the first coordination sphere in the proposed model fits the EXAFS data well. Fitting Co-MFU-4*l* with other models have been examined, including a total coordination number of 6 or a coordination number of 4 but with different numbers of neighbor (N versus Cl), which all lead to significantly poorer fits. Note that this model does not attempt to fit the EXAFS data beyond the primary coordination sphere, hence the poor correlation between the fit and experimental data at R > 2 Å in Figure S10.3.

**Table S10.2**. Quantitative evaluation of the EXAFS fit (Artemis Software)

| Sample | Scattering Pair | $S_0^2$ * | CN | Bond Length (Å) * | $\Delta E_0$ (eV) * | $\Delta\sigma^2$ (Å$^2$) * |
|---|---|---|---|---|---|---|
| Tp$_2$Co | Co−N | 0.90 | 6 | 2.14 | 4.2 | 0.007 |
| CoCl$_2$ | Co−Cl | 0.90 | 6 | 2.42 | -1.9 | 0.010 |
| Co-MFU-4l | Co−N | 0.90 | 3 | 2.02 | -6.8 | 0.011 |
| | Co−Cl | | 1 | 2.15 | | 0.007 |

* The average error (if not fixed) in $S_0^2$ is 0.14, in bond length is 0.02 Å, in $\Delta E_0$ is 1.4 eV and in $\Delta\sigma^2$ is 0.003 Å$^2$.
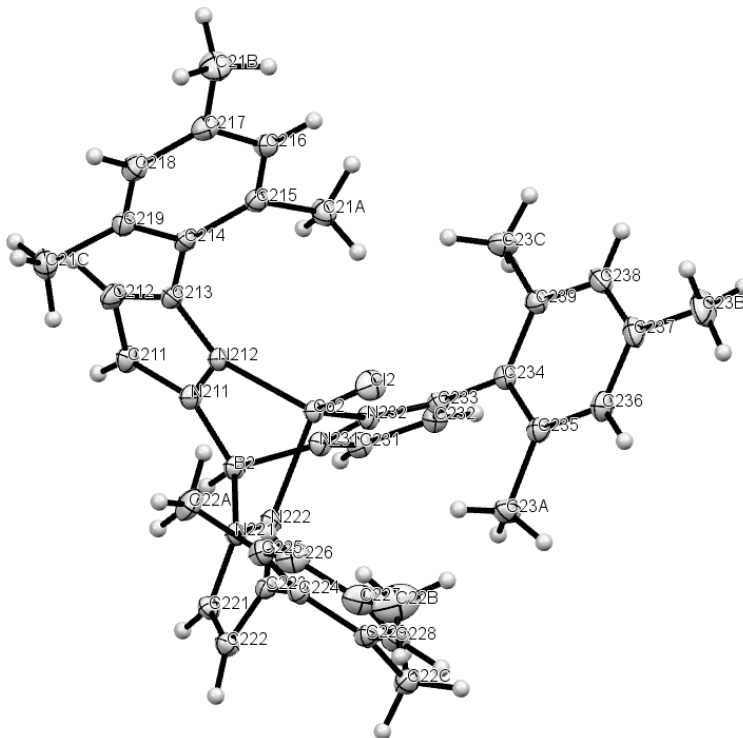
# 11. Crystallographic Data.

## 11.1. Tp$^{Mes}$CoCl.



**Figure S11.1.** Ellipsoid representation of the crystal structure of the Tp$^{Mes}$CoCl complex.

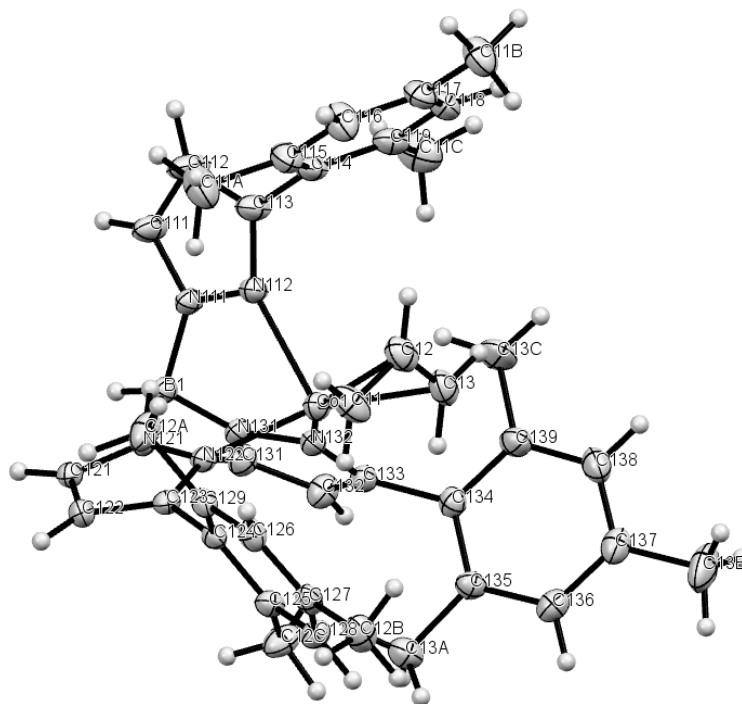**Table S11.1.** Selected bond angles from the Tp$^{Mes}$CoCl complex.

| Atom 1 | Atom 2 | Atom 3 | Angle | Atom 1 | Atom 2 | Atom 3 | Angle |
|--------|--------|--------|-------|--------|--------|--------|-------|
| Cl2 | Co2 | N212 | 127.18(5) | Co2 | N212 | C213 | 140.4(1) |
| Cl2 | Co2 | N222 | 116.62(5) | Co2 | N222 | C233 | 139.0(1) |
| Cl2 | Co2 | N232 | 125.30(5) | Co2 | N232 | C233 | 139.4(1) |
| N212 | Co2 | N222 | 94.56(7) | N212 | C213 | C214 | 122.7(2) |
| N212 | Co2 | N232 | 92.90(7) | N232 | C233 | C234 | 121.0(2) |
| N222 | Co2 | N232 | 91.22(7) | N222 | C223 | C224 | 120.1(2) |

**Procedure**: A solvated, diffraction-quality single crystal of Tp$^{Mes}$CoCl, was mounted in paratone oil on a Kapton loop. Room temperature (293(2) K) diffraction data ($\varphi$- and $\omega$-scans) were collected on a Bruker-AXS X8 Kappa Duo diffractometer coupled to a Smart APEX II CCD detector with MoK$_\alpha$ radiation ($\lambda$ = 0.71073 Å) from a *IμS*-micro source.

Absorption and other corrections were applied using SADABS.[14] The structure was solved by direct methods using SHELXS[15] and refined against $F^2$ on all data by full-matrix least squares with SHELXL-97.[15] All non-hydrogen atoms were refined anisotropically. Hydrogen atoms were included in the model at geometrically calculated positions.

**Table S11.2.** Crystallographic data and structure refinement for $Tp^{Mes}CoCl$.

| | |
|---|---|
| Empirical formula | $C_{36}H_{40}N_6BClCo$ |
| Formula weight | 661.93 |
| $T$ (K) | 293(2) |
| Radiation (Å) | MoKα (λ = 0.71073) |
| Crystal system | triclinic |
| Space group | P1 |
| Unit cell (Å) | a = 9.1600(18)  b = 10.940(2)  c = 17.452(4) |
| | α = 102.47(2)°  β = 97.46(3)°  γ = 95.07(3)° |
| V (Å³) | 1680.8(6) |
| Z | 2 |
| $\rho_{calc}$ (g/cm³) | 1.308 |
| Abs. coeff μ(mm⁻¹) | 0.625 |
| $2\theta$ range for data collection (°) | 3.84 to 62.066 |
| Index ranges | -13 ≤ h ≤ 13, -15 ≤ k ≤ 15 -25 ≤ l ≤ 25 |
| Reflections collected | 254071 |
| Independent reflections | 21429 [$R_{int}$ = 0.0462, $R_{sigma}$ = 0.0227] |
| Data/restraints/parameters | 21429/5/835 |
| GOF on F² | 1.029 |
| R1 (I > 2$\sigma$ (I)) | 0.0280 |
| xR₂ (all data) | 0.0721 |
| Largest diff. peak, hole (eÅ⁻³) | 0.29/-0.31 |
| Flack Parameter | -0.003(2) |

## 11.2. Tp^Mes^Co-allyl.



**Figure S11.2.** Ellipsoid representation of the crystal structure of the Tp$^{Mes}$Co-allyl complex.

**Table S11.3.** Selected bond angles from the Tp$^{Mes}$Co-allyl complex.

| Atom 1 | Atom 2 | Atom 3 | Angle | Atom 1 | Atom 2 | Atom 3 | Angle |
|--------|--------|--------|-------|--------|--------|--------|-------|
| N112 | Co1 | C12 | 96.2(1) | N112 | C113 | C114 | 123.8(3) |
| N132 | Co1 | C12 | 136.2(1) | N122 | C123 | C124 | 122.0(3) |
| N122 | Co1 | C12 | 133.2(1) | N132 | C133 | C134 | 122.1(2) |
| Co1 | N112 | C113 | 140.8(2) | C11 | C12 | C13 | 120.0(4) |
| Co1 | N122 | C123 | 136.4(2) | N122 | Co1 | C11 | 95.7(1) |
| Co1 | N132 | C133 | 138.4(2) | N132 | Co1 | C13 | 97.9(1) |

**Procedure**: A solvated, diffraction-quality single crystal of Tp$^{Mes}$CoCl, was mounted in paratone oil on a Kapton loop. Low temperature (100 K) diffraction data ($\varphi$- and $\omega$-scans) were collected on a Bruker-AXS X8 Kappa Duo diffractometer coupled to a Smart APEX II CCD detector with MoK$_\alpha$ radiation ($\lambda = 0.71073$ Å) from a *IμS*-micro source. Absorption and other corrections were applied using SADABS.[14] The structure was solved by direct methods using SHELXS[15] and refined against $F^2$ on all data by full-

matrix least squares with SHELXL-97[15]. All non-hydrogen atoms were refined anisotropically. Hydrogen atoms were included in the model at geometrically calculated positions.

**Table S11.4.** Crystallographic data and structure refinement for $Tp^{Mes}Co$-allyl.

| | |
|---|---|
| Empirical formula | $C_{39}H_{45}N_6BCo$ |
| Formula weight | 667.55 |
| $T$ (K) | 100(2) |
| Radiation (Å) | MoKα (λ = 0.71073) |
| Crystal system | triclinic |
| Space group | P1 |
| Unit cell (Å) | a = 9.0038(14)   b = 11.3166(17)   c = 17.839(3) |
| | α = 103.802(3)°   β = 95.013(3)°   γ = 94.018(3)° |
| V (Å³) | 1750.6(5) |
| Z | 2 |
| $\rho_{calc}$ (g/cm³) | 1.266 |
| Abs. coeff μ(mm⁻¹) | 0.527 |
| $2\theta$ range for data collection (°) | 3.722 to 62.214 |
| Index ranges | -13 ≤ h ≤ 13, -16 ≤ k ≤ 16, -25 ≤ l ≤ 25 |
| Reflections collected | 112018 |
| Independent reflections | 22086 [$R_{int}$ = 0.0532, $R_{sigma}$ = 0.0531] |
| Data/restraints/parameters | 22086/605/871 |
| GOF on F² | 1.036 |
| R1 (I > 2$\sigma$ (I)) | 0.0444 |
| xR2 (all data) | 0.1154 |
| Largest diff. peak, hole (eÅ⁻³) | 0.70/-0.67 |
| Flack Parameter | 0.035(3) |

# 12. Notes and References.

1. Perrin, D. D.; Armarego, W. L. F. *Purification of Laboratory Chemicals*. 3rd ed., Pergamon Press, Oxford, 1988.

2. Denysenko, D.; Grzywa, M.; Tonigold, M.; Streppel, B.; Krkljus, I.; Hirscher, M.; Mugnaioli, E.; Kolb, U.; Hanss, J.; Volkmer, D. *Chem. - A Eur. J.* **2011**, *17*, 1837.

3. Comito, R. J.; Fritzsching, K. J.; Sundell, B. J.; Schmidt-Rohr, K.; Dincă, M. *J. Am. Chem. Soc.* **2016**, *138*, 10232.

4. Denysenko, D.; Jelic, J.; Reuter, K.; Volkmer, D. *Chem. - A Eur. J.* **2015**, *21*, 8188.

5. Metzger, E. D.; Brozek, C. K.; Comito, R. J.; Dincă, M. *ACS Cent. Sci.* **2016**, *2*, 148.

6. Denysenko, D.; Werner, T.; Grzywa, M.; Puls, A.; Hagen, V.; Eickerling, G.; Jelic, J.; Reuter, K.; Volkmer, D. *Chem. Commun.* **2012**, *48*, 1236.

7. Furukawa, J.; Kobayashi, E.; Katsuki, N.; Kawagoe, T. *Die Makromol. Chemie* **1974**, *175*, 237.

8. Santee, E. R.; Chang, R.; Morton, M. *J. Polym. Sci. Polym. Lett. Ed.* **1973**, *11*, 449.

9. Silas, R. S.; Yates, J.; Thornton, V. *Anal. Chem.* **1959**, *31*, 529.

10. Comito, R. J.; Metzger, E. D.; Wu, Z.; Zhang, G.; Hendon, C. H.; Miller, J. T.; Dincă, M. *Organometallics* **2017**, *36*, 1681-1683.

11. Ravel, B.; Newville, M. ATHENA, ARTEMIS, HEPHAESTUS: data analysis for X-ray absorption spectroscopy using IFEFFIT. *Journal of Synchotron Radiation* **2005**, *12*, 537.

12. $Co_4Cl_4Zn(BTDD)_3$ was used for XAS studies.

13. Myers, W. K.; Duesler, E. N.; Tierney, D. L. *Inorg. Chem.* **2008**, *47*, 6701.

14. Sheldrick, G. M. *SADABS - A program for area detector absorption corrections* **2004**.

15. G. M. Sheldrick, *Acta Cryst. Sect. A* **1990**, *46*, 467.